Universität Potsdam
Institut für Biochemie und Biologie

Engineered human cytochrome c: Investigation of superoxide and protein-protein interaction and application in bioelectronic systems

Dissertation
zur Erlangung des akademischen Grades
"doctor rerum naturalium"
(Dr. rer. nat.)
in der Wissenschaftsdisziplin "Biochemie"

eingereicht an der
Mathematisch-Naturwissenschaftlichen Fakultät
der Universität Potsdam

von
Franziska Wegerich

Potsdam, den 15. September 2010

Published online at the
Institutional Repository of the University of Potsdam:
URL http://opus.kobv.de/ubp/volltexte/2011/5078/
URN urn:nbn:de:kobv:517-opus-50782
http://nbn-resolving.org/urn:nbn:de:kobv:517-opus-50782

LIST OF ABBREVIATIONS

ET	electron transfer
PECT	proton coupled electron transfer
SAM	Self-assembled monolayer

Proteins

cyt c	Cytochrome c
XOD	Xanthine oxidase
BOD	Bilirubin oxidase
SOX	Sulfite oxidase
SOD	Superoxide dismutase
Moco	Molybdenum cofactor
WT	wild-type

Chemicals

MUA	11-Mercaptoundecanoic acid
MU	11-Mercaptoundecanol
MPA	Mercaptopropionic acid
PASA	Poly(anilinesulfonic acid)
HX	Hypoxanthine
DTT	Dithiothreitol
IPTG	β-D-1-thiogalactopyranoside
EDC	N-Ethyl-N′-(3-dimethylaminopropyl)carbodiimide hydrochloride

Methods

CV	Cyclic voltammetry
AFM	Atomic force microscopy
SPR	Surface plasmon resonance spectroscopy
LbL	Layer-by-Layer
LB	Langmuir-Blodgett
NMR	nuclear magnetic resonance spectroscopy
^{1}H NMR	one dimensional ^{1}H NMR…
^{1}H-^{15}N HSQC NMR	two-dimensional ^{1}H-^{15}N heteronuclear single quantum coherence NMR

Units

Da	Dalton
M	Molar
A	Ampere
V	Volt
k	kilo- (10^{-3})
m	mili- (10^{-3})
µ	micro- (10^{-6})
n	nano- (10^{-9})
p	pico- (10^{-12})

TABLE OF CONTENTS

1 INTRODUCTION

1.1 General motivations for this work

The small redox protein cytochrome c is an all-time-favorite in biochemical and biophysical research since it is easy to handle and well characterized. But also from another point of view this protein is still in the focus of researchers: Cytochrome c is a good negative example of the paradigm one gene → one protein → one function. Beside its considered main function as electron carrier between complex III and IV in the respiratory chain, cytochrome c has also other physiological roles in different cell compartments. For example it accepts electrons from other proteins in the mitochondria like sulfite oxidase, and during the last decade it could be shown that cytochrome c can also act as apoptosis-triggering agent. Both the study of electron transfer reactions in proteins with cytochrome c as model protein and the role of cytochrome c in the apoptotic pathway are research topics of high interest today.

For electron transfer reactions to and from the heme group of cytochrome c the solvent-exposed heme edge surrounded by lysine residues forming a positively charged patch, is considered to be a relevant surface site for electron transfer, supported by electrostatic interactions with redox partner proteins. Thus, the introduction of additional electrostatic interaction points in the cytochrome c molecule represents a possible way to influence the reaction with other redox proteins. This provides not only further understanding of these reactions, but also can be applied in biomimetic systems where the electrochemical functionality is dependent on the protein-protein interaction. As an example, protein multilayer electrodes with cytochrome c embedded with other proteins can be accentuated here.

However, biological electron transfer reactions differ from most redox processes involving small molecules. For example, for the known reaction of the superoxide radical with cytochrome c neither exist a clear evidence for an outer or inner sphere reaction mechanism nor it is proven which part of the protein is relevant for this reaction. The reaction is of great relevance, because the superoxide-induced reduction of cytochrome c is used since many years for measuring the concentration of superoxide in tissues and other samples. For example, cytochrome c can be used as recognition element in an electrochemical superoxide biosensor, being immobilized on a SAM modified gold electrode. Here, the reaction rate of cytochrome c with superoxide is one sensitivity-limiting factor. The potential chance of enhancing the reaction rate via altering the electrostatics on the surface of cytochrome c and thereby improving the guidance of the negatively charged superoxide radical is one of the main motivations of this thesis.

The detection of superoxide is of particular interest, since this reactive oxygen species (ROS) has many physiological functions which are far from being fully understood. As already

mentioned, in the last few years the role of cytochrome c during ROS-induced cell death became also a highly discussed research field. Recent work suggests also a natural relevance of superoxide conversion via cytochrome c, which brings even more interest to the mechanism of this particular reaction and could provide another hint for an even further extended physiological role of the cytochrome c molecule.

In the past the role of particular amino acids of the cytochrome c molecule with respect to electron transfer reactions with proteins and other smaller compounds was mainly investigated using chemically-modified amino acids. Here, often a negative charge was added to positions with positively charged amino acids, which limits however the field of investigations. Modern molecular biology offers tools that provide the site specific exchange of an amino acid of a protein by any other amino acid of interest. In this way mutated protein forms with tailor made functions at specific positions within the protein can be produced. This possibility can be used to introduce additional positively charged amino acids into cytochrome c and to study the impact of these mutations on the properties of the engineered cytochrome c molecules.

Thereby protein engineering not only offers a great chance to investigate the reaction between the radical or other proteins with cytochrome c, but also provides a method for optimizing this reaction in order to build a superoxide sensor with an enhanced performance and to investigate electron transfer reactions within multilayer assemblies based on direct electron exchange between immobilized protein molecules.

Furthermore, the recombinant expression of cytochrome c allows the convenient production of the human form of the redox protein and permits the study of the protein's reactions in a more medically relevant context, since in the major part of *in vitro* investigation in literature only cytochrome c from yeast or horse was used.

1.2 Aim of this work

The aim of this thesis is the design, expression and purification of human cytochrome c mutants and their characterization with regard to electrochemical and structural properties as well as with respect to the reaction with the superoxide radical and the two selected proteins sulfite oxidase and bilirubin oxidase. Out of these investigation suitable cytochrome c mutants should be chosen for incorporation in two bioelectronic systems: an electrochemical superoxide biosensor with an enhanced sensitivity and a protein multilayer assembly with and without bilirubin oxidase on electrodes. All aspects of the investigations shall furthermore be compared with the attributes of unmutated human and horse heart wild-type cytochrome c.

2 LITERATURE SURVEY

2.1 Redox proteins and enzymes

Redox reactions are involved in many important biological reactions and are defined as reactions where electrons are transferred from a donor to an acceptor molecule. Biological electron transfer reactions differ from most redox processes involving small molecules. They occur rapidly over long distances (>10 Å) and are often accompanied by only small changes at the active site. Enzymes catalyzing redox reactions are called oxidoreductases and are conflated in the enzyme class EC 1 which can be further classified into 22 subclasses. Redox proteins are carriers of electrons and have the role of mediators in redox reactions. Often these proteins and enzymes have metal centers and are therefore known as metalloproteins.

In this thesis, reactions involving the redox protein cytochrome c (cyt c) from human, the oxidoreductases sulfite oxidase (SOX) from human and bilirubin oxidase (BOD) from fungi are investigated. The most important facts about these proteins are compiled below. Also the oxidoreductase superoxide dismutase (SOD) will be introduced for the comparison with the cyt c – superoxide reaction.

2.1.1 Cytochrome c

Cytochrome c is small globular redox protein with a molecular weight of 12 kDa. It contains a single polypeptide chain of about 100 residues (in mammals 104 amino acids) and a single c-type heme as prosthetic group (protoporphyrin IX, see Figure 1) which is covalently bound to two cysteine residues (Cys-14 and Cys-17). The actual electron carrier of cyt c is the heme iron which is coordinately bound to the ligands His-18 and Met-80. It can exist in the oxidized (ferric, Fe^{3+}) or the reduced (ferrous, Fe^{2+}) form. The heme group is also responsible for its red color.

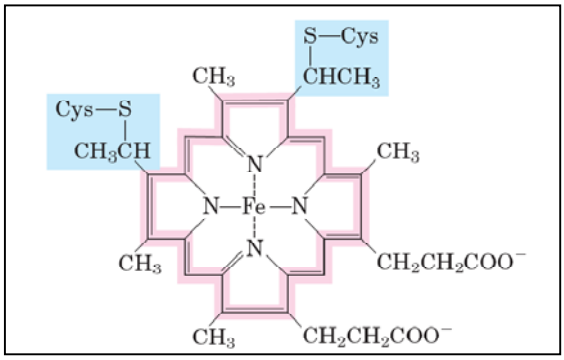

Figure 1 Structure of heme c of c-type cytochromes (Lehninger et al. 2005)

About 40% of the polypeptide is in α-helical segments the rest of the cyt c chain contains turns and irregularly coiled and extended segments but no β sheets (Figure 2). The characteristic fold of cyt c contains four α-helices which go from the N to the C terminus in the following order: Helix 1 (H1) with residues 5-14, Helix 2 (H2) with residues 50-54, Helix 3 (H3) with residues 61-68 and Helix 4 (H4) with residues 88-102 (De Biase et al. 2009).

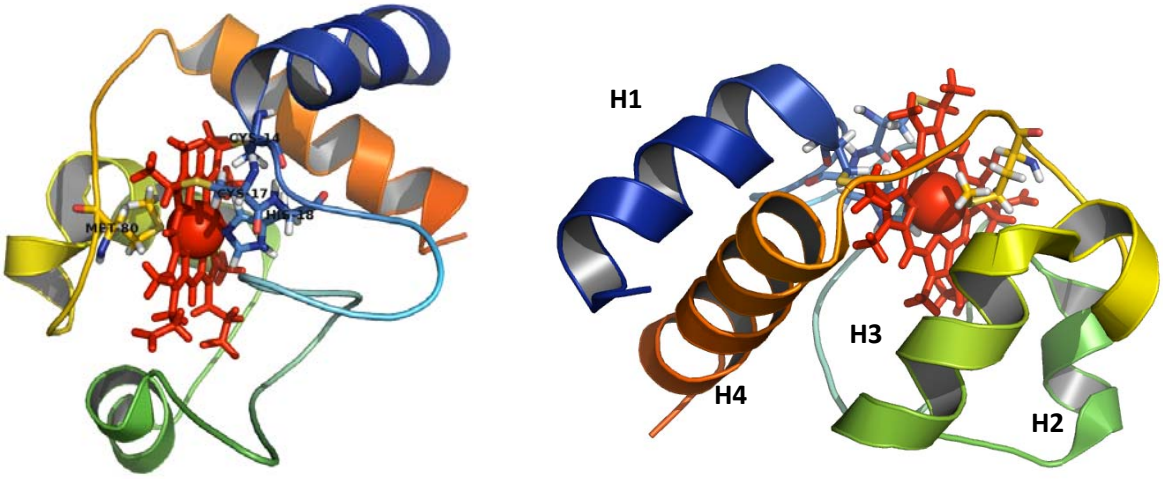

Figure 2 Cartoon representation of the structure of human cytochrome c. The iron ligands as well as the cysteines bound to the heme group are represented as sticks. The heme group is represented by red sticks and the heme iron as red sphere. Colors are going from blue over green and yellow to orange representing the peptide chain going from the N to the C terminus. Picture made with Pymol and the pdb-file 1J3S.

Cyt c is highly soluble in contrast to other cytochromes with a solubility of about 100 g/l. The 18 positively charged lysine residues contribute largely to the basic isoelectric point in the range of 10.0 – 10.5 (Van Gelder et al. 1962). The redox potential of cyt c is 250 mV vs NHE at pH 7 and 25°C.

2.1.1.1 The role of cytochrome c in nature

Cyt c is present in many species ranging from eukaryotes to bacteria and Achaea (Bertini et al. 2006). In eukaryotes cyt c is mainly located on the outer surface of the inner mitochondrial membrane (Figure 3 A). From the total amount of cyt c in mitochondria 15% can be found free in the intermembrane space and the rest is loosely (70%) and tightly (15%) bound to the phospholipid cardiolipin of the outer leaflet of the inner mitochondrial membrane via electrostatic interactions (Ow et al. 2008). But also interaction of an acyl chain of the anionic lipid with a hydrophobic channel of cyt c was suggested (Sinibaldi et al. 2010).

The main role of cyt c in the mitochondria is the capability of shuttling electrons between Complex III (cyt c reductase) and Complex IV (cyt c oxidase) during oxidative phosphorylation in

the respiratory chain (Figure 3 B). In chloroplasts, cyt c transfers electrons from the cytochrome *bf* complex to photosystem I. In prokaryotes, cyt c is involved in both aerobic and anaerobic respiration.

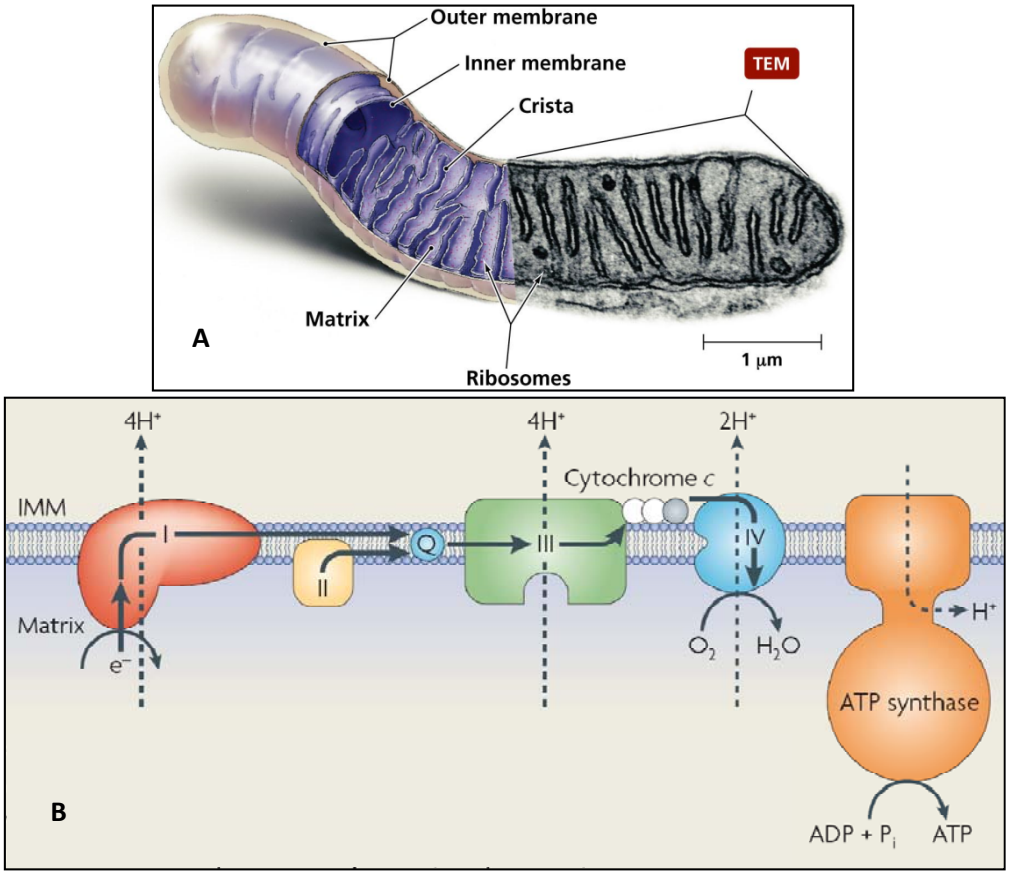

Figure 3 A: Demonstration of the mitochondrion structure (Pearson Education). B: role of cyt c electron transfer carrier between complex III and IV within the respiratory chain (Q – ubiquinone, IMM – inner mitochondrial membrane) (Ow et al. 2008).

The dogma of the apparent simplicity of the cyt c function was shaken in 1996 when Wang and co-workers (X. Liu et al. 1996) discovered that this protein is somehow involved in apoptosis.

It is now widely accepted that cyt c is involved in the intrinsic pathway of apoptosis (Caroppi et al. 2009; Ow et al. 2008; L. Wang et al. 2008), which is being initiated in mitochondria. Its activation includes the release of cyt c and other pro-apoptotic factors from the mitochondrial intermembrane space. In the cytosol, cytochrome c exerts its pro-apoptotic action. It binds to the apoptosis protease activation factor (APAf-1) and forms a complex indicated as 'apoptosome'. The complex-induced activation of pro-caspase 9 initiates an enzymatic reaction cascade, leading to the execution of apoptosis in cells (Figure 4) (Bayir et al. 2008).

A ‘‘pro-apoptotic’’ conformer of cyt c with increased peroxidase activity was identified (Kagan et al. 2005). It is suggested that the mobilization of cyt c from the membrane is conserted with cardiolipin peroxidation, resulting in MOMP (mitochondrial outer membrane permeabilization), the release of pro-apoptotic factors and the above described apoptotic cascade (Basova et al. 2007; Gonzalvez et al. 2007; Ying et al. 2010)

.

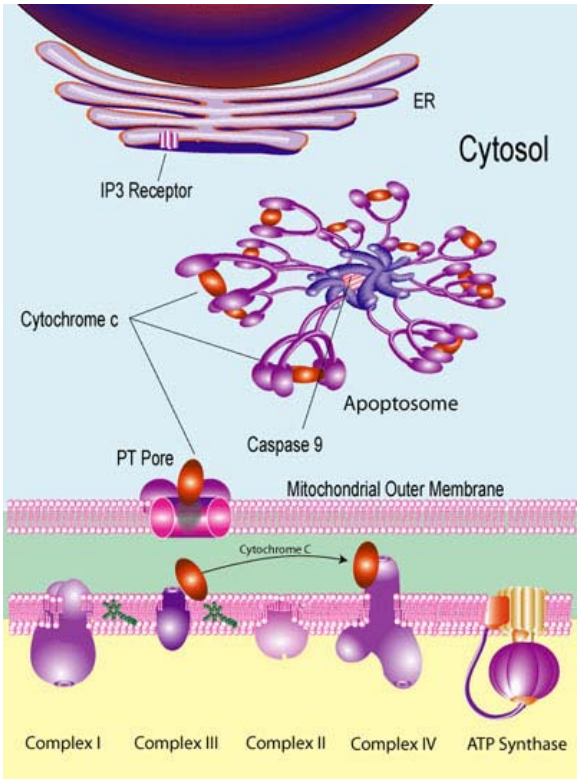

Figure 4 Schematic representation of the cyt c induced apoptotic intrinsic pathway (www.sigmaaldrich.com/life-science/metabolomics/enzyme-explorer/learning-center/cytochrome-c.html)

The complex role of cyt c during apoptosis is further underlined with the recent observations that tRNA can bind to cyt c preventing the cyt c-induced apoptosis pathway (Mei et al. 2010). Another function of cyt c is the ability to be bind to the growth factor adapter Shc ($p66^{Shc}$) in mitochondria, providing then electrons for the $p66^{Shc}$ catalyzed formation of ROS, which trigger mitochondrial apoptosis (Giorgio et al. 2005; Pinton et al. 2007). Scavenging superoxide and hydrogen peroxide in mitochondria (Min et al. 2007; Pereverzev et al. 2003) may also be connected to the apoptosis, since ROS are shown to act as redox signal molecules (see 2.1.1.2 and 2.3.1).

For the binding of cyt c to acidic partner proteins, prior studies have clearly established the important role of cyt c’s lysine-rich front face, and a series of apparently very different proteins and protein complexes recognize this surface domain on the cyt c molecule (Moore et al. 1990; Scott et al. 1996; Brautigan et al. 1978). In Figure 5 the asymmetric spatial charge distribution

and the positively charged front face of cyt c which surrounds the heme cleft can clearly be seen. Even when not all lysines at the front face of cyt c are directly involved in the binding, they may also contribute to its orientation. In many cases the positive charges on the five or six lysine groups immediately surrounding the heme cleft are involved in complementary charge interactions with negatively charged carboxyl groups on the other partner proteins (Webb et al. 1980).

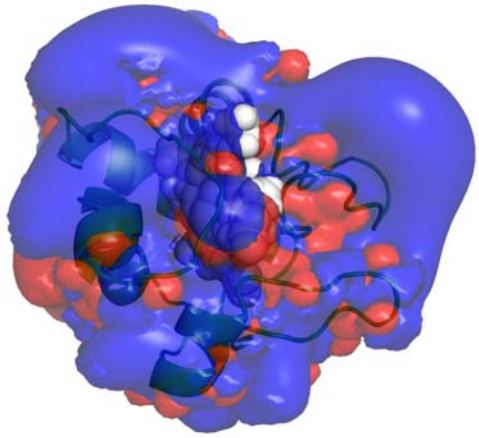

Figure 5 Electrostatic potential around human cyt c. The potential surface is transparent showing the underlying cartoon representation of the cyt c structure. The heme group is depicted in white spheres and is partly exposed. The surface potential was calculated by Andrea Giachetti from the University of Florence using the pdb file 1J3S. Regions where the electrostatic potential is <-1 kT are red, while those >+2 kT are blue (k, Boltzmann constant; T, absolute temperature). Picture made with Pymol.

These binding mechanism is established not only for its reaction partners in the respiratory chain, such cyt bc_1 complex of cyt c reductase(Rieder et al. 1980) and cyt c oxidase (Döpner et al. 1999), but can also be related to other proteins such as cyt c_1 (Rieder et al. 1980), cyt b_5 (Volkov et al. 2005) and SOX (see 2.1.4). However, the distinct importance of the lysines involved in binding differs for the different reaction partners (Pepelina et al. 2010).

For the proteins cyt c_1 of cyt c reductase and cyt c peroxidase it was shown that also hydrophobic interactions are of crucial importance for the binding (Bertini et al. 2006). Further e.g. in Apaf-1 binding, it seems that cyt c uses not only this front face, but also an opposite surface placed around positions 39 and 62–65 (Yu et al. 2001; Mufazalov et al. 2009; Ow et al. 2008).

The discoveries of cyt c functions beyond that of an electron carrier in respiration seem still not to be finished and contribute to the still ongoing high interest for this protein.

2.1.1.2 The reaction of cytochrome c with superoxide

In 1968 McCord and coworkers described for the first time the reduction of cytochrome c in the presence of the superoxide-generating enzyme xanthine oxidase (McCord et al. 1968). Since SOD competes for the reaction with superoxide and thereby inhibits the reduction of cytochrome c, a spectrophotometric assay for the quantification of the enzyme superoxide dismutase (SOD) in tissue was developed on this basis (McCord et al. 1969; 1970). Cyt c oxidizes superoxide to molecular oxygen:

$O_2^{\cdot-}$ + cyt c^{3+} → O_2 + cyt c^{2+}

Although the cytochrome c reduction assay is widely used since decades, only very few literature sources suggesting a natural role of superoxide conversion via cyt c can be found. Recently, parallel with the deep investigations of the role of ROS and cytochrome c in mitochondria and during the apoptotic pathway, some hints for a relevance of this reaction in nature were found. First in Skulachev's laboratory, the antioxidant properties of cytochrome c were confirmed in experiments with isolated mitochondria (Korshunov et al. 1999; V. P. Skulachev 1998). It could be shown that only free cyt c (not the membrane-bound one) is able to reduce superoxide. The latter one exhibits a peroxidase activity (Korshunov et al. 1999). Pereverzev declared cyt c even as an "ideal antioxidant" due to its ability to generate useful metabolic energy upon detoxifying potentially harmful superoxide (Pereverzev et al. 2003). In contrast to the SOD system, no hydrogen peroxide is generated here. It was postulated that the oxidation of superoxide-reduced cyt c by cytochrome c oxidase could generate a proton motive force (Mailer 1990), that mitochondria can use to produce ATP. Recently, it could also be demonstrated that cyt c, released in the yeast apoptotic pathway, can be reduced by superoxide and reoxidized by cyt c oxidase showing a further indication of its antioxidant activity (Giannattasio et al. 2008). Another recent paper suggests that superoxide is one of the cyt c reducing species, responsible for the steady-state redox state of cyt c which is supposed to regulate apoptosis, since reduced cyt c cannot activate the apoptosome (see 2.1.1.1). Therefore, it does not promote apoptosis, whereas the reoxidation of cyt c and the enhanced availability of cyt c oxidase after apoptotic permeabilization of the mitochondrion membrane lead to activation of the apoptotic pathway via oxidized cyt c (G. C. Brown et al. 2008). Another theory is linked to the loss of cyt c during apoptosis and the observed immediate burst of ROS: The absence of the ROS-scavenging function of cyt c could contribute to this burst of ROS. (Ow et al. 2008; Min et al. 2007).

Combining the above mentioned findings with the observations of an apoptosis inhibitory effect for a higher ratio of superoxide/H_2O_2 (see 2.3.1 and (Pervaiz et al. 2002)), one could speculate that superoxide oxidation via cyt c is also relevant for the apoptosis pathway due to

the competition with SOD in superoxide scavenging, together with the fact that cyt c, in contrast to SOD, does not cause the formation of hydrogen peroxide. Furthermore, a higher ratio of superoxide to hydrogen peroxide could also guarantee an efficient reduction of cyt c and thereby could hinder the cyt c^{3+}-induced apoptosis cascade.

Nevertheless the physiological role of superoxide as putative redox signal molecule in combination with cyt c and the *in vivo* efficiency of this superoxide scavenging system remain to be explored.

However, if this reaction is of relevance in nature, a conserved reaction pathway should exist. Only three works were dedicated to investigate the reaction pathway for the reduction of cyt c by superoxide up to date (Butler et al. 1975; Butler, W. H. Koppenol, et al. 1982; Cudd et al. 1982).

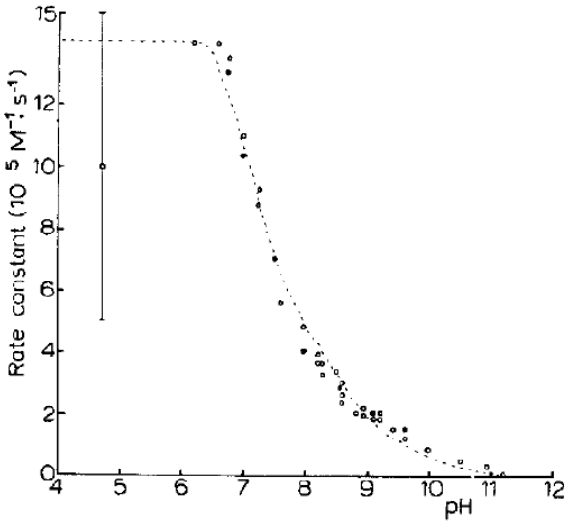

Figure 6 Effect of pH on the rate constant for the reaction of O_2^- with ferricyt c at 20 °C., (o) horse heart cytochrome c, (•) tuna heart cytochrome c. The point at pH 4.7 with the large error was estimated. Taken from (Butler et al. 1975).

In the first work the reaction rates were investigated at different pH (see Figure 6 (Butler et al. 1975)). Several conclusions were made: the most significant change of the rate constant occurs at pH 7.45, and it was supposed that an inner sphere reaction at the exposed heme edge is not likely due the cluster of positively charged amino acids around the heme edge. Further they examined the sequence of cyt c and identified two blocks of invariant residues (47-53 and 63-83), which border a distinct channel into the cytochrome interior, with some of the side chains (for example the aromatic residues tyrosine 67 and 74 and tryptophan 59) being along the channel. The suggestion was done that superoxide may transfer its electron to the heme group through this track. With respect to the pH change, it was proposed that protonation of some amino acids at pH values below 7.45 enhances the electron transfer either because superoxide reacts more rapidly with the protonated group or because protonation opens up the

way through the track. Newly obtained results in the field of electron transfer in proteins in the context of diverse tunneling mechanisms, lead to the arisen interest of a further investigation of this hypothesis.

However, the latter two works focused on the role of lysine residues around the exposed heme edge. Cudd and coworkers proposed a similar electrostatic facilitation effect like for the SOD owing to measurements at different ionic strength (Cudd et al. 1982).

In the later work of Butler et al. chemically modified lysine residues were used to investigate the influence of these amino acids on the reaction with superoxide. The modified lysines introduced a negative charge in the cyt c molecule. The reaction rate of the unmodified cyt c molecule was determined to be (2.6 ± 0.1) x 10^5 M^{-1} s^{-1}. The modified residue with most decreasing effect on the reaction rate was K72 following by K86, K27, K87, K13 and K60. This order differed from the order measured with other anionic reductants (where K13 was most influencing) (Butler et al. 1981; G. Williams et al. 1982). However, considering superoxide as the best representative of a small negative point charge, the authors concluded that the radical might be able to by-pass the normal orientations required for reaction with the enzymes such as cytochrome c oxidase and reductase, sulfite oxidase, and cytochrome c peroxidase, as well as with the non physiological reactants. Moreover, it has been stated that the cytochromes, modified at positions 87, 86, and 72, which are located to the left of the exposed heme edge, have activities much less than expected from the electrostatic correlation. Hence, they concluded that this might be the result of steric and short-range electrostatic effects, causing the superoxide reactions at the left of the heme edge.

The negative influence of the exchange of positive charges with negative charges on the reaction rate implies the possibility to enhance the reaction rate by introducing additional positively charged lysines. On the other hand these kinds of investigations could elucidate the reaction mechanism; since it remains unclear which reaction pathway is relevant upon reduction of the heme iron by superoxide. Possibilities include diffusing to the heme, followed by a direct reaction (inner sphere mechanism) or tunneling through outer amino acids (outer sphere reaction). In the latter case several electron transfer mechanisms can be considered.

Protein engineering offers here the chance to investigate the chemically unmodified protein, allowing the study of human cyt c as superoxide oxidant. This has never been investigated before with regard to the reaction with superoxide, but might be from greater medical relevance.

2.1.1.3 Comparison of human and horse cytochrome c structure

Although the tertiary structure of human and horse cyt c is very similar (Figure 7, right), there are twelve amino acids differing between the horse and human form of cyt c at the

following positions (horse→human): F46Y, T47S, D50A, K60G, V11I, Q12M, A15S, T58I, E62D, A83V, T89E, and E92A. The location of the sequence changes can be found in Figure 7 (left). As it can be seen, many of the positions are located at the surface of the protein. Also in the loop containing the residues 71 to 85 where some important lysine residues (Lys72, Lys73, Lys79) are located, one amino acid is changed. In most cases the changes are accompanied by a change in hydrophobicity and cause a more hydrophobic surface of human cyt c compared to the horse form. The apparent pK value (pKa) of human cyt c (pKa=9.9) is higher than those of horse cyt c (pKa=9.4) (Ying, F. Zhong, et al. 2009). There are obvious differences found in alkaline isomerization between these two proteins (Ying, F. Zhong, et al. 2009). The stability of human cyt c was found to be higher (Olteanu et al. 2003). The electrostatic surface potential of the two protein forms are shown to be strikingly similar (Banci et al. 1999). However, Rodríguez-Roldán et al. have recently reported that human cyt c exhibits remarkable differences compared to the horse form when interacting with horse cytochrome c oxidase (Rodríguez-Roldán et al. 2006).

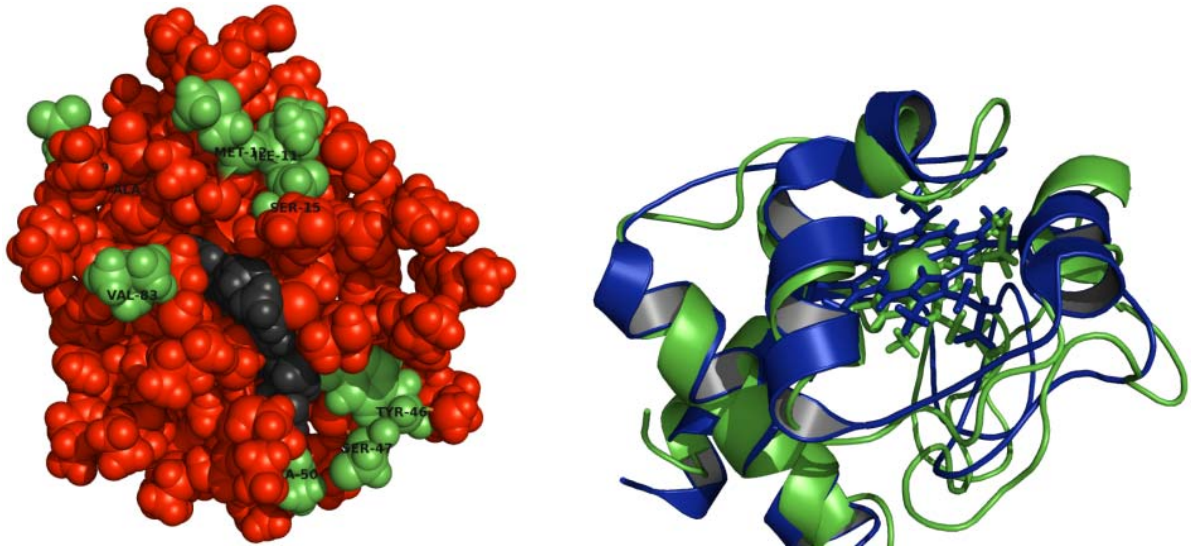

Figure 7 Left: Sphere representation of human cyt c with amino acid positions differing in comparison to horse cyt c marked in green. Heme is depicted in black spheres. Right: Structure alignment of the human (blue, pdb file 1J3S) and horse form (green, pdb file 2GIW) of cyt c. The heme group is depicted as sticks and the heme iron as green sphere. Pictures are made with Pymol.

2.1.1.4 Examples of mutational studies with cytochrome c

Former investigations with the aim to identify amino acids of cyt c involved in binding to reaction partners often include chemical modification of the protein (Rieder et al. 1980; Butler, W. H. Koppenol, et al. 1982; Speck et al. 1981). However, this resulted in an artificial protein and the modifications were limited to charged amino acids as targets for the modification. In

contrast, the site directed mutagenesis of proteins offers the chance to probe the properties of tailored proteins.

For example, the importance of distinct lysine for the binding to cyt c oxidase could be shown with mutated cyt c (Döpner et al. 1999; Pepelina et al. 2010). Engineered cyt c was also used to map the electron transfer interface between cyt c and cyt b_5 (Ren et al. 2004). Furthermore, cyt c mutants could help to identify the binding domains for the binding to Apaf-1 (Yu et al. 2001). For the mutants K72A and K72W an inhibition effect on apoptosis was demonstrated (Mufazalov et al. 2009). A similar effect was observed for the mutation of Y48 (Pecina et al. 2010).

A mutation at position F82 caused changes in global stability and of the local structure (Greene et al. 1993; Inglis et al. 1991). The role of histidines in the structure and stability of cyt c was also investigated (Sinibaldi et al. 2006).

Also the reaction with small compounds was shown to be changed upon mutation of cyt c. Mutations at position 67 can increase the peroxidase activity (Ying, Z.-H. Wang, et al. 2009; Casalini et al. 2010). The K73H mutant of yeast iso-1-cyt c exhibits a different electron transfer rate for the reaction with the positively charged hexaammineruthenium(II) chloride (Baddam et al. 2005).

Furthermore, the electron transfer (ET) from cyt c to modified electrodes was shown to be changed with the rat and yeast cyt c mutant K12A and K13R. Whereas the substitution of a lysine residue with alanine at position 13 lowers the interfacial ET rate more than 5 orders of magnitude; the charge conservative mutation K13R still causes a 100 fold decrease for the ET rate which highlighted the role of this lysine residue for the heterogeneous ET (Katsumi Niki et al. 2003; Katsumi Niki 2002).

For multiple Lys to Ala variants at the surface lysines 72, 73, and 79 an altered formal redox potential when adsorbed to modified gold was observed (Battistuzzi et al. 2007).

2.1.2 Superoxide dismutase

The enzyme family of superoxide dismutases (SODs) converts superoxide to oxygen and hydrogen peroxide, a relatively stable molecule. Although the dismutation of superoxide to hydrogen peroxide can occur spontaneously (see 2.3), the role of SODs is to increase the rate of the reaction to that of a diffusion-controlled process (Abreu et al. 2010). SODs are subdivided in three subclasses according to their folding with four different metal cofactors: Copper-zinc SODs (Cu,ZnSOD), manganese SODs/iron SODs (MnSOD/FeSOD) and nickel SODs (NiSOD). All SOD types can be found in prokaryotic organisms. In Eukaryotes FeSOD can be found in chloroplasts. In the mitochondria of animals the corresponding MnSOD can be found in the matrix and

Cu,ZnSOD in the intermembrane space (Abreu et al. 2010). Cu,ZnSOD as the most abundant SOD is also the most thoroughly studied SOD.

All SODs have in common the disproportionation reaction, occurring through alternate oxidation and reduction of their catalytic metal ions (M). This mechanism is called a "ping-pong" mechanism (Perry et al. 2010) and can be described in general as:

$M^{(n+1)} + O_2^- \rightarrow M^{n+} + O_2$

$M^{n+} + O_2^- (+2H^+) \rightarrow M^{(n+1)} + H_2O_2$

Overall: $2O_2^- + 2H^+ \rightarrow O_2 + H_2O_2$

Although the protein architectures of the three SOD classes are distinct, all of them crucially provide electrostatic guidance for the superoxide radical and alter the metal ion redox potential to a range suitable for superoxide disproportionation (Perry et al. 2010).

Figure 8 One subunit of human Cu,ZnSOD with the channel towards the copper ion (green sphere) lined with positively charged amino acids (positive surface potential marked in blue, negative surface potential marked in red). Figures made with PyMol and the pdB file 1HL5.

The overall structure and the channel towards the copper ion in human Cu,ZnSOD is presented in Figure 8. Under physiological conditions, the rate of the Cu,ZnSOD reaction with the radical is ca. 10^4 times faster (2×10^9 M^{-1} s^{-1}) than that of the spontaneous disproportionation of superoxide in solution(Smirnov et al. 2006).

A lot of work was done including genetic engineering and Brownian dynamics simulations to identify amino acids responsible for this fast reaction especially for Cu,ZnSOD: a couple of positively charged lysines were found around the active site, providing an electrostatic potential distribution which attracts the negatively charged superoxide radical to this region (Figure 8)

while the rest of the protein is mainly negative charged (Stroppolo et al. 2001; Getzoff et al. 1983). Additionally, the evolutionary conserved arginine residue at position 143 was shown to play an important role in catalysis by steering the superoxide towards the copper ion (Fisher et al. 1994; Y.-H. Zhou et al. 2007). Mutational exchange at this position with a still positively charged lysine residue reduced the activity to 10%, indicating the importance of the local charge distribution.

Several attempts were made to further increase the reaction rate with superoxide with enhanced electrostatic guidance by engineering of SOD (Getzoff et al. 1992; Folcarelli et al. 1999; Polticelli et al. 1998): substitutions of negatively charged glutamates by uncharged glutamines near the superoxide channel resulted in a two- to threefold arisen activity of the protein. However, a further increase of local positive charges (by introducing a positively charged amino acid) was not successful, indicating that preorientation factors may also be relevant for the correct attraction of the substrate toward the active site.

The possibility to increase the rate by improved electrostatic guidance in SOD provides the motivation to apply this approach for the enhancement of the rate of superoxide oxidation by cyt c as it will be shown in this thesis. Besides, SOD is also a popular recognition element in superoxide biosensors (see 2.3.2).

However, one has to take into account possible side effects of the mutation conducted: unwanted reactivities may occur or the stability of the protein might be decreased.

2.1.3 Bilirubin oxidase

The monomeric enzyme bilirubin oxidase (BOD; EC 1.3.3.5) belongs to the family of multicopper oxidases and is found in the fungi Myrothecium verrucaria. BOD has a molecular weight of about 64 kDa. It catalyzes the oxidation of bilirubin to biliverdin with oxygen as electron acceptor in the following way:

bilirubin + O_2 = 2 biliverdin + 2 H_2O

In diagnostic analysis BOD is used to determine levels of bilirubin in serum (Kosaka et al. 1987). Due to its high reactivity at neutral pH in comparison to other multicopper oxygen consuming enzymes like laccases, it has also attracted attention as an enzymatic catalyst for the cathode of biofuel cells (Cracknell et al. 2008). Recently, the X-ray structure of BOD was resolved (K. Mizutani et al. 2010). It was shown that the structure as well as the four copper binding sites are very similar to other multicopper oxidases. The protein is folded into three domains, domain one and three contain the copper binding sites (Figure 9). The enzyme contains one type I, one

type II and two (one pair of) type III coppers. The type II and III coppers form a trinuclear centre that reduces oxygen to water molecules and the type I copper functions as the electron mediator from the substrate to the trinuclear centre (Shleev et al. 2005). In the crystal structure a hydrophilic asparagine residue was identified close to type I copper (where in other multicopper oxidases a hydrophobic residue can be found) and it was suggested that this amino acid contributes to the characteristically high redox potential of BOD (490 mV vs. NHE) (K. Mizutani et al. 2010; F. Xu et al. 1996)).

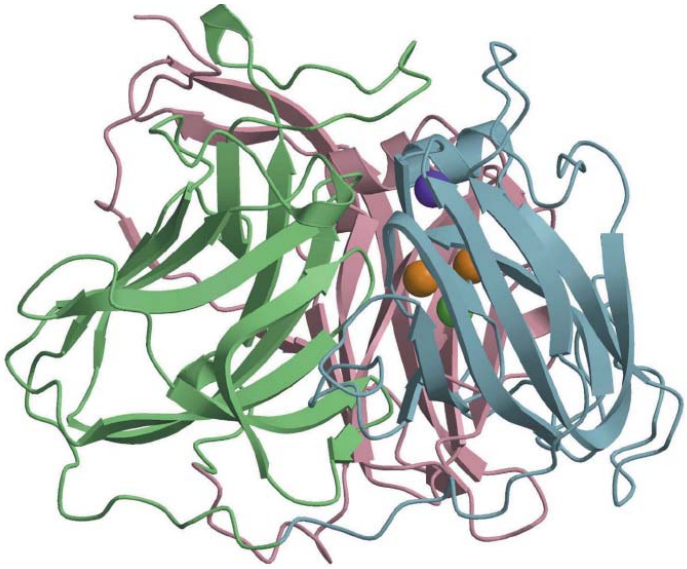

Figure 9 Crystal Structure of fungi BOD. Domains 1, 2 and 3 are shown in pink, green and blue, respectively. Type I Cu, type II Cu and type III Cu ions are depicted as purple, green and orange spheres, respectively (K. Mizutani et al. 2010).

Recently it was demonstrated that also cyt c can act as electron donor instead of bilirubin in solution and in bioelectronic multilayer assemblies on electrodes (Dronov, Kurth, Frieder W. Scheller, et al. 2007; Dronov, Kurth, Möhwald, Frieder W. Scheller, and Lisdat 2008). But also modified electrodes can be used to contact BOD directly (Shleev et al. 2005).

2.1.4 Sulfite oxidase

The homodimeric enzyme sulfite oxidase (SOX, EC 1.8.3.1) has a molecular weight of 110 kDa and belongs to the family of molybdo-enzymes with a molybdopterin (MPT) cofactor. This family also includes DMSO reductase, xanthine oxidase and nitrite reductase (Kisker et al. 1997). It catalyzes the oxidation of sulfite to sulfate (Figure 10 left) as the final step in the oxidative degradation of the sulfur-containing amino acids cysteine and methionine. SOX also plays an important role in detoxifying exogenously supplied sulfite and sulfur dioxide (Jean L Johnson

2003). Loss of SOX activity, due to either a defect in one of the proteins in the synthesis pathway for the MPT cofactor or a mutation in the SOX gene itself (isolated SO deficiency), leads to severe birth defects and neurological problems that usually result in death at an early age (Jean L Johnson 2003).

Animal SOX is located in the intermembrane space of mitochondria with ferricyt c as physiological electron acceptor (C. Feng et al. 2007). High activity is found in liver, kidney and heart tissues. The only crystal structure of active animal SOX solved so far, is that of chicken liver SOX (Kisker et al. 1997). Each 52 kDa subunit of the homodimeric chicken SOX contains a 10 kDa N-terminal b_5-type cytochrome c domain, a MPT cofactor binding domain and a C-terminal interface domain (Figure 11). The MPT domain and the heme b_5 domain are linked by a flexible peptide loop. The structure of the human heme b_5 domain is also solved (Rudolph et al. 2003).

The overall SOX reaction cycle (Figure 10) can be divided into reductive and oxidative half-reactions (Garrett et al. 1998). The reductive half reaction portion of the catalytic sequence involves the reaction of sulfite with oxidized enzyme to yield the reduced enzyme (and sulfate), and the oxidative half reaction involves the reaction of SOX with cyt c to yield oxidized enzyme and reduced cyt c. The proposed catalytic mechanism of animal SOX involves two intramolecular one-electron transfer steps from the MPT to the heme b_5 iron, and two intermolecular one-electron steps from the heme b_5 domain to exogenous cyt c.

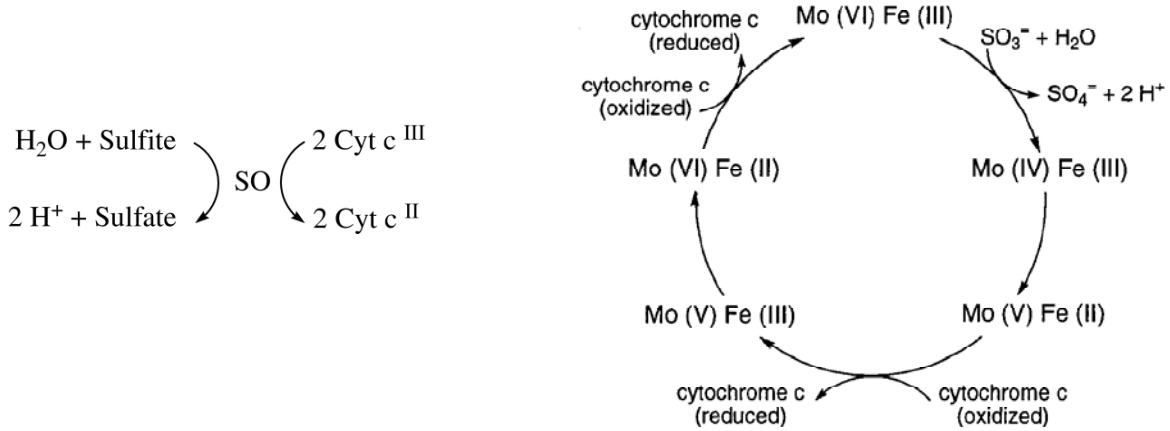

Figure 10 Overall reaction (left) and proposed reaction mechanism for animal SOX (right) (Garrett et al. 1998).

The distance between the Mo and Fe atoms in the two domains of SOX in the crystal structure is 32 Å, which did not suit to the rapid ET rate constants (k_{ET} > 1000 s^{-1}) observed for this enzyme (Sullivan et al. 1993). It was suggested that during the reaction cycle two domains adopt a conformation that brings the MPT and heme centers much closer to each other. Indeed, the rate constant for intramolecular ET decreases with an increase in the viscosity of the

solution, indicating that domain movement is essential for the efficient ET between the heme b_5 and MPT domains of SOX (C. Feng et al. 2007). The flexible loop probably provides the mobility of the heme b_5 domain to allow its negatively charged exposed edge to interact electrostatically with the positively charged MPT domain (Moco domain in Figure 11) as well as with the positively charged surface of cyt c. It was shown that in the reduction half cycle the intraprotein ET is the limiting step, probably due to the conformational change which is necessary to bring the heme b_5 domain close to the MPT cofactor to conduct reduction of heme b_5 (C. Feng et al. 2007).

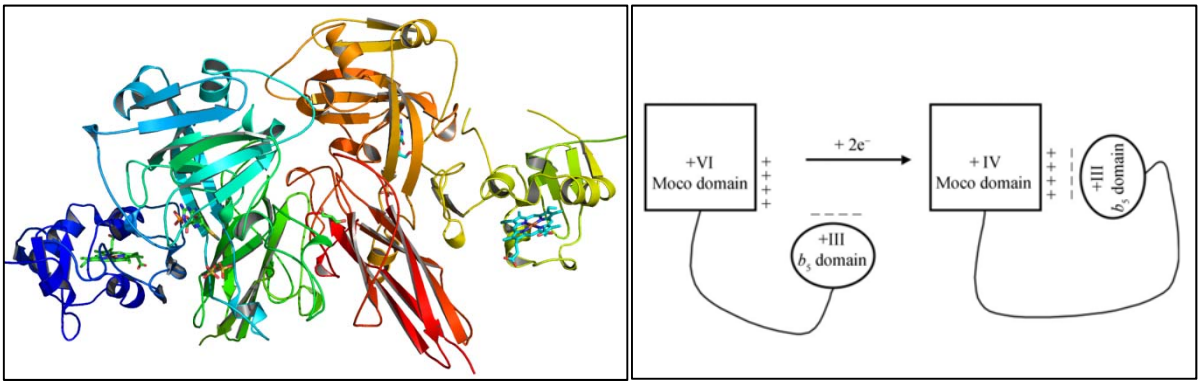

Figure 11 Left: X-ray dimeric structure of chicken liver SOX (made with PyMol and pdb file 1SOX.pdb (Kisker et al., 1997)). The two heme b5 domains are depicted in yellow in blue, the two Moco domains in orange an cyan respectively. Right: Schematic presentation of the intraprotein ET from the Moco domain to the heme b5 domain (Rudolph et al. 2003).

Many studies were done to determine the binding sites of cytochrome b_5 and cyt c (Ren et al. 2004; Volkov et al. 2005) but it was also found that this cannot be compared with the heme b_5 domain of SOX since there is only 42% sequence identity (Ritzmann et al. 1988; Rudolph et al. 2003). However, similar to the cyt b_5-cyt c interaction the analysis of the electrostatic surface potential of cyt c and the SOX heme b_5 domain as well as chemical modifications of the lysine residues of cyt c indicated that the lysines around the heme crevice are important for the interaction with the negatively charged area of the heme b_5 domain of SOX (Rudolph et al. 2003; Speck et al. 1981; Webb et al. 1980). These are the same lysines identified to be important also for the binding to cyt c oxidase (see 2.1.1.1).

SOX was applied in several bioelectronic systems. It was shown that SOX accepts also modified electrodes as electron acceptor instead of cyt c (Ferapontova et al. 2003; Spricigo et al. 2010; Sezer et al. 2010). Furthermore, it could be also embedded in a multilayer assembly together with cyt c (Spricigo et al. 2008; Dronov, Kurth, Möhwald, Roberto Spricigo, Leimkühler, et al. 2008b). A sulfite biosensor with SOX as recognition element could be constructed with

(Spricigo et al. 2009; Hart et al. 2002) and without cyt c as mediator (Ferapontova et al. 2003; Spricigo et al. 2010).

2.2 Biosensors

Biosensor can be defined as a "compact analytical device or unit incorporating a biological or biologically derived sensitive 'recognition' element integrated or associated with a physio-chemical transducer" (Turner 2000). The first biosensor was developed in 1967 and consisted of an enzyme electrode with glucose oxidase for the measurement of glucose (Updike et al. 1967). Up to day the glucose biosensors have the highest commercial success in this field. The schematic representation of the general biosensor configuration is depicted in Figure 12.

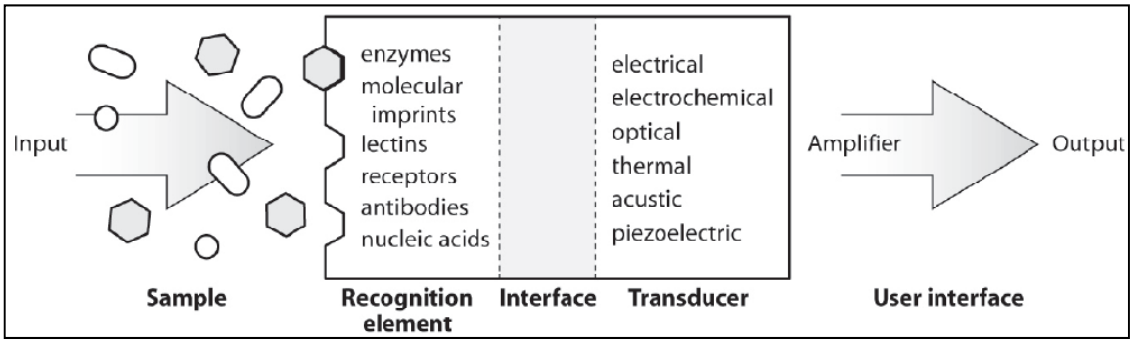

Figure 12 Configuration of a biosensor showing biorecognition, interface, and transduction elements (Chambers et al. 2008).

Biological recognition elements can be enzymes, proteins, antibodies, receptors, nucleic acids, aptamers, lectins and molecular imprints. An overview of the different recognition elements can be found in a review published by Chamber et al. (Chambers et al. 2008).

Biosensors can be also divided by the type of transducer used: signal transformation can be achieved via a physicochemical way, as well as optical, piezoelectric, electrochemical, acoustic or thermal ways.

2.2.1 Electrochemical biosensors based on direct protein electrochemistry

Electrochemical biosensors are bioelectronic devices normally based on reactions that produce or consume electrons (Privett et al. 2010). Therefore, redox proteins and oxidoreductases are often employed as recognition elements. Different potentiometric (e.g. ISFETs), voltammetric and amperometric methods exist, where either the potential or the current change depending on the concentration of the analyte can be measured.

Electrochemical biosensors can be divided in three different generations: First generation sensors measure directly the product of the reaction. To avoid interferences second generation biosensors use mediators which mediate the electron transfer between the product of the reaction and the electrode. Third generation electrochemical biosensors are based on direct protein electrochemistry i.e. direct electron transfer (DET) between the electrode and the protein (Figure 13 left). Basic principles of this kind of biosensor are reviewed by Wu et al. (Y. Wu et al. 2007).

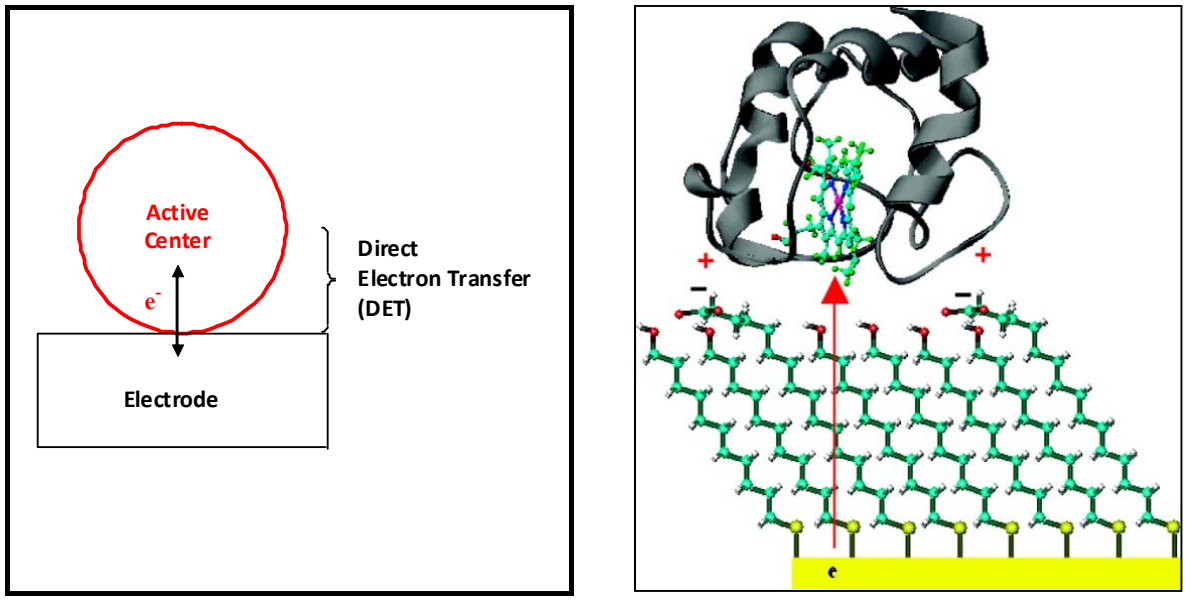

Figure 13 Left: Principle of direct protein electrochemistry which is applied in third generation electrochemical biosensors. Right: Schematic representation of the DET between cyt c and a modified gold electrode (Yue et al. 2008).

The main advantage of a third generation biosensor is a superior selectivity since no mediator is used which diminishes the influence of potential interferences. An additional advantage of systems based on DET is the possibility of modulating the desired properties of an analytical device using protein modification with genetic or chemical engineering techniques as well as novel interfacial technologies.

The rate of the DET is an important feature of a third generation biosensors and depends strongly on the potential difference and the distance between the two redox sites according to the Marcus theory (Marcus et al. 1985). Hence special attention has to be made during immobilization of the protein to guarantee a close approach of the active site to the electrode. Often, immobilization on bare metal electrodes results in irreversible adsorption and denaturation of the proteins and hence a hindered ET. Modifications of the electrode with promoters may solve this problem. Thiol-based promoters have achieved a broad usage, because they can easily bind to gold surfaces by simple adsorption and without any complex reaction

step, since they rely on self-assembly (self assembling monolayers – SAMs). The end group of the acyl chain may also be chosen depending on the protein immobilization strategy.

In the case of cyt c the positively charged lysines around the heme cleft can be used for an oriented immobilization of the protein via electrostatic interaction with the negatively charged carboxyl group of the SAM modified electrode (Figure 13, right). Adsorption and also covalent immobilization are possible with this arrangement. The length and composition of the SAM promoter crucially influences the electron transfer rate of cyt c to the electrode (L. Wang et al. 2008; Davis et al. 2008; Alvarez-Paggi et al. 2010; Ly et al. 2010; Z. Feng et al. 1997; Ge et al. 2002; Arnold et al. 1997; Yue et al. 2008; Battistuzzi et al. 2007). These features are also important for the selectivity in the sensor application (see 2.3.2).

New surface modifications used by nanotechnology open a new field in the direct protein electrochemistry research field. For example carbon nanotubes (Schubert et al. 2009), quantum dots (Stoll et al. 2008) and mesoporous indium tin oxide (Frasca et al. 2010) can be used for immobilization. These techniques increase the surface area of the electrode and thereby allow the immobilization of a high protein amount which increases the sensitivity of the biosensor. Also protein multilayers can increase the amount of the recognition element on the electrode (see 2.2.3).

2.2.2 Examples of protein engineering for biosensor applications

Outside the field of biosensors protein engineering represents usually a popular tool to understand reaction mechanisms in proteins and enzymes. For example it could be shown that the lysine residues near the heme edge of cyt c are important for the ET to cyt c oxidase (Döpner et al. 1999) and mutants of cellobiose dehydrogenase exhibited a drastically altered substrate specificity which provided hints for the role of the active site during catalysis (S. Ferri et al. 2010).

The knowledge and control of the interaction site position on the surface of the enzyme is crucial in the field of biosensors. Besides, tailored protein mutants can also be beneficial for the application in biosensors and biofuel cells. The particular advantages offered by genetically engineered recognition elements in bioelectronic devices were reviewed recently (Campàs et al. 2009; Caruana et al. 2010). The main goals of site directed mutagenesis in this field are: creation of more sensitive or specific enzymes, designing new enzyme immobilization techniques to increase the stability of the sensor and the enhancement of ET to the electrode.

The approach for the enhancement of the enzyme sensitivity is based on the increase of the affinity for the target analyte by favoring the accessibility of the active site. For example, the active site in the *drosophila* acetylcholinesterase is buried and the entrance is therefore very

narrow. Mutations in this precise region, i.e. the exchange of distinct tyrosines, not only enhanced the sensitivity of an anatoxid-a(s) biosensor but also improved the selectivity since it was shown to be resistant to most insecticides (Devic et al. 2002).

Another elegant approach is the usage of engineered PQQ-dependent glucose dehydrogenase with altered K_m values. Combination of two mutants with a decreased and increased K_m value, respectively, together with the wild type protein extended the dynamic range of the glucose sensor significantly. Additionally the sensor showed also a higher specificity (Yamazaki et al. 2000).

Biosensors based on new immobilization techniques with protein mutants include approaches for an easier electrical communication between the redox center of the protein and the electrode; a covalent anchoring of the redox centers to the protein matrix to prevent the loss in hostile environments; and an increased stability of the protein over a wide range of temperatures and pH (Maly et al. 2002). For example, the insertion of cysteine residues in the protein can be used for an oriented immobilization on gold surfaces as it was shown for SOD (Moritz Karl Beissenhirtz et al. 2006)and plastocyanin (Andolfi et al. 2002). Similarly, the introduction of histidines can also be used for an enhanced immobilization (Andreescu et al. 2002; Ferapontova et al. 2001).

An example of an electrochemical biosensor based on enhanced electron transfer is the genetic addition of a poly-l-lysine chain to glucose oxidase and the linkage of the redox mediator ferrocenecarboxylic acid to it. This resulted in higher electro-catalytic currents, a wider linear range of the sensor and a higher stability (L.-Q. Chen et al. 2002).

Also cyt c was already subject to protein engineering in the context of tailored recognition elements for biosensors: Site directed mutagenesis of yeast-1-iso cyt c at position M80 and Y67 resulted in an increased peroxidase activity of cyt c which was applied in an electrochemical hydrogen peroxide sensor (Casalini et al. 2010). The cyt c mutant M80A showed also changed catalytic properties: the mutation caused the ability to react with oxygen and nitrite. This mutant was investigated in an oxygen biosensor (Casalini, Battistuzzi, Borsari, Bortolotti, et al. 2008; Casalini, Battistuzzi, Borsari, Ranieri, et al. 2008).

2.2.3 Layer-by-Layer technique for biosensor applications

The construction of protein multilayer films on electrodes by layer-by-layer technique is a popular research area, especially in the field of biosensors, since the significant increase in the surface concentration of the biological recognition element can be achieved in a controlled way (Z. Tang et al. 2006; Lisdat et al. 2009; Ariga et al. 2006; Caruso et al. 1997; W. Zhao et al. 2006; Rusling et al. 2008). Synthetic polyelectrolytes are often applied as building blocks (Decher et al.

1998; S. Song et al. 2009; Lutkenhaus et al. 2007; Calvo et al. 2001; Calvo et al. 2010) but also other materials such as DNA (Rusling et al. 2008; Sarauli et al. 2009; Lvov et al. 1998) or nanoparticles (Katz et al. 2004; Bonk et al. 2009; H. Tang et al. 2007) can be used to successfully incorporate biological compounds within the films.

The assembly of the multilayer is in most cases driven by electrostatic interactions: basically a charged surface is immersed alternately in two solutions containing oppositely charged building blocks until a desired film thickness is achieved (Figure 14). The incorporated biomolecule can represent hereby also the charged building block itself.

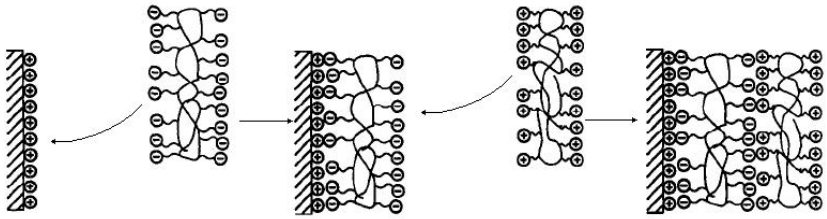

Figure 14 Formation of a multilayer structure on a positively charged substrate using charged polyelectrolytes (Decher et al. 1992).

Communication within such assemblies however is an issue since the ET distance drastically increases with the number of deposited layers (Ma et al. 2000). Thus, shuttle molecules are often used in order to transfer the information of a conversion at the protein molecule to the electrode (Moraes et al. 2007; Rusling et al. 2008; L. Shi et al. 2003).

The small heme protein cyt c is the first redox protein which could be successfully incorporated in a fully redox-active multilayer assembly using sulfonated polyaniline (PASA) as a counter polyelectrolyte (Moritz Karl Beissenhirtz et al. 2004; Moritz Karl Beissenhirtz et al. 2005). A biosensor for superoxide radicals based on this architecture was reported with a much higher sensitivity in comparison to a cyt c monolayer system (M.K. Beissenhirtz, F.W. Scheller, et al. 2004).

A more sophisticated approach is the embedment of other enzymes in these layers to form a bi-protein artificial signal chain (Lisdat et al. 2009). Cyt c can act here as an electron transfer protein, which can provide the electron transfer between the electrode and the enzyme without any external mediator. First assemblies with cyt c and xanthine oxidase still relied on the generation of an internal shuttle molecule (Dronov, Kurth, Helmuth Möhwald, et al. 2007). However, reaction partners of cyt c such as SOX (Dronov, Kurth, Möhwald, Roberto Spricigo, Leimkühler, et al. 2008b; Spricigo et al. 2008; Spricigo et al. 2009) , laccase (Balkenhohl et al. 2008) or BOD (Dronov, Kurth, Möhwald, Frieder W. Scheller, and Lisdat 2008) allow the construction of electrode assemblies without the need of any diffusing shuttle molecules. Such electrodes are capable of sensing of sulfite and oxygen. However, limited stability is still a

drawback in terms of application of protein multilayer electrodes, and some attempts as a thermal treatment were done to increase stability (M.K. Beissenhirtz, F.W. Scheller, et al. 2004).

2.3 Superoxide radicals

The superoxide anion radical belongs to the so called reactive oxygen species (ROS), and is produced by the one-electron transfer to oxygen. It has a high reactivity acting both as a reductant and an oxidant. Superoxide is the first ROS generated *in vivo* during the stepwise four electron reduction of oxygen (Fridovich 1978):

$$O_2 + e^- \rightarrow O_2^-$$

$$O_2^- + e^- + 2H^+ \rightarrow H_2O_2$$

$$H_2O_2 + e^- + H^+ \rightarrow HO^{\cdot} + H_2O$$

$$HO^{\cdot} + e^- + H^+ \rightarrow H_2O$$

Superoxide can undergo spontaneous dismutation being the conjugate base of the hydroperoxyl radical $HO_2^{\cdot}$(Behar et al. 1970), and the dominating dismutation reactions are the following:

$$HO_2 + HO_2 \rightarrow H_2O_2 + O_2$$

$$HO_2 + O_2^- + H^+ \rightarrow H_2O_2 + O_2$$

At physiological pH value of 7.5 the rate of dismutation is determined to be 2.3×10^5 M^{-1} s^{-1} (Behar et al. 1970). The dismutation reaction $2O_2^- + 2H^+ \rightarrow O_2 + H_2O_2$ is to slow to contribute to the overall rate (Behar et al. 1970). The short life-time of the radical is dependent on its concentration and ranges from milliseconds to seconds (Fridovich 1972).

2.3.1 Role of superoxide radicals in nature

Several enzymes can produce superoxide under certain conditions. The respiratory chain in mitochondria is an important source for superoxide within most mammalian cells (Murphy 2009). Also other biological reactions e.g. reactions involving xanthine oxidase (Hille 2006) and the reactions of the bacterial and plant photosynthesis are sources of superoxide (Scarpeci et al. 2008). External addition of the herbicide paraquat can also induce superoxide formation. In mitochondria superoxide can be produced by respiratory complexes. Complex I in the brain and complex III in the heart and lung seem to be the primary sources of mitochondrial superoxide production (Figure 15) (Bayir et al. 2008). In the presence of iron superoxide can be converted via the Fenton reaction to the even more reactive hydroxyl radical. Together with nitric oxide superoxide can form the highly reactive peroxynitrite. The concentration of superoxide is estimated to be 10-200 pM *in vivo*. However, the concentration inside mitochondria *in vivo* is not

known, since only measurements with isolated mitochondria were possible up to date (Murphy 2009).

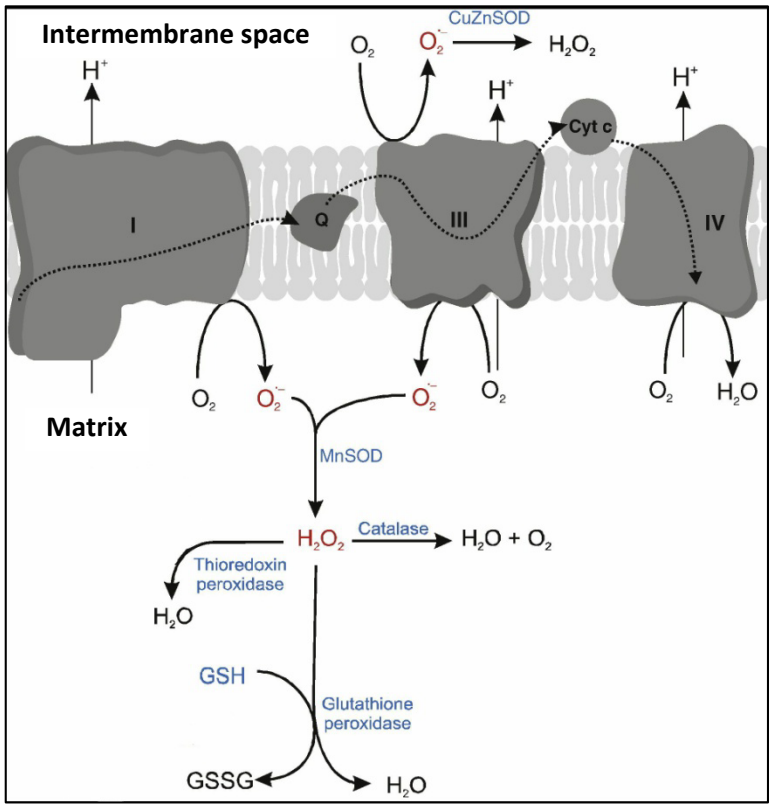

Figure 15 Places of superoxide generation in the mitochondrial respiratory chain (Cyt c, cytochrome c; $O_2^{\cdot-}$, superoxide; Q, ubiquinone) (Kowaltowski et al. 2009).

Superoxide is detoxified by superoxide dismutases (SODs) to hydrogen peroxide (H_2O_2) in the mitochondria and glutathione peroxidases convert hydrogen peroxide to water (Figure 15). In peroxisomes catalases convert superoxide to oxygen and water. The fact that virtually all living organisms possess either one of these enzymes is, per se, remarkable evidence for the importance of superoxide in biology. Lately also cyt c was considered as an ideal antioxidant oxidizing superoxide without formation of H_2O_2 (Pereverzev et al. 2003). Also other non-enzymatic compounds are able to act as antioxidants such as tocopherol and ascorbate (Imlay 2008).

For many years superoxide is considered only as by-product with dominating negative cell compound damaging effects. But it is also deployed by the immune system as a mechanism to destroy the invading microorganisms (Craig et al. 2009). Additionally more recently the role of superoxide as cell signaling molecule has been discovered in a variety of physiological responses such as transcriptional activation, bioenergy output, cell proliferation, and apoptosis (Bartosz 2009; Sarsour et al. 2009; Z. Wu et al. 2010; Jones 2006). For apoptotic signaling a function of a tight balance between the levels of superoxide and hydrogen peroxide is supposed (Pervaiz et al. 2002). It is suggested that under normal physiological conditions redox-optimized ROS balance

(with both ROS production and ROS scavenging) obeys the evolutionary drive toward maximal energy output and the ROS-dependent signaling function of mitochondria (Aon et al. 2010). If under stress situations this equilibrium is disturbed and the body can no longer compensate for the production of superoxide, several pathological events can occur which includes damage of DNA, proteins and lipids (Sarsour et al. 2009). One example is ROS damage during ischemia and reperfusion involving XOD (Kevin et al. 2003; Becker et al. 1999). Furthermore, it could be shown that superoxide is involved in several diseases like cancer (Pervaiz et al. 2007) and Alzheimer (Z. Wu et al. 2010). Together with the role of superoxide during apoptosis it is suggested that superoxide and other ROS are also involved in the aging process (G. Paradies et al. 2010). However, although the correlation of oxidative damage with aging is generally accepted, the proof of causality for ROS as aging accelerator is still lacking (Bokov et al. 2004).

Since the role of superoxide in diseases and cell signaling e.g. in apoptosis is far from fully understood it is necessary to quantify superoxide under different conditions and at different locations *in vivo*. Particularly in the medical field there is a large interest to follow the radical's concentration on-line *in vivo*.

2.3.2 Detection methods for superoxide

The short life span of superoxide makes it difficult to measure and only a few techniques can be utilized. Indirect spectrophotometric assays rely on the reduction of dyes (Fink et al. 2004) but are not specific for superoxide, which limits its use. The same is valid also for the direct spectrophotometric measurement at 250 nm (Marklund 1976). Chemiluminescent methods have been used frequently for vascular tissue samples because they are more sensitive than other conventional methods (C. Lu et al. 2006). Fluorescence-based assays have also been widely used in cultured cells and vascular tissues (X. Xu et al. 2010; Seitz et al. 2010). Electron spin resonance (ESR) spectroscopy, also known as electron paramagnetic resonance (EPR), quantitatively measures superoxide concentration but is less suitable for its *in vivo* detection (R. Chen et al. 2004). Among the indirect methods the spectrophotometric measurement of cyt c reduction by superoxide is the most widely employed technique due to its great sensitivity and simple assay design (Quick 2000; Sanders et al. 1994).

Electrochemical sensors based on cytochrome c reduction or superoxide dismutase (SOD) enzymatic reaction have been developed for the sensitive real-time monitoring of superoxide (Tian et al. 2006; Borgmann 2009; Yuasa et al. 2005). First-generation SOD-based biosensors detect superoxide indirectly by measuring hydrogen peroxide concentration (McNeil et al. 1989). H_2O_2 is enzymatically generated during superoxide reaction within immobilized SOD and then further oxidized at the electrode surface. Several approaches have been developed to

enhance the selectivity for these types of sensors: a H_2O_2-impermeable Teflon membrane (M. I. Song et al. 1995), combination with horseradish peroxidase (Lvovich et al. 1997) the entrapment of SOD between two membranes (Campanella et al. 2003) and the incorporation of SOD in a polypyrrol film (Descroix et al. 2001; Mesaros et al. 1998).

Another approach (second-generation SOD-based biosensors) used different mediators, such as ferrocene-carboxyaldehyde or methyl viologen, to enable electron transfer from SOD to the electrode (Endo et al. 2002; Ohsaka et al. 2002). Since the direct electron transfer of SOD to electrodes, without the need of mediators, results in a simple sensor design with high sensitivity and selectivity, third-generation biosensors have gained considerable attraction. The electron transfer to SOD was shown to be promoted using thiol self-assembled monolayers (SAMs)(Ge et al. 2003; Tian et al. 2002; Tian et al. 2004; Tian et al. 2005) an electroactive sol-gel film (J. W. Di et al. 2004), or a ZnO nanodisc film (Deng et al. 2008). SOD was also directly immobilized on gold using SOD mutants with additional cysteine residues (Moritz Karl Beissenhirtz et al. 2006; Kapp et al. 2006). Superoxide biosensors using SOD often lack reproducibility due to immobilization problems. In contrast, third-generation cyt c based superoxide sensors are more stable and have already been used for in vivo applications (Buttemeyer et al. 2002; Frieder W. Scheller et al. 1999). Here the reduction of the heme protein by superoxide and subsequent reoxidation by an electrode is used. The detection principle is depicted in Figure 16.

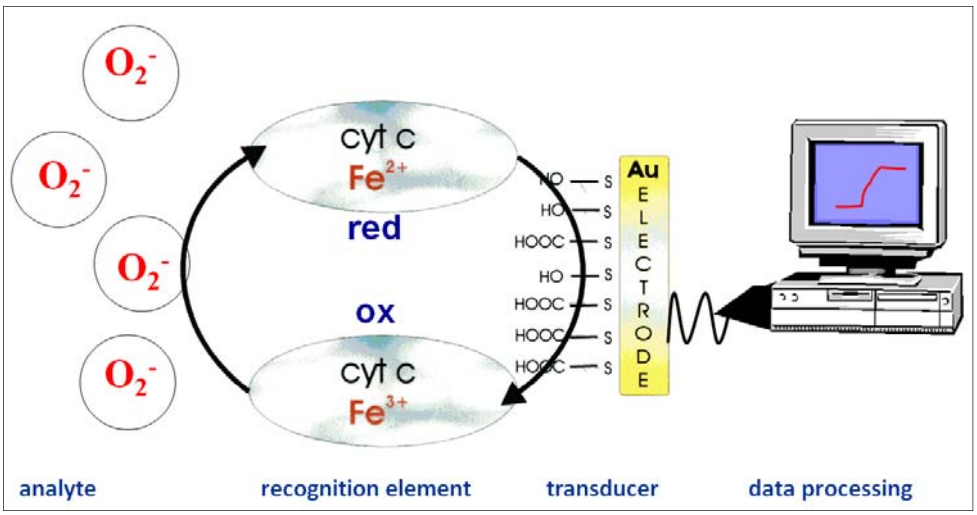

Figure 16 Principle for the detection of superoxide with an amperometric cyt c based biosensor.

Short-chain thiol-modified gold electrodes used for the immobilization of cyt c show a highly efficient communication between cyt c and the electrode and have been applied for cyt c based superoxide sensors (Tammeveski et al. 1998) e.g. in isolated mitochondria (Henderson et al. 2009). However, they are not completely blocking the electrode surface. For this reason, sensor electrodes using long-chain thiols have been developed to diminish effectively electroactive

interferences. These cyt c electrodes have been applied for in vitro measurements of the radical (Moritz Karl Beissenhirtz et al. 2003; Ignatov et al. 2002; Krylov et al. 2007; Lisdat, Ge, Ehrentreich-Forster, et al. 1999; Lisdat, Ge, Reszka, et al. 1999; M.K. Beissenhirtz, R.C.H. Kwan, et al. 2004) as for in vivo studies (Buttemeyer et al. 2002; Frieder W. Scheller et al. 1999).

The sensitivity of these cyt c electrodes is dependent on the amount of electroactive protein and the reaction rate of protein with the radical. Thus, different approaches have been used for sensitivity enhancement: optimization of the promotor layer (Ge et al. 2002; Gobi et al. 2000), increasing the surface roughness (Krylov et al. 2004) and the construction of protein multilayer electrodes (M.K. Beissenhirtz, F.W. Scheller, et al. 2004). A possibility to enhance the reaction rate of cyt c with superoxide may be directed protein engineering as it is an approach in this thesis. This could also lead to a superoxide sensor with increased sensitivity.

3 MATERIALS AND METHODS

3.1 Materials

3.1.1 Materials

Xanthine Oxidase (XOD) was purchased from Roche (Mannheim, Germany). Horse-heart cytochrome c, bovine erythrocyte superoxide dismutase (SOD), Bilirubin oxidase from *Myrothecium verrucaria* (EC 1.3.3.5), lysozyme, hypoxanthine, H_2O_2 (30% solution in water), isopropyl β-D-1-thiogalactopyranoside (IPTG), dithiothreitol (DTT), 1-ethyl-3(3-dimethyl aminopropyl) carbodiimide (EDC), 11-mercapto-1-undecanoic acid (MUA), 11-mercapto-1-undecanol (MU), 3-mercapto-1-propanol, deuterium oxide (D_2O), potassium hydroxide and ferriycyanide were provided by Sigma-Aldrich (Taufkirchen, Germany). Potassium dihydrogen phosphate (KH_2PO_4), dipotassium hydrogen phosphate(K_2HPO_4), disodium sulfite, sodium dihydrogen phosphate (NaH_2PO_4), disodium hydrogen phosphate (Na_2HPO_4), and potassium chloride were purchased from Merck (Darmstadt, Germany). Purified sulfite oxidase was received as a gift from the group of Prof. Silke Leimkühler from the University of Potsdam, Germany.

Gold wire electrodes with a diameter of 0.5 mm were provided by Goodfellow (Bad Nauheim, Germany).

All solutions were prepared in 18 MΩ Millipore water (Millipore, Eschborn, Germany).

3.1.2 Buffers

For the preparation of the sodium phosphate buffer (50 mM and 10 mM), Na_2HPO_4 or NaH_2PO_4 was used with the pH adjustment using sodium hydroxide or phosphoric acid. The 10 mM sodium phosphate buffer containing 1 M KCl was adjusted for pH after KCl addition.

The potassium phosphate buffers (0.5 mM and 5 mM) were made with K_2HPO_4 or KH_2PO_4 salts and the pH was adjusted using hydrochloric acid or potassium hydroxide respectively.

3.2 Methods

3.2.1 Preparation of cytochrome c mutants

3.2.1.1 Mutation of human cytochrome c

The plasmid pET21a-CCHL-hCYC provided by Chuang and coworkers (Jeng et al. 2002) carries the human cytochrome c gene, converted from yeast cyt c with long primers, and the CCHL genes of the yeast heme lyase (Pollock et al. 1998). The heme lyase attaches the heme covalently to apocytochrome c (Allen et al. 2003).

This plasmid was used for introducing additional mutations and is further referred as wild-type (WT). Primers for mutation were designed with the web-based software PrimerX (http://bioinformatics.org/primerx/). Mutations were introduced using the QuickChange site-directed mutagenesis kit from Stratagene (La Jolla, USA) following the provided protocol. Gene sequencing was done to confirm the mutations.

3.2.1.2 Recombinant expression and purification of wild-type and mutated human cytochrome c

Human cytochrome c was expressed and purified using adapted protocols from the literature (Jeng et al. 2002; Rivera & Walker 1995; Bertini, Chevance, Turano submitted). It was coexpressed with heme lyase and other cytochrome c maturation proteins: Competent BL21(DE3)C41 E. coli cells were used for transformation of the plasmid DNA with the mutated cyt c gene and the yeast heme lyase. These cells contained an additional pEC86 plasmid which expressed the bacterial cytochrome c maturation genes ccmABCDEFGH under the control of the tet promoter (Arslan et al. 1998). The complex cyt c biogenesis system containing these eight genes is arranged in one operon in *E. coli* (Meyer et al. 2005). CcmE acts e.g. as heme chaperon during cyt c maturation (Schulz et al. 1998).

The cells were cultivated in minimal media M9 supplemented with minerals, vitamins and glycerol in a shaker at 37 °C and 180 rpm until OD_{600} reached 1.0. The expression started after addition of IPTG (1 mM final concentration) and $FeSO_4$ (100 mg/l final concentration) and the culture was incubated for 72 h at 30 °C and 60 rpm (Figure 17a). After harvesting by centrifugation (Figure 17b), the cells were lysated using lysozyme and sonication. Purification of cyt c, involved two chromatography steps, first, the supernatant of the centrifuged lysate was loaded onto a 5 ml SP Sepharose cationic exchange column (Figure 17c, GE Healthcare, Sweden)

and eluted with a linear NaCl gradient (0-500 mM) in 50 mM sodium phosphate buffer, pH 6.8. Pertinent fractions (Figure 17d) were determined by SDS-PAGE, and those containing cyt c were concentrated using an Amicon ultra centrifugal filter device with a molecular weight cutoff of 5000 kDa (Millipore, USA). The sample was then loaded onto a 120 ml dextran size exclusion column and eluted with 50 mM sodium phosphate buffer, pH 6.8. Fractions were monitored by UV/VIS spectroscopy and pooled together to obtain a final cyt c sample.

Figure 17 Pictures of some cyt c expression and purification steps from left (a) to right (d): a - culture after 72 h; b - cell paste after harvesting by centrifugation; c - cyt c running through a cationic exchange column; d - final fractions of cyt c after size exclusion chromatography

3.2.2 NMR measurements

NMR measurements were conducted by Prof. Paola Turano from the University of Florence, Italy (CERM, Magnetic Resonance Center) who was involved as cooperation partner in the project of this thesis.

Unlabelled and ^{15}N-labelled cytochrome c samples, in both diamagnetic ferrous and paramagnetic ferric forms, were used for the NMR characterization. The reduced and oxidized states of the proteins were obtained by addition of dithiothreitol (DTT) and an excess of ferricyanide, respectively. The oxidizing agent was then removed by ultra-filtration before NMR data acquisition. Typical protein concentrations were in the 200 μM – 1 mM range (samples were concentrated to reach this range with a Centricon centrifugal filter device, containing a molecular weight cut off of 5000 kDa), in 20-50 mM phosphate buffer, pH 6.8 with 10 % D_2O.

NMR experiments were carried out at 300 K on a Bruker 800 MHz spectrometer equipped with a TXI cryoprobe. Uni-dimensional ^{1}H NMR spectra were recorded over a spectral width of 20 ppm and a 1.2 s recycle delay. Water suppression was achieved using excitation sculpting (Hwang 1995). The ferric form of the protein required detection of hyperfine shifted resonances, achieved using a larger spectral width (100 ppm), faster repetition rates (600 ms), and presaturation for efficient water suppression. Two-dimensional ^{1}H-^{15}N heteronuclear single quantum correlation (HSQC) experiments (Sklenar 1993) were acquired with 1024 × 256 data

points, over a spectral width of 14 ppm for ^{1}H and 40 ppm for ^{15}N. Spectra were processed and analyzed with the Bruker Topspin software package.

3.2.3 Spectrophotometric measurements

Spectrophotometric measurements were performed with an UV-250 1PC UV-VIS spectrophotometer (Shimadzu Sientific Instruments, Kyoto, Japan), a DU 7400 spectrophotometer (Beckman Coulter, USA), a Spectronic Helios Alpha spectrophotometer (Thermo Fisher Scientific, USA) and a stopped-flow spectrometer (Stopped Flow SX.18MV Reaction Analyzer, Applied Photophysics, United Kingdom). Spectra were obtained between 350 to 650 nm for a 5 µM cyt c solution. In order to fully oxidize or reduce the protein, DTT or sodiumdithionite and excess ferricyanide were used respectively.

3.2.3.1 Reaction with superoxide

To guarantee ultrapure samples for the determination of the reaction rate of cyt c with superoxide, mutant and wild type cyt c were dialyzed before the spectrophotometric kinetic measurements with 50 mM sodium phosphate buffer pH 7.5 using the Slide-A-Lyzer dialyses cassettes (Thermo Scientific, Rockford, USA) with a molecular weight cut off of 3500 kDa. The amount of oxidized (ox) cyt c used for this measurement was calculated according to the absorption spectra of the dialyzed protein before each measurement and the total amount of cyt c in the sample which could be retrieved from the absorption spectra of reduced (red) cyt c (treated with DTT or sodiumdithionite). In case of a totally oxidized sample the equation

$$[cyt\ c]_{ox} = \frac{(A_{550-red} - A_{542-red}) \times dilution\ factor + (A_{542-ox} - A_{550-ox}) \times dilution\ factor}{(\varepsilon_{550-red} - \varepsilon_{550ox})}$$

was used, and in case of a partly oxidized cyt c sample the following equation was used

$$[cyt\ c]_{ox} = \frac{A_{550-untreated} \times dilution\ factor - A_{550-red} \times dilution\ factor}{(\varepsilon_{550-ox} - \varepsilon_{550red})}$$

with $\varepsilon_{550\text{-}ox}$= 7.4 $mM^{-1}\ cm^{-1}$ and $\varepsilon_{550\text{-}red}$ = 32.02 $mM^{-1}\ cm^{-1}$ (determined with horse heart cyt c in 50 mM sodium phosphate buffer pH 7.5).

A steady state superoxide concentration was generated *in vitro* using the enzyme xanthine oxidase (XOD) and its substrate hypoxanthine (Ge et al. 2002). The increase of absorbance at

550 nm after addition of XOD, with a final concentration of 30 mU/ml, was recorded for 60 seconds in the presence of 100 µM hypoxanthine with a spectrophotometer or a stopped-flow spectrometer (Stopped Flow SX.18MV Reaction Analyzer, Applied Photophysics, United Kingdom). This corresponds to a steady-state superoxide concentration of about 520 nM calculated using the following formula (Ge et al. 2002):

$$[O_2^-] = \sqrt{\frac{k_3}{2\,k_4}[XOD]}$$

The rate constant for the enzymatic superoxide generation with XOD, k_3, was determined photometrically to be 0.015 µM ml s^{-1} mU^{-1}. The rate constant of spontaneous dismutation k_4 at pH 7.5 is given as 2.3×10^5 M^{-1} s^{-1}(Behar et al. 1970).

The initial rate of reduction of cyt c was measured for seven different cyt c concentrations (0.2 to 5 µM cyt c) for each cyt c form. This was performed at least twice. The resulting slope divided by the superoxide concentration determined the reaction rate constant k_1 for the reaction of cyt c and superoxide in solution.

3.2.4 SPR measurements

A Biacore X (Biacore AB, Sweden) was used to monitor the multilayer formation by SPR spectroscopy. A flat gold sensor chip was cleaned by a 10 min incubation with 96 % (w/w) H_2SO_4 / 30 % (w/w) H_2O_2 (3:1) solution. Then the chip was incubated in a MUA/MU (1:3) ethanolic solution for 72 hours, and subsequently washed with Millipore water and installed into the Biacore flow system. The following solutions (all in 0.5 mM potassium phosphate buffer, pH 5) were injected subsequently with a flow rate of 1 µl/min: buffer, cyt c (5 min), PASA (5 min), and cyt c (5 min). The latter two steps were repeated four times.

3.2.5 Electrochemical measurements

Cyclic voltammetry was performed with an Autolab PGSTAT 20 and a µAutolab Type II potentiostat (Metrohm, Germany). Amperometric measurements were conducted on a model 720 A potentiostat from CHI Instruments (Austin, TX, USA).

For the electrochemical studies, a custom-made 1-ml measurement cell (Figure 18), a Ag/AgCl/1 M KCl reference electrode with a potential of +0.237 V vs. NHE (Biometra, Göttingen, Germany), and a platinum counter electrode was used. Gold wire electrodes were cleaned following an established protocol (Ge et al. 2002): First the wires were boiled in 2.5 M KOH for four hours, then rinsed with water and finally put in concentrated (98 % (w/w)) H_2SO_4 at least

overnight. Just before modification the electrodes were incubated for 10 minutes in concentrated HNO_3 (65 % (w/w)). The immersion depth of the electrodes during the measurements was 4 mm. The experiments were all carried out at room temperature.

Figure 18 Custom-made 1-ml measurement cell with a gold needle working electrode immersed in a cyt c solution.

3.2.5.1 Measurements with cytochrome c in solution

Electrochemical studies of cyt c in solution were carried out with mercaptopropanol-modified electrodes (incubation 24 h in 20 mM mercaptopropanol). Cyclic voltammograms were recorded with 20 µM cyt c in 1 M KCl and 10 mM sodium phosphate buffer, pH 7.0. The redox potential E_0 was calculated as mean of the midpoint potentials between the anodic and cathodic peak potentials at different scan rates (50-400mV/s). This is appropriate since R, the ET coefficient, is found to be approximately 0.5 and E_f is almost independent of the scan rate in the range of 0.50-400 mV/s. Diffusion coefficients were calculated from the peak currents at different scan rates according the Randles-Sevcik equation (Bard et al. 1980).

3.2.5.2 Measurements with adsorbed cytochrome c

For the electrochemical investigations of adsorbed cyt c on gold electrodes, the needle electrodes were modified with mercaptoundecanoic acid and mercaptoundecanol (MUA/MU, incubation for 48 to 72 h in 5 mM solutions with a volume ratio of 1/3). Subsequently the electrodes were incubated for two hours in 30 µM cyt c (in 5 mM potassium phosphate buffer pH 7).

Cyclic voltammograms were recorded between -300 and +300 mV vs. Ag/AgCl at a scan rate of 100 mV/s (step potential 0.3 mV). The formal potential E_f was calculated as mean of the midpoint potentials between the anodic and cathodic peak potentials at low scan rates (where no tendency of E_f could be observed). The heterogeneous electron transfer rate constant k_s was

determined by the variation of the scan rate between 100 mV/s and 15 V/s followed by an evaluation of the peak separation according to the Laviron method (Laviron 1979). The amount of redox active cyt c (surface coverage Γ) was derived from the mean of the oxidation and reduction peak area (charge) using Faraday's law. The charge and the half peak width were determined with the Autolab software (GPES version 4.8 and 4.9).

3.2.5.3 Construction and usage of the superoxide sensor electrodes

In order to construct sensor electrodes for the amperometric measurement of superoxide, cyt c was immobilized covalently by incubation of the electrodes in 2.5 mM EDC, 30 µM cyt c (in 5 mM potassium phosphate buffer, pH 7.0) for 30 minutes. After washing with 5 mM potassium phosphate buffer, they were stored in the same buffer until they were measured. For long time storage, electrodes were kept in buffer or dry in closed 1.5 ml reaction vials at 4 °C. The amperometric measurements were performed at +150 mV vs. Ag/AgCl under constant stirring in 1 ml 50 mM sodium phosphate buffer, pH 7.5. 10 µl of 50 mM hypoxanthine was added after reaching a stable baseline.

Enzymatic superoxide generation was performed by adding 2.5, 5, 10, or 15 µl of a 1 U/ml XOD solution. The sensor signal was derived from the steady state current after baseline subtraction. The sensor was calibrated using the fact that the superoxide concentration corresponds to the square root of the XOD concentration (Ge et al. 2002). At least three electrodes were measured for each cyt c type.

The effect of pseudoperoxidase activity of cyt c was investigated with covalently immobilized cyt c on gold electrodes using cyclic voltammetry within the range of -150 mV up to +250 mV at a scan rate of 20 mV/s (with step potential of 0.3 mV). The difference between the cathodic current at 0 V in the absence and presence of 5 mM H_2O_2 was evaluated. The amperometric pseudoperoxidase control measurements were conducted at +0.15 V in the presence of up to 300 mM H_2O_2.

3.2.5.4 Reaction of cytochrome c with sulfite oxidase and bilirubin oxidase in solution

MUA/MU modified gold electrodes (see 3.2.5.2) were used to investigate the reaction of cyt c with BOD and SOX in solution. Cyclic voltammetry with SOX was carried out in 50 mM sodium phosphate buffer pH 8.5 and in the presence of 10 µM cyt c and 2 mM sulfite. The concentration of SOX was varied from 0.1 to 3 µM and the scan rate from 2 to 32 mV/s.

For the BOD measurements 10 µM cyt c prepared in air saturated 50 mM phosphate buffer pH 7.0 was used. The scan rate variation was conducted from 4 to 16 mV/s for BOD concentratios of 50 to 350 nM.

3.2.5.5 Construction of the cyt c / BOD multilayer electrodes

The multilayer assembly was performed with a MUA/MU modified gold electrode with a cyt c monolayer adsorbed (see 3.2.5.2). The electrodes were incubated up to 6 times alternating in a 2 mg/ml PASA solution and a 20 µM cyt c solution (or for the BOD multilayers a protein mixture of 20 µM cyt c and 200 nM BOD) for each 10 minutes. Between the incubations steps the electrodes were dipped 10 times in 0.5 mM potassium phosphate buffer pH 5. The solutions were also prepared with this buffer. The electrochemical response of the electrodes was controlled by cyclic voltammetry in air saturated 5 mM potassium phosphate buffer pH 7. The oxidation peak currents and the reduction peak or catalytic currents were evaluated at fixed potentials and as absolute current values (without baseline usage).

4 RESULTS AND DISCUSSION

This chapter is divided into four sections. The first part of the thesis (4.1) is dedicated to the design, expression and characterization of the mutants. The electrochemical characterization of the mutants in solution and their behavior being immobilized on electrodes are here accentuated. Moreover, the reaction of these mutants with superoxide is investigated and the possible mechanism of the reaction is discussed.

In the second part (4.2) an amperometric superoxide biosensor with selected human cytochrome c mutants is constructed and the performance of the sensor electrodes is studied.

In the third part (4.3) of the thesis the reaction of human cyt c mutants with two selected proteins sulfite oxidase and bilirubin oxidase, is studied electrochemically, and the influence of the mutations on the electron transfer reactions is discussed.

Finally, protein multilayer electrodes with cytochrome c mutants are investigated (4.4). Furthermore, bilirubin oxidase and the engineered cyt c are embedded in a multilayer assembly. The relevant electron transfer steps and the kinetic behavior of the multilayer electrodes are discussed.

4.1 Study of the reaction between cytochrome c mutants and superoxide: structure-function relationships

In this section the motivation for the selection of mutation sites for human cytochrome c is described. Then the reaction rate of the expressed mutants with superoxide is determined, and the mutants are characterized thoroughly by spectroscopic and electrochemical analysis.

4.1.1 Selection of mutation sites

Based on earlier studies on the mechanism of O_2^- conversion by SOD (Getzoff et al. 1992) and the reaction of cyt c with the radical (Butler et al. 1982, see also section 2.1.2 and 2.1.1.2), it can be presumed that an increased positive charge could enhance the guidance of superoxide to the heme iron by electrostatic interaction. This would potentially increase the reaction rate of cyt c with superoxide, which could impose a higher sensitivity of a cyt c based biosensor. In the case of cyt c it could be also shown that chemical modification of lysines slows down the reaction rate (Butler, W. H. Koppenol, et al. 1982). Furthermore it is well known that positively charged amino acids like lysines play a key role during recognition and binding of other redox partner proteins like cytochrome c oxidase (Döpner et al. 1999) or sulfite oxidase (Webb et al. 1980).

For this purpose positively charged lysines are introduced into cytochrome c by site directed mutagenesis.

In this work human cyt c was chosen as template protein, although in former work with cyt c electrodes or for studies with superoxide the commercially available horse heart cyt c was used in most cases. The motivation for the human version of cyt c as template protein is the availability of a well established protein expression system in *E. coli* at the Center of Magnetic Resonance (CERM) at the University of Florence (Bertini, Chevance, Turano submitted). It involves the coexpression of a yeast heme lyase which plays a role in the covalent attachment of heme to apocyt c and the coexpression of other *E. coli* cyt c maturation genes (see 3.2.1). Furthermore, it was reported that human cyt c is more stable compared to cyt c of other eukaryotic species like horse and yeast (Olteanu et al. 2003). Besides, human cyt has never been investigated before on gold electrodes or with respect to the reaction with superoxide and other proteins as BOD and human SOX. Thereby, it offers also the chance of comparing not only different cyt c mutants but also the behavior of different cyt c species.

The following criteria were applied during the selection of mutation sites: Neutral or negatively charged amino acids are chosen in order to alter the charge environment to a positive direction. The positions need to be selected near the surface to take advantage of electrostatic interaction, but also in a pertinent location near the heme group allowing proper guidance of the superoxide to a site close to the iron center. One caveat is that the structural integrity and the electrochemical properties, e.g. the redox potential of cyt c, need to be maintained. A further criterion is the fact found in the literature, describing two regions which might play an important role: the left side of the heme edge (Butler, W. H. Koppenol, et al. 1982) (left site in right structure of Figure 19) and a hydrophobic channel framed by the amino acids 51-71 (Butler et al. 1975) (see also 2.1.1.2).

The selection of mutation sites has been conducted iteratively in three rounds. In the first mutation round eight hydrophobic residues have been selected to be replaced with lysine: Tyr46Lys, Ala50Lys, Ala51Lys, Tyr74Lys, Ile75, Gly77Lys, Ile81Lys, Phe82Lys. Furthermore, four positions are chosen to introduce lysines instead of negatively charged glutamic acids and aspartic acids: Glu61Lys, Asp62Lys, Glu66Lys and Glu69Lys. After evaluation of the mutation sites (see 4.1.3 - 4.1.5) further five positions were chosen for a second mutation round: Ile57Lys, Thr63Lys, Asn70Lys, Val83Lys and Ile85Lys. Here also a double mutant was expressed, combining two single mutants with high reaction rate constants determined after the first round (Glu66Lys-Phe82Lys).

Finally, in the last round a second lysine double mutant (Thr63Lys-Glu66Lys) and two single arginine mutants were selected (T63Arg and Glu66Arg). Arginine was chosen to probe the superoxide electron pathway. It is not clear whether superoxide reacts directly with the heme

(so called inner sphere electron transfer) or via tunneling through outer amino acids (outer sphere electron transfer, see 2.1.1.2). That is why the question arises if the enhanced reaction rate with superoxide found for some mutants presents a more effective electron tunnel pathway or is due to electrostatic guidance of the radical to the heme iron. Niki and coworkers could show that the electron transfer of cytochrome c towards the SAM via arginine is 100 times slower than through lysine at position 13 (Katsumi Niki et al. 2003). It can be assumed that if the electrons of superoxide are transferred via the lysines, the reaction rate with superoxide would be also smaller for the arginine mutants.

Fifteen of the selected seventeen single mutations sites are not conserved within the different eukaryotic sequences, thus are supposed to be not crucial for the stable structure of the protein. Just Phe82 and Gly77 are strictly invariant positions in eukaryotic cytochromes c (Pielak et al. 1987).

Figure 19 shows all selected single mutation sites and their position within the human cyt c molecule with different colors with respect to the mutation round. Considering the heme as a disc dividing the molecule in two parts, the mutation sites are concentrated on the left side.

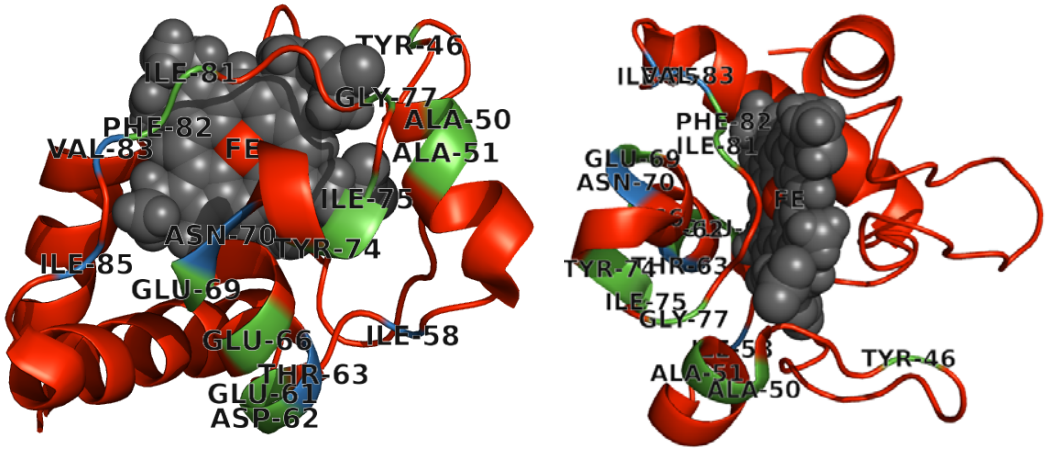

Figure 19 NMR structure of human cyt c with single mutation sites shown as cartoon from two different views. Selected positions of the first round are marked in green and sites of the second round in blue. The heme cofactor is shown as grey spheres with the iron as red sphere. The image was built with the software Pymol (http://pymol.sourceforge.net) using the pdb file 1J3S.

4.1.2 Expression and purification of the mutants

The mutates plasmids were transferred to *E. coli* cells for expression and the cyt c further purified as described in 3.2.1.2. During the first purification step the cell lysate was purified with a cationic exchange column taking advantage of the positive net charge of cyt c at neutral pH. The cyt c protein was eluted using a sodium chloride gradient. In Figure 20 (left) a typical chromatogram of a run with a cationic exchange column is depicted. There are two cyt c peaks

during elution. The first one corresponds to reduced cytochrome c which has a lower net charge (+6.6) compared to oxidized cyt c (+7.1; Trewhella et al. 1988). The fact that the difference is not one unit may be ascribed to the fact that there is an internal relaxation within the protein buffering it. Then with increasing salt concentration oxidized cyt c elutes in a second fraction. Both fractions were pooled and given to a size exclusion column for further purification. Two typical chromatograms of this step are shown in Figure 20 (right), where the cyt c peak is followed by a colorless second peak. This peak can be attributed to apocyt c, thus heme incorporation did not succeed for all expressed cyt c peptide chains. Interestingly the ratio of these two peaks differs for some mutants: whereas for the wild-type the ratio of holocyt c to apocyt c is circa 3.7/1 for F82K for example the peak of apocyt c is much higher (ratio: 1.1/1) indicating a lower efficiency in heme incorporation (red curve in the right diagram of Figure 20).

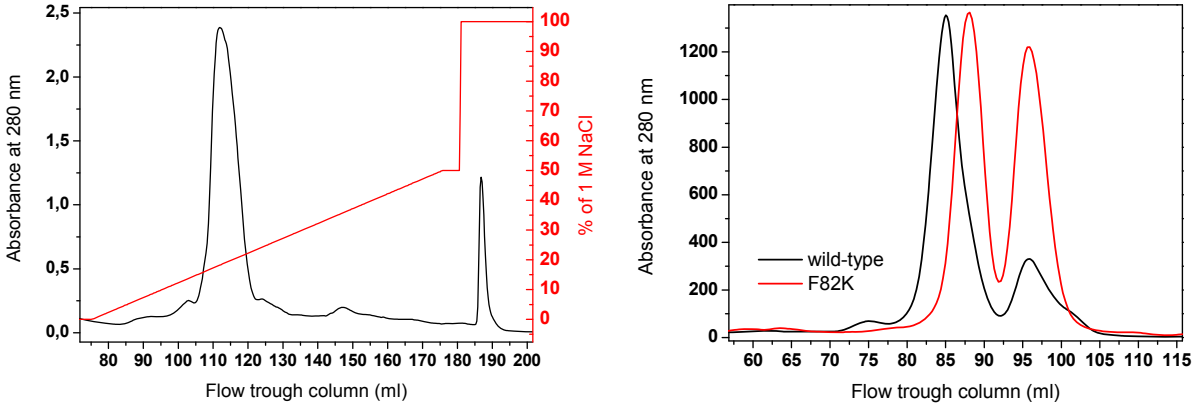

Figure 20 Chromatograms of the two purification steps of wild-type cyt c: cationic exchange chromatography (left) and size exclusion chromatography (right)

After the two chromatography steps pure fractions of cyt c were pooled together and quantity as well as purity were checked with UV-Vis spectroscopy. In addition SDS gel electrophoresis was conducted (Figure 21). The total yield of pure cyt c was in average circa 5 mg/l culture.

From the twenty-one chosen cyt c mutants 20 could be expressed and purified successfully:

- Single lysine mutants: Y46K, A50K, A51K, I57K, E61K, D62K, T63K, E66K, E69K, N70K, Y74K, G77K, I81K, F82K, V83K, I85K
- Double lysine mutants: E66K-F82K, T63K-E66K
- Single arginine mutants: T63R, E66R

Only the single lysine mutant Ile75Lys could not be expressed successfully. In this case folding and/or heme incorporation did not work properly. One reason could be the importance of this rather conservative amino acid to build hydrogen bonds to a catalytically important water molecule (Qi et al. 1994).

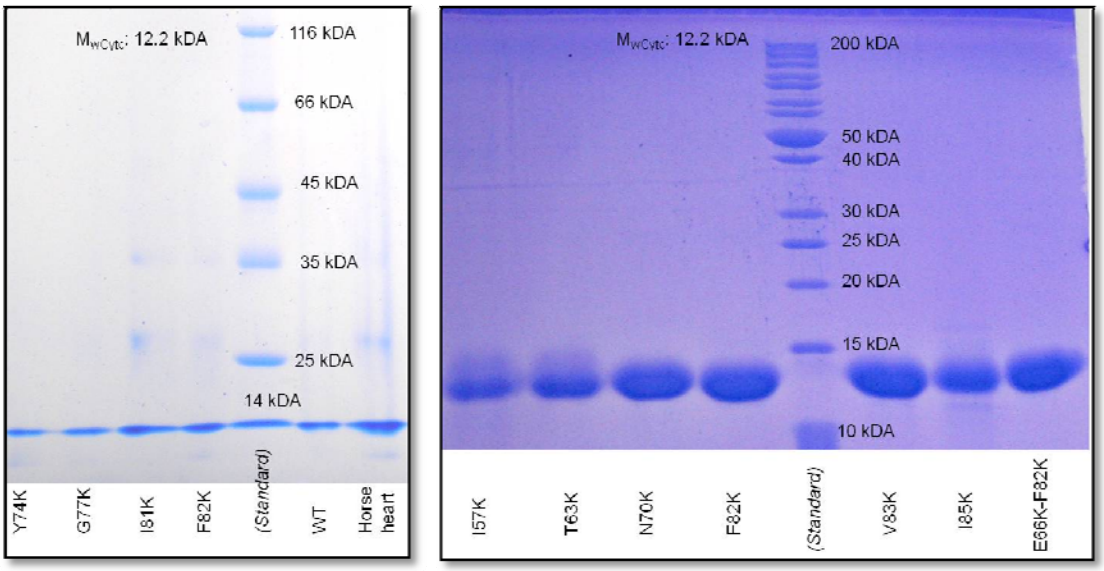

Figure 21 Stained SDS gel of some expressed and purified cyt c mutants

4.1.3 The reaction rate with superoxide in solution

For all mutants, wild type human cyt c and horse heart cyt c, the reaction rate constants with superoxide are determined in solution by recording the cyt c reduction rate at 550 nm in the presence of the superoxide radical. In the left diagram of Figure 22 two kinetic flow curves are plotted, showing different reduction rates for the same cyt c concentration of wild-type and the mutant T63K. These initial rates are then plotted versus the different cyt c concentrations as shown in the right diagram of Figure 22. The slope of these lines divided by the superoxide concentration gave the reaction rate constant k_1 for the reaction of cyt c and superoxide in solution. The rate constants for the mutants differ according to the difference in slopes. The results for all twenty-two proteins are collected in Table 1.

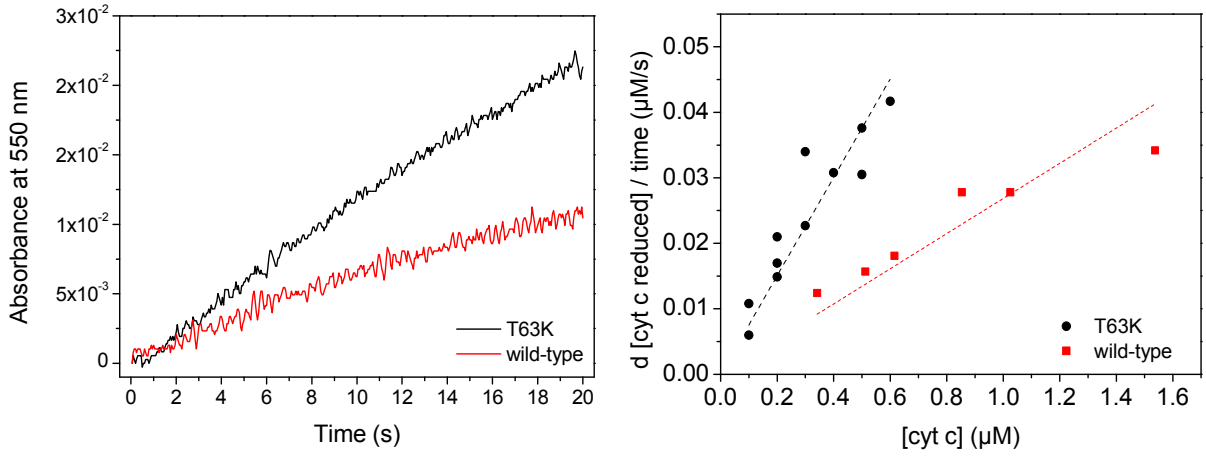

Figure 22 Left: Stopped-flow measurement of 1 µM cyt c in 50 mM sodium phosphate buffer pH 7.5. The absorbance was measured at 550 nm in the presence of 30 mU/ml XOD and 100 µM HX. The values were set to zero at time = 0 s. Right: cyt c reduction rate for different cyt c concentrations

Table 1 Reaction rate constants with superoxide for horse heart, human wild-type and all mutants.

mutant		***reaction with O_2^- in solution***
		$k_1 / 10^4$ (M^{-1} s^{-1})
unmutated cyt c	horse heart	6.7
	human wild type	6.6
single lysine mutants	Y46K	2.5
	A50K	5
	A51K	3
	I57K	2
	E61K	7
	D62K	6
	T63K	11.3
	E66K	12.5
	E69K	8.8
	N70K	6.4
	Y74K	10.7
	G77K	6
	I81K	6.5
	F82K	10.7
	V83K	4.3
	I85K	2.1
double lysine mutants	E66K-F82K	2
	T63K-E66K	1.8
single arginine mutants	T63R	6.4
	E66R	5.3

Horse heart and human wild-type cyt c show nearly the same reaction rate constants of about 7×10^4 $M^{-1}s^{-1}$. The value for horse heart cyt c was also determined by the group of Butler in 1982 (Butler, W. H. Koppenol, et al. 1982) to be 2.6×10^5 $M^{-1}s^{-1}$ which is almost 4 times higher than the value determined in this work. The usage of 100 mM EDTA by Butler et al. may cause this obvious artifact due to the direct reduction of cytochrome c by Fe^{2+}-EDTA (Butler and B. Halliwell 1982). Another contribution might arise from the different sources of superoxide radicals used (pulse-radiolysis).

The four single lysine mutants T63K, E66K, Y74K, and F82K show a higher rate constant for the reaction with superoxide compared to the human wild type (11.3×10^4 $M^{-1}s^{-1}$, 12.5×10^4 $M^{-1}s^{-1}$, 10.7×10^4 $M^{-1}s^{-1}$ and 10.7×10^4 $M^{-1}s^{-1}$, respectively). Figure 23 depicts these amino acids in green for a better visualization. The E69K variant has a reaction rate constant of 8.8×10^4 $M^{-1}s^{-1}$, i.e. only slightly higher than in the case of wild type protein. For several single lysine mutants the reaction rate is not influenced, whereas six mutants (Y46K, A50K, A51K, I57K, V83K and I85K) show a reduced reaction with superoxide. In Figure 23 these mutation sites are marked in blue and orange, respectively. Figure 23 suggests two areas of mutation sites, one with positive effects and one with negative effects (higher and lower reaction rates, respectively). The area with positive effects is clustered at the 60's helix and may be related to a possible access pathway for superoxide, which can guide the radical to the heme group. The proposed pocked lies between the 60's helix (helix-3), the 70's turn and the 50's helix (helix-2) which is further

supported by the fact that for E61K and D62K no enhancement was found. These two amino acids are pointing away from this pocket.

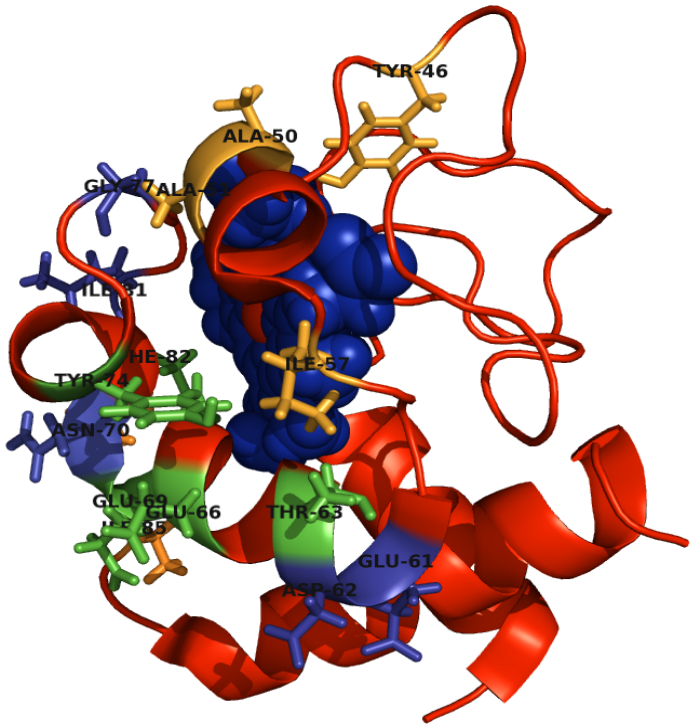

Figure 23 NMR structure of human cyt c with single mutation sites [green, higher reaction rate with superoxide (T63, E66, E69, Y74, F82); orange, lower reaction rate (Y46, A50, A51, I57, V83, I85); blue, reaction rate not affected (E61, D62; N70, G77, I81)]. The mutant E66K with the highest reaction rate with superoxide is marked with a green arrow. The heme cofactor is shown as blue spheres with iron as red sphere. The image was built with the software Pymol (http://pymol.sourceforge.net) using the pdb file 1J3S.

The decrease in the reaction rate with the radical, observed for some mutants, may be due to addition of a positive charge far from the access channel slowing the entrance of superoxide by misguiding the radical. Y46K and I57K have other factors contributing to the decreased reaction rate. This will be discussed in more detail in the following sections of this work.

These results show that the reaction rate of cyt c with the superoxide radical can be enhanced by introducing extra positive charges in form of lysines. However, a further enhancement of the reaction rate by combining "high-rate" mutation sites did not succeed. Both double mutants exhibit a decreased reaction rate with superoxide. Reasons can be various, and further structural and electrochemical characterizations are necessary before conclusion can be made. This is done in the sections 4.1.4 - 4.1.6.

The arginine mutants neither exhibit a higher reaction rate with superoxide nor a huge decrease of the rate constant, which can be a first hint for an outer sphere mechanism or for a less efficient guidance to the heme iron in comparison with the lysine mutants. However, the

effect of another charge distribution can cause several changes, which will be discussed in section 4.1.6 after further characterization of the mutants.

4.1.4 Electrochemical characterization of the mutants

In the following two subsections the mutants are characterized electrochemically in solution and adsorbed on modified gold electrodes. Cyclic voltammetry is a convenient method to determine several relevant properties such as the redox potential, the diffusion coefficient and the heterogeneous electron transfer rate constant.

4.1.4.1 Electrochemical characterization in solution

Information about the thermodynamic and diffusional properties of all 22 cyt c forms has been obtained by electrochemical investigations in solution with mercaptopropanol modified gold electrodes. Here a SAM with short chains was used since the diffusion constant was determined at high ionic strength for comparative reasons and the electron transfer rate for longer chain lengths as for MUA decreases drastically at higher ionic strength and no evaluable cyclic voltammogram can be detected in the range of 20-40 µM cyt c. This can be explained in terms of a shielding effect of the high ionic strength buffer on the electrostatic interaction sites of cyt c and the SAM surface. It has already been shown that electron transfer rates through short alkanethiol chains are independent of the ionic strength of the solution (Avila et al. 2000; Terrettaz et al. 1996).

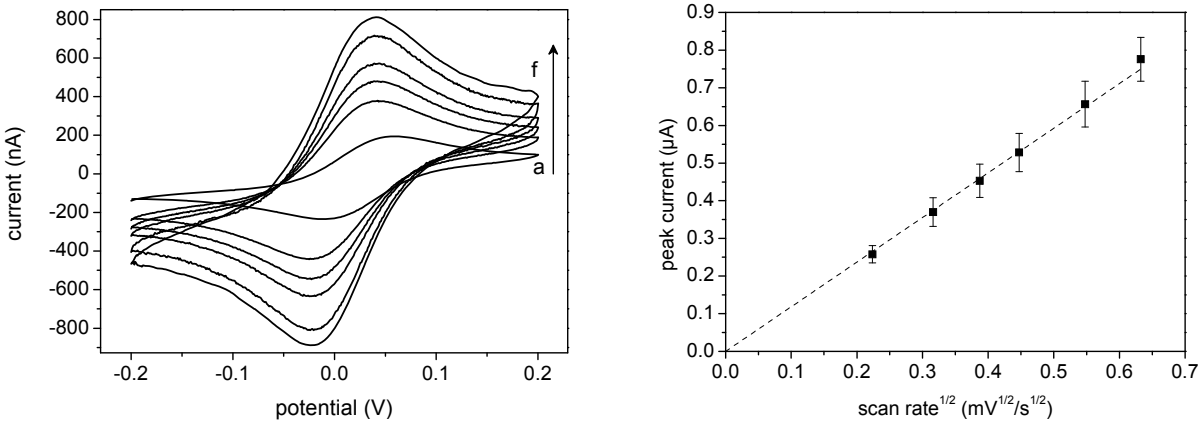

Figure 24 Left: cyclic voltammograms of the mutant T63R in solution (38 µM) with increasing scan rates (a 50, b 100,c 150, d 200, e 300, and f 400 mV/s; 10 mM sodium phosphate, pH 7.0, 1 M KCl with MPA modified gold electrodes). Right: Peak currents vs. the square root of the scan rate for T63R in solution.

Cyclic voltammetry has been performed at different scan rates to deduce the formal redox potential and the diffusion coefficients of the different mutants. All results are summarized in Table 2, and an example of a typical cyclic voltammogram is shown in Figure 24, left. The linear dependence of the peak current on the square root of the scan rate can be obtained, for T63R as example, in Figure 24, right. This dependence is typical for redox active species in solution according to the Randles-Sevcik equation.

Table 2 Electrochemical properties of cyt c in solution. Values were obtained in 10 mM sodium phosphate buffer; pH 7.0, 1 M KCl with MPA modified gold electrodes and a Ag/AgCl/1M KCl reference electrode. Average errors on E_0, and D are 5 mV and 4×10^{-7} cm² s^{-1} mV respectively.

mutant		***Electrochemical properties in solution***	
		E_0 (mV)	D x 10^6 (cm²/s)
unmutated cyt c	horse heart	15	2.3
	human wild type	17	1.7
single lysine mutants	Y46K	-40	0.9
	A50K	13	1.3
	A51K	14	1.9
	I57K	-30	1.8
	E61K	18	3.1
	D62K	13	1.4
	T63K	7	1.9
	E66K	20	1.6
	E69K	11	1.6
	N70K	22	1.3
	Y74K	15	2.6
	G77K	12	1.5
	I81K	18	1.2
	F82K	2	0.4
	V83K	17	1.4
	I85K	18	1.9
double lysine mutants	E66K-F82K	10	0.1
	T63K-E66K	10	0.3
single arginine mutants	T63R	15	3.2
	E66R	24	1.5

The formal redox potential E_0 was calculated as mean of the midpoint potentials between the anodic and cathodic peak potentials at different scan rates (50-400mV/s), since no dependence of the potential on the scan rate was observed in this range. For 17 out of 20 mutants no remarkable influence of the introduced amino acid on E_0 has been observed. However, the formal redox potential of Y46K is -40 mV (±5 mV) versus Ag/AgCl and for a I57K a value of -30 mV (±5 mV) versus Ag/ AgCl was determined which is clearly below the range of the other proteins; hence, the oxidized state of Y46K and I57K gets stabilized by the mutations, probably due to some structural changes in the vicinity of the heme group. This on the other hand diminishes the driving force for the superoxide oxidation and contributes to the low reaction rate constant mentioned in 4.1.3.

A slight decrease of -15 mV for E_0 was observed for the mutant F82K. This suits to the suggestion that the conserved phenylalanine at this position contributes to the hydrophobic

environment of the heme and thereby gives cyt c its large positive redox potential (Pielak et al. 1987). Nevertheless the reaction rate with superoxide is increased for this mutant. A first explanation can be provided by the analysis of the diffusion behavior.

Diffusion coefficients, calculated from the voltammetric measurements are found to be in general above literature values for horse heart cyt c determined electrochemically and with fluorescence recovery after photobleaching (4.7×10^{-7} cm^2s^{-1} in Terrettaz et al. 1996, $8.5\ 10^{-7}$ cm^2s^{-1} in Mozaffari et al. 2009 and 1×10^{-6} cm^2s^{-1} in Gupte et al. 1988). This might be due to the different modification of the gold surface and the lower temperature during the experiments in the literature. For human cyt c a slightly lower diffusion coefficient compared to horse cyt c was determined. The data in Table 2 also reveal that the diffusion coefficients vary among the mutants. E61K and T63R show a 1.7 fold increased value compared with the wild-type, whereas F82K has a four-fold decreased diffusion coefficient with respect to the wild type; the experimental error is approximately 20 %. These variations can be explained by small conformational changes caused by the mutations and thus a change in the solvent accessible surface area (Penna et al. 2007). For F82K an increased surface area could be due to a less compact structure and cause a better accessibility of the heme for superoxide. This can be an explanation for the increased reaction rate although a slightly decreased formal redox potential was observed. Also for Y46K a smaller diffusion coefficient was determined. However, for the reaction with superoxide obviously the reduced E_0 has a larger influence on the rate constant. A remarkable decrease of the diffusion coefficient was also observed for both double mutants. For E66K-F82K it seems that the mutation of F82 causes the decrease of D like it was observed for the single mutant. However, at this point it is still unclear whether the less compact structure, which was also observed for the mutant T63K-E66K, can be related to the decreased reaction rates with superoxide measured for both double mutants. Further structural investigations are necessary and will be discussed in section 4.1.6.

4.1.4.2 Mutants adsorbed on gold electrodes

The thermodynamic and kinetic properties of horse heart, human wild type, six single lysine mutant forms of cyt c, which reveal a higher radical reaction rate constant, together with the two double mutants and the two arginine mutants, have been characterized electrochemically, while the protein is adsorbed on a promoter modified gold electrode. In this way for the five single lysine mutants, with the highest reaction rate with superoxide, also the possible usage as a recognition element in a biosensor for the detection of superoxide was investigated.

First, all chosen mutants can be adsorbed on the negatively charged mercaptoundecanoic acid/mercaptoundecanol (MU/MUA) layer. Figure 26 (left) demonstrates that the cyclic

voltammograms of the mutants are similar to those achieved with the wild type. The behavior is also studied kinetically and the values for the formal potential and the heterogeneous electron transfer rate constants (k_s) are presented in Table 3. The formal potential E_f was calculated as mean of the midpoint potentials between the anodic and cathodic peak potentials at low scan rates (where no change of E_f could be observed). For two cyt c forms the plot of k'_s vs. scan rate is depicted in Figure 26 (right). The rather similar redox properties and surface coverage of the five lysine mutants with the highest reaction rate, compared with the values for the wild type and horse heart cyt c, are promising for a sensor application.

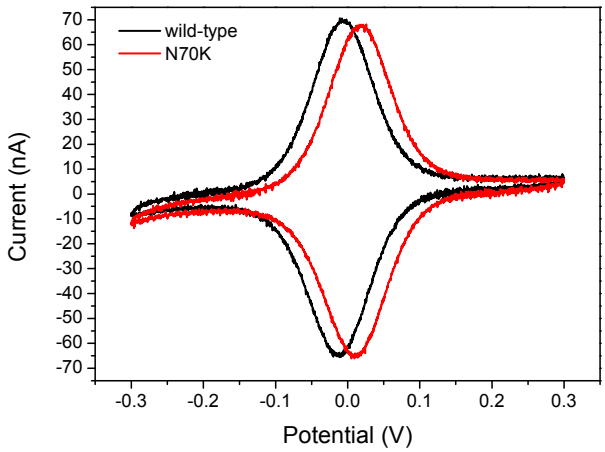

Figure 25 Cyclic voltammograms of the mutant N70K and human wild-type cyt c adsorbed on MUA/MU modified gold electrodes (5 mM sodium phosphate, pH 7, scan rate 100 mV/s).

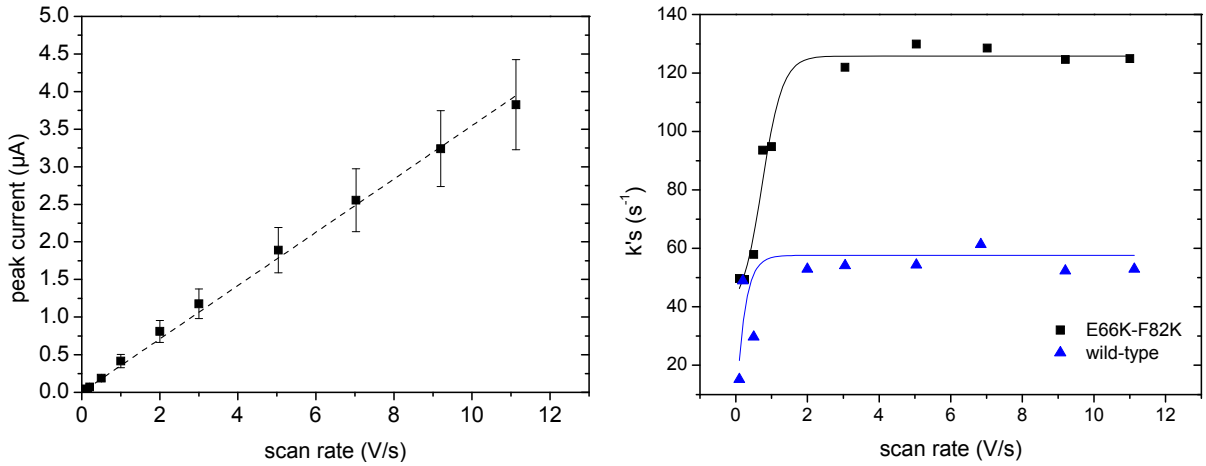

Figure 26 Left: peak currents of wild-type cyt c on MUA/MU modified gold electrodes at different scan rates. Right: Plot of k'_s vs. scan rate for human wild-type cyt c and the mutant E66K-F82K, lines represent a Boltzmann fit, k_s values correspond to the plateau of these lines. (5 mM sodium phosphate, pH 7)

However, a more detailed evaluation of the determined values reveals some differences. The formal potential of all cyt c forms lies in general below the formal redox potentials of the solution state cyt c. This can be explained by the electrostatic stabilization of the more positive

oxidized state over the reduced state of immobilized cyt c due to the negatively charged SAM surface which was observed also in other work (Battistuzzi et al. 2007). The slight decrease of the formal potential of the mutant F82K corresponds to the slight decrease observed also in the solution state. On the other hand for three mutants the change of E_f does not reflect the differences found in solution.

Table 3 Electrochemical properties of cyt c adsorbed on MUA/MU modified gold electrodes. Values were obtained in 5 mM potassium phosphate buffer, pH 7. Average errors on E_f, Γ, k_s, and $Ew_{1/2}$ are 5 mV, 3 pmol/cm², 8 s^{-1} and 5 mV respectively.

mutant		***Electrochemical properties adsorbed on modiefied Au electrodes***			
		E_f (mV)	Γ (pmol/cm²)	k_s (s^{-1})	$Ew_{1/2}$ (mV)
unmutated cyt c	horse heart	-7	13	55	102
	human wild type	-8.6	10.7	61	101
single lysine mutants	T63K	-9.5	9.1	47	97
	E66K	1	12	55	109
	E69K	2	11	47	106
	N70K	9.1	10.3	45	101
	Y74K	0	7	113	97
	F82K	-19	6	139	96
double lysine mutants	E66K-F82K	3.6	3.8	125	91
	T63K-E66K	7.5	2.8	27	141
single arginine mutants	T63R	-14.8	5.6	68	110
	E66R	-1.4	6.9	60	125

N70K and the double mutant T63K-E66K reveal a slight increase of E_f compared with the wild-type. In case of the double mutants T63K-E66K this could be attributed to a less effective electrostatic stabilization of the oxidized state due to a different orientation of the protein. The orientation of adsorbed cyt c on negatively charged SAMs, proposed by (J. Xu et al. 2006) is depicted in Figure 27. Both exchanged amino acids of the double mutant - E66 and T63 - are normally not "visible" for the electrode. In the case of the introduced positively charged lysines it is reasonable that the two charges cause a different orientation. This can be supported also by the decreased electron transfer rate k_s and the increased half peak width $Ew_{1/2}$ determined for this mutant. The different orientation can cause a less effective heterogeneous electron transfer, probably due to a larger distance between the heme and the electrode. Also the smaller amount of protein which could be adsorbed on the electrode for these mutants supports the described altered situation.

For N70K the increased formal potential without any other significantly changed feature, might be due to local structure changes in the heme environment, which occur only after immobilization of the protein.

A smaller amount of redox active protein could be immobilized on the electrodes for F82K, E66K-F82K, T63K-E66K and the two arginine mutants. Here probably the binding efficiency of the second binding region containing the residues 73, 79, 87 and 88 (J. Xu et al. 2006; Davis et al.

2008) is diminished due to the mutations near this region. In the case of the mutant F82K with a higher reaction rate the decreased surface coverage can be a disadvantage for a sensor application, since the amount of immobilized recognition elements limits the sensitivity.

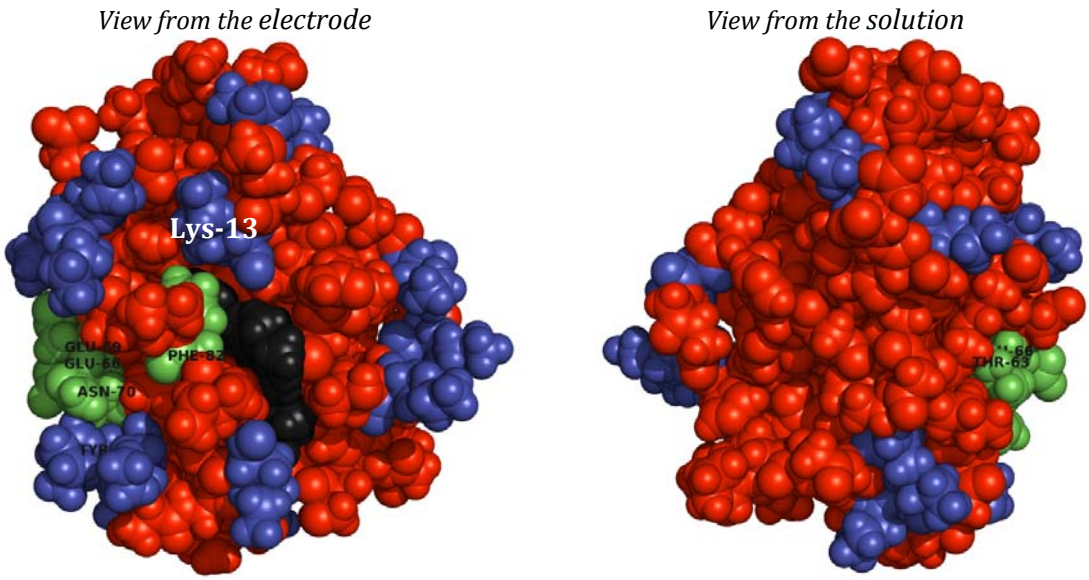

Figure 27 Orientation of cyt c immobilized on SAM modified electrode according to (J. Xu et al. 2006). Hemes are depicted as black, mutation sites as green spheres. Blue spheres represent positively charged lysine residues. Left: view from the electrode. Right: view from the solution.

A two-fold increase of the electron transfer rate constant k_s is found for Y74K, F82K and E66K-F82K. It was suggested that the lysine residue K13 plays an important role for the ET to the SAM-Au electrode (Katsumi Niki et al. 2003; Katsumi Niki 2002). Figure 27 shows the close proximity of this residue to F82K. One might speculate that a positively charged lysine at position 82 allows an even closer approach of the protein's face (including K13) to the negatively charged SAM surface and thereby facilitates electron transfer. Structural changes may also be responsible for the observed effects. This point is discussed in 4.1.6.

The increased electron transfer rate found for Y74K may also be related to the influence on the structure of the 70's loop, which is part of the second binding region to the SAM mentioned above. Similar to the effect of nitration of Y74 in human cyt c this loop could get more flexible (García-Heredia et al. 2010) and thereby permit a closer approach of the heme to the surface.

For a potential superoxide sensor the investigations of the immobilized state show no hindrance for the construction of the sensor electrodes for all mutants with a higher reaction rate apart from F82K, where the smaller surface coverage might be a disadvantage.

4.1.5 Spectroscopic UV/VIS characterization

Table 4 summarizes the results of mutant characterization by UV/VIS spectroscopy and the spectra of two cyt c forms are depicted in Figure 28.

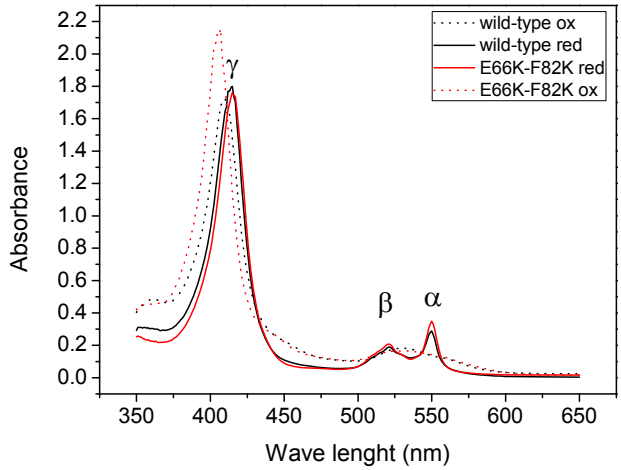

Figure 28 UV/VIS spectra of the reduced (line) and oxidized (dotted line) wild type (black) and the mutant E66K-F82K (red), 5 µM protein sample in 50 mM sodium phosphate buffer pH 7.5.

Table 4 Spectrophotometric properties of wild type and variant forms of human cyt c (50 mM sodium phosphate buffer pH 7.5)

mutant		***spectrophotometrical properties***		
		max γ ox (nm)	max γ red (nm)	max α red (nm)
unmutated cyt c	horse heart	409	415	550
	human wild type	410	415	549
single lysine mutants	Y46K	406	415	549
	A50K	410	415	549
	A51K	408	415	549
	I57K	409	416	550
	E61K	410	415	549
	D62K	410	415	549
	T63K	410	415	550
	E66K	410	415	549
	E69K	410	415	549
	N70K	409	416	550
	Y74K	407	415	549
	G77K	410	415	549
	I81K	410	415	549
	F82K	406	415	549
	V83K	410	415	550
	I85K	407	417	550
double lysine mutants	E66K-F82K	406	415	550
	T63K-E66K	409.5	416	550
single arginine mutants	T63R	409	415	550
	E66R	410	416	550

It can be noted that almost all mutants show the typical absorption maxima in the reduced state (Soret (γ), alpha, and beta bands) at the same wavelength as the wild type cyt c. The

gamma band in the oxidized state slightly varies among a few mutants. Five variants (Y46K, Y74K, F82K, I85K and E66K-F82K) show hypsochromic shifts like E66K-F82K (Figure 28) consistent with a slight change in the heme group environment toward the non-polar direction. Here, obviously some structural changes near the heme group occur upon mutation.

4.1.6 Summary of the observed mutant properties and their possible explanation using NMR investigations and energy minimization calculations

Significant differences in the reaction rate with superoxide, the formal redox potential, the diffusion constant and the behavior at SAM coated electrodes were found for a number of the human cyt c mutants characterized. The hypsochromic shifts of the γ bands in the UV-Vis spectra found for some mutants in the oxidized state already indicate that mutation can cause a structural change of the cyt c molecule, which can be a reason for the observed changes compared to the wild-type. In order to rationalize the observed behavior mono-dimensional ^{1}H NMR as a fingerprint to check the integrity of the iron-Met80 bond in the entire series of expressed mutants was performed by Prof. Paola Turano in the Magnetic Resonance Center of the Univerity of Florence (Italy) where the author of this thesis has also expressed and purified all cyt c mutants. For the most significantly affected mutants the folding was also studied in both redox states using two dimensional ^{1}H-^{15}N HSQC NMR.

Single lysine mutants

The single lysine mutants represent the first focus within this discussion. For the two single lysine mutants Y46K and I57K the decreased reaction rate with superoxide is related to the reduced formal redox potential which diminishes the driving force for the oxidation of superoxide. A structural change in the heme environment is hence likely. Slight shifts in the UV/VIS spectra could provide a first confirmation. However, there are larger shifts for the mutant Y46K where a lysine residue replaces the aromatic Tyr46, a rather conserved sequence site of cyt c (Pielak et al. 1987). Also the diffusion coefficient is reduced for this mutant. The two dimensional ^{1}H-^{15}N HSQC NMR spectrum suggests an induced partial unfolding of the human cyt c structure of this mutant, as indicated by the appearance of broad resonances in the random coil and collapse of several of the Gln/Asn side chain resonances in the spectra of both the ferrous and the ferric forms (Appendix A1, A2). The ^{1}H NMR spectrum of the ferric Y46K protein (Appendix A3) displays only slightly altered chemical shift patterns for heme methyl resonances and Met80 side chain, but all the hyperfine-shifted resonances are much broader than for the wild type protein, consistent with a conformational equilibrium. Partial unfolding of the

structure could account for the observed reduction in the diffusion coefficient and formal redox potential (Gunner et al. 1991), while the decreased reaction rate may be correlated to a partial disruption of the structure which affects the entrance of superoxide, in addition to the diminished driving force for superoxide oxidation due to the lower E_0 value.

In contrast to Y46K there are indications that for two mutants (Y74K and F82K) a changed tertiary structure has an influence on the enhancement of the reaction rate with superoxide.

The increased reaction rate with the radical for F82K is accompanied by a slightly decreased formal potential in solution and in the adsorbed state. Furthermore the diffusion coefficient as well as the immobilization efficiency in the adsorbed and covalently attached state are decreased and a higher electron transfer rate in the adsorbed state and hypsochromic γ band shifts in the UV-Vis spectra could be observed. In literature one can find a hint that underlines the structural importance of the strictly invariant Phe at position 82 in cyt c: Greene and coworkers observed a destabilizing effect (20%) with a different mutation at the same position (F82Y) in the yeast form of cyt c (Greene et al. 1993). Indeed, the NMR investigations reveal greater structural changes for this mutant: The ferrous F82K has a ^{1}H-^{15}N HSQC spectrum that shows only subtle chemical shift variations for residues located in the proximity of amino acid 82 on the distal site (see the local environment of F82 in Figure 29 and Appendix A4). However, the spectra of the ferric form of F82K indicate occurrence of larger changes. Chemical shift variations in the ^{1}H-^{15}N HSQC spectrum (Appendix A5) are observed for backbone amides of essentially all protein residues and additionally in the ^{1}H NMR spectrum on the full spectral width (Appendix A6); neither the heme methyl signals above 30 ppm nor the Met80 upfield signals are visible. The ^{1}H chemical shift pattern of heme methyl substitutions in low spin ferri-heme proteins reflects the nature and the relative orientation of axial ligands (Bertini et al. 1999); the spectral features of the oxidized protein suggest important structural changes for the ferric form of F82K. A different axial ligation only in the oxidized state is very likely, but the change in E_0 compared to the wild type remains rather small. Inspection of the wild type protein structure suggests Lys82 would hang from the 80´s loop, with its positive end in proximity to the heme iron. The combined effect of electrostatic repulsion between the ferric center and Lys82 with the intrinsically lower stability of the bond between the Met80 sulfur and iron(III) (Berners-Price et al. 2004; Winkler et al. 1997; Turano 2004) may cause an opening in the mutant structure, allowing better access to the heme center for electron transfer and superoxide interaction, compared to the wild type. In addition, this conformational change may also be responsible for the lowered covalent coupling efficiency of the protein NH_2-groups with carboxylic groups on the modified electrode surface found during sensor investigations, and the diminished diffusion coefficient.

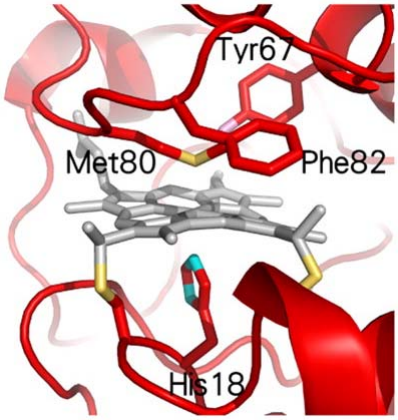

Figure 29 Structural environment of Phe82 in wild-type human cyt c (NMR structure, pdb file 1J3S), the heme group is presented as grey sticks, sulfur atoms of the side chains are marked in yellow and nitrogen atoms of Hi18 in blue.

Substitution of Tyr74 (on helix-4) with Lys slightly affects the chemical shift values of residues on helix-3 and on the facing helix-2 in both the ferric and ferrous forms. Introducing a positive charge at position 74 may induce electrostatic repulsion on the existing Lys55 on helix 2, whose side chain points toward the helix-3 (60's helix) and may induce ionic interaction with the negatively charged Glu 66 (Figure 30). Both could provide a facilitated entrance to the pocket for the path of superoxide to the heme iron. Additionally two structural water molecules in the horse heart x-ray structure are found to be hydrogen bonded to the ring hydroxyl of Tyr74 (Qi et al. 1994). Hence a mutation of this site may diminish hydrogen bonds to this water and cause small structural changes.

No differences can be observed in terms of axial ligation, even in the ferric form. Consistently, smaller property changes compared with F82K are found. However this region might be also important for the cyt c peroxidase activity, which is found to be increased with this mutant (see 4.2.2.2). In recent literature it could be shown that the exchange of another very closely situated tyrosine Y67 with a positively charged arginine led to an increased peroxidase activity (Ying, Z.-H. Wang, et al. 2009). Therefore one might also speculate that changes in this region are involved in the induced peroxidase activity of cyt c after binding to cardiolipin in the inner mitochondria membrane which might also be related to the apoptotic pathway in mitochondria (see literature section 2.1.1.1).

For the two mutants with the highest reaction rate with superoxide - T63K and E66K – none of the electrochemical properties or the UV-Vis spectra were changed compared to the wild-type. The ^{1}H-^{15}N HSQC spectra of T63K and E66K are essentially superimposable with those of the wild type protein in both oxidation states (Appendix A7-A10). In addition, the ^{1}H spectrum over the full spectral width for the ferric forms is identical to that of the wild type protein (Appendix A11-A13). Such an invariant signature is indicative of an intact structure.

Consistently, the formal redox potential, the surface coverage of the covalently fixed protein, as well as the electron transfer kinetics are not changed compared to the wild type. The increased reaction rate with superoxide is therefore attributable to a real electrostatic guidance. As it is apparent from Figure 30 in these cyt c variants the replacement of the neutral and negatively charged amino acids with a positively charged lysine occurs in a solvent exposed position and relatively far from the heme. It is therefore proposed that the observed positive effect is related to the good accessibility for the superoxide anion and thus can help to attract the radical to this protein region in a more efficient way.

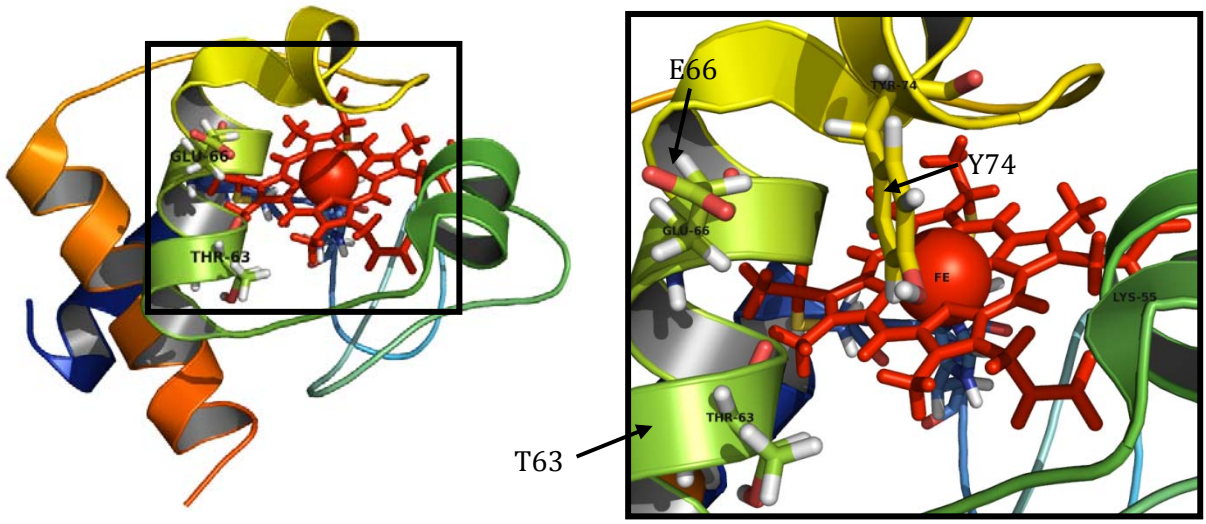

Figure 30 Proposed pocket for the reaction of superoxide with cyt c. Left: location of the pocket in the molecule. Right: close up of the pocket. Colors: blue – helix-1; dark green – helix-2; light green – helix-3; yellow - hydrogen bonded turn; orange – helix-4.

Taking together all positive and negative effects on the reaction rate for all exchanged amino acids - where structure changes are not involved (no shifts in the NMR spectra) - one can identify a positive-effect region (see Figure 23 and description in section 4.1.3). Hence, it can be concluded that the pocket presented here in Figure 30 represents a kind of access region for the superoxide radical. This is also consistent with three literature suggestions: It was proposed that this region represents a possible pathway for the electron transfer from and to cyt c in general (Dickerson et al. 1971) and also in the special case of superoxide it was suggested that this pocket play an important role (Butler et al. 1975) and that the reaction site may be situated on the left site of the molecule (in Figure 23) with respect to the heme group (Butler, W. H. Koppenol, et al. 1982) (see also section 2.1.1.2).

Potential implications for the mechanism of the reaction of superoxide with cytochrome c

Although it could be shown in this thesis that additional positive charges in the mentioned putative superoxide reaction pocket can enhance the reaction rate with cytochrome c due to electrostatic guidance, it cannot be concluded what the reaction mechanism in detail is. One can propose two general possibilities: an inner and an outer sphere mechanism. In the case of an inner sphere mechanism superoxide would react directly with the heme or the heme iron and the pocket in Figure 30 could represent a channel for the superoxide radical towards the heme or the heme iron. Also the superoxide dismutase (SOD) has a channel which guides the radical towards the copper so that the inner sphere reaction takes place (see 2.1.2). However, the copper site in SOD is less buried under the protein's solvent accessible surface than in the case of the heme iron (see Figure 8 in section 2.1.2), and as described in section 2.1.1.2 there are also hints for the outer sphere reaction of superoxide via a tunneling mechanism. In this context the mentioned pocket could also represent a kind of tunneling pathway through the heme. The introduced lysine residues could attract the superoxide radical towards this region and increase in this case the probability for the tunneling event.

Inside the pocket three evolutionary conserved (Pielak et al. 1987) aromatic residues including one tryptophane and two tyrosines can be found (Figure 31), which could provide also conditions for tunneling via an electron-hopping pathway with W59, Y67 and Y74 as possible hopping step stones. A putative role of these three amino acids for the reaction of cyt c with superoxide was already suggested before (Butler et al. 1975).

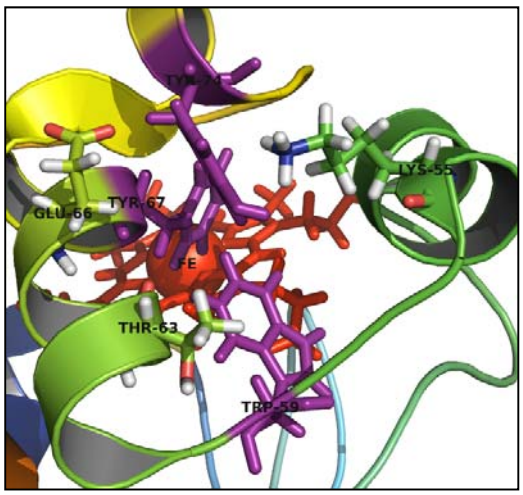

Figure 31 Position of three aromatic residues in purple (Trp59, Tyr67 and Y74) inside the putative superoxide reaction pocket of human cyt c (figure created with Pymol and pdb file 1J3S).

The triad of aromatic amino acids (Y74-W59-Y67) can be compared for example with a similar triad found in the R2 subunit of class I ribonucleotide reductases (Reece et al. 2005).

Since it was shown that also methionines can act as stepping stones in multistep electron hopping (M. Wang et al. 2009) Met80 in the case of cyt c might also play a role in the electron transport chain, reducing the heme iron since it is very close to Y67 (Figure 32). A possible pathway could be like follows: Y74 → W59 → Y67 → M80 → Fe^{3+}. The positions of these amino acids are highly conserved and a comparison between horse heart and human cyt c NMR structures with respect to the mentioned residues is presented in Figure 32, which shows that the amino acids are almost superimposible for both species.

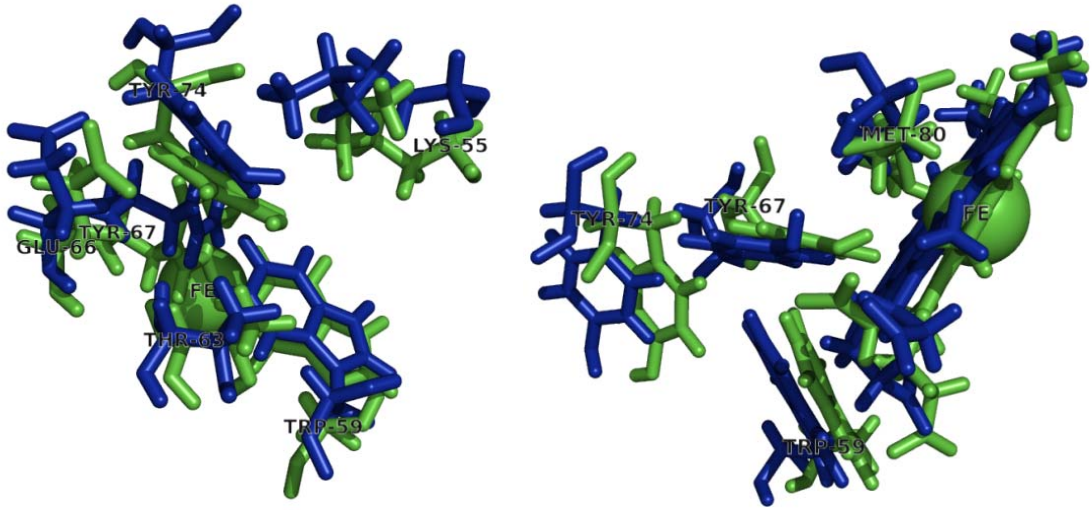

Figure 32 Superposition of the positions of amino acids putative important for the reaction of superoxide with cyt c in two different views (blue – human cyt c; green – horse heart cyt c).

The role of a multistep tunneling mechanism involving tyrosine and tryptophane has been discussed for several biological electron transfer processes and often proton coupled electron transfer (PCET) is related to these reactions (Cordes et al. 2009; Shih et al. 2008). From the crystal structure of horse heart cyt c it is known that between W59 and Y67 a buried water molecule is situated having a hydrogen bond to Y67, and hydrogen bonds between Y67 and the iron ligand M80 as well as between the heme and W59 were observed (Bushnell et al. 1990) (Qi et al. 1994). These hydrogen bonds could be involved in a putative PCET from superoxide to cyt c. Often also basic groups, such as the side chains of lysine or histidine, are generally available around active sites (including aromatic amino acids) with hydrogen bonds to them to support the PCET mechanism in redox proteins (Reece et al. 2005; Supporting Information in Chen et al. 2009; Pond et al. 2001). In human cyt c Lys55 is situated in direct neighborhood to Tyr74 (Figure 31), probably forming a hydrogen bond to it and thereby may support the PCET. Also the lysines in T63K and E66K may have in addition to their supporting role for the electrostatic attraction of superoxide also a PCET supporting effect. In a recent published work a base assisting proton regulated electron-hopping was suggested for the electron transfer from

tyrosine to tryptophane with a basic group accepting a proton from the phenol group during electron transfer to tryptophan (X. Chen et al. 2009). One might speculate that the mentioned lysine residues in cyt c might also be involved in such a mechanism with Tyr74 as proton donor.

Single arginine mutants

The prepared arginine mutants T63R and E66R are dedicated to elucidate the electron transfer mechanism from superoxide to the heme iron. As described above, basic amino acids near the reaction pocket might conduct electrostatic attraction and/or support proton regulated or coupled electron hopping via the aromatic amino acids inside the pocket.

Since arginine has a different charge distribution (Figure 33 left) they will have on the one hand different electrostatic features but on the other hand might alter also the hydrogen bond network and thereby the tunneling efficiency.

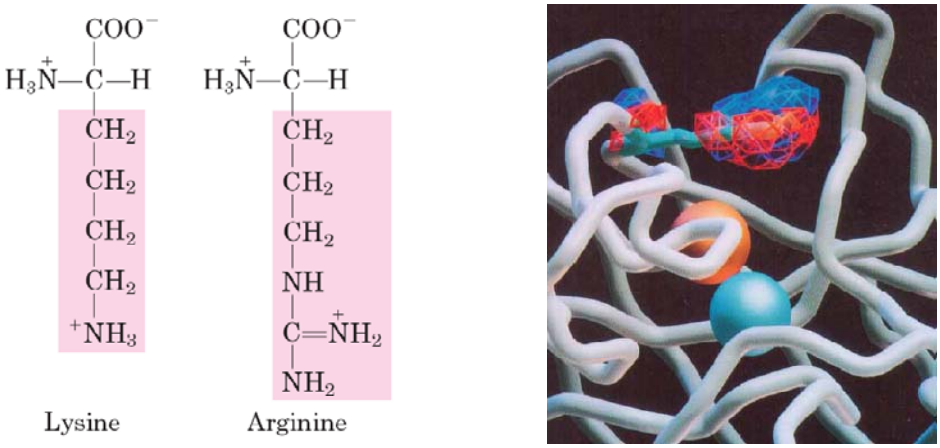

Figure 33 Left: Structural formula of lysine and arginine. Right: Difference grid between the electrostatic potentials of the wild-type SOD (red) and R143K mutant enzyme (blue), illustrating the specific local differences in the distribution of positive potential near the active site. Excess positive potential in the wild-type enzyme, which occurs directly adjacent to the superoxide binding site, is indicated by red shading, excess positive potential in the lys mutant, which occurs away from the superoxide binding site, is indicated by blue shading. The enzyme fold (white tubes) is shown with the Arg-143 side chain (blue tubes), the copper ion (orange sphere) and the zinc ion (blue sphere) (Fisher et al. 1994).

Niki and coworkers could show that the electron transfer from cytochrome c towards SAM modified electrodes via arginine is 100 times slower than through lysine at position 13 (Katsumi Niki et al. 2003). In this thesis the mutants E66R and T63R did not show an increased reaction rate with superoxide, while for both mutants one and two dimensional NMR did not show any significant structural change compared to the wild type. However, ^{1}H ^{15}N HSQC NMR revealed some minor shifts comparing T63K and T63R confining to residues 52, 56, 57, 59, 66, 67, 69 and 74 (Appendix A9, A10), which include the above discussed aromatic residues in the proposed

pocket. But they are too small to provide evidence for any structural change. Despite the influence on the electronic coupling mechanism less effective electrostatic guidance for the arginine mutants might play also a role for the moderate reaction rate constants. To explore the role of the surface potential for the electrostatic attraction Andrea Giachetti from the University of Florence conducted some energy minimization calculations. In Figure 34 the surface potentials of the four mutants compared with the wild-type cyt c are presented.

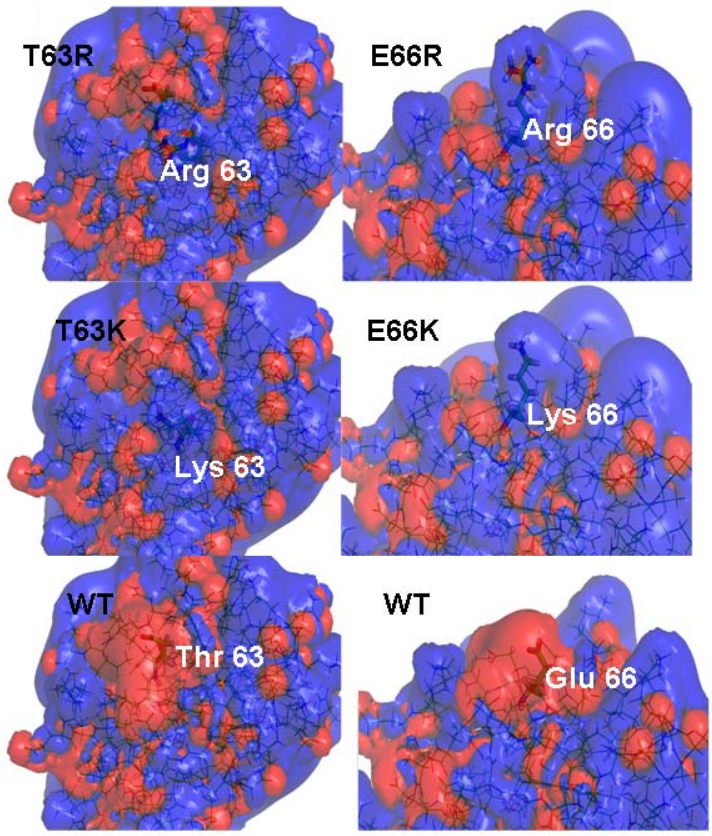

Figure 34 Surface potential representation of the area around residue 63 (left) and 66 (right) in human cyt c: regions where the electrostatic potential is <-1 kT are red, while those >+2 kT are blue (k, Boltzmann constant; T, absolute temperature). The wild-type, lysine and arginine variants are represented in the bottom, middle and top panels, respectively. The residues at position 63 and 66 are shown as sticks and visible in transparency. The residue label has been added at the terminal part of the side chains, to show its orientation. The structures in the left and right panels have different orientations, to better show the involved protein surface area.

It can be observed that for both positions the lysine residues are a little bit more effective in reducing the negative charge patch than the arginine mutants. Although the magnitude of the differences observed for the reaction rate is rather small, the differences for the surface potential in Figure 34 do not provide an adequate explanation for the differences found for the reaction rate constants. This puts the focus also to local electrostatics and the hydrogen bond network.

Due to its different charge distribution compared with lysine, arginine could induce a different direction of the induced electrostatic field. Calculations providing the direction of the field vectors could help to investigate this hypothesis. For the Cu,Zn SOD it was also shown that the exchange of the arginine 143 with lysine at the same position directly situated above the copper ion (Figure 33 right) causes a 2-fold drop of the reaction rate (Fisher et al. 1994). A different charge distribution compared with lysine was calculated and it was concluded that arginine contributes to the local electrostatic environment necessary for binding superoxide and/or facilitating proton transfer from solvent.

In addition to the different charge distribution of the two amino acids, it is known that arginine is able to form multiple hydrogen bonds and may thereby change the hydrogen bond network of the pocket in a different way as lysine does. This might influence the PCET. In the case of the arginine mutants, a supporting hydrogen bond - like it might be induced by the lysine mutants - may not be created and hence, rates comparable with the wild-type were measured. This would underline the importance of the local amino acid architecture in case of an outer sphere electron transfer mechanism for superoxide with cyt c.

Another example for the importance of the type of positive amino acid near catalytic redox centers could be shown for the R481K mutant of cyt c oxidase. It was demonstrated that the exchange of arginine with lysine in the vicinity of the heme propionates can even cause a different redox potential and a different behavior for the electron and proton transfer (Mills et al. 2005).

Double lysine mutants

Finally the effects of the two double mutants will be discussed. In both cases the reaction rate could not be further enhanced compared to the single mutants. The rate constant was even clearly decreased compared to the wild-type. For the mutant E66K-F82K ^{1}H NMR spectra revealed the same structural changes as found for the single F82K mutant (Appendix A14). Regarding the electrochemical properties as k_s, D and Γ as well as to the UV/VIS spectra, the same changes were observed. However, this does not explain why these far from each other situated amino acids which reveal enhanced rates in the single mutant form, exhibit a decreased reaction rate in the double mutant form. One can think of a possible “competition” of the two positively charged residues which results in an ineffective electrostatic guidance.

For the mutant T63K-E66K ^{1}H and ^{1}H ^{15}N HSQC NMR show clearly that there are no structural changes compared to the wild-type (Appendix A15-A120). However, in addition to the slow reaction rate several electrochemical and UV/VIS parameters are changed, which did not occur in the single mutant forms: decreased D, Γ and k_s, increased $Ew_{1/2}$ and hypsochromic shifts

of the γ bands in the UV-Vis spectra. Whereas the changes for the adsorbed cyt c can be related to a different orientation induced by the two extra charges, the decreased reaction rate and the diffusion coefficient remain to be explained. For this purpose Andrea Giachetti has calculated the electrostatic potential of this double mutant, presented in Figure 35.

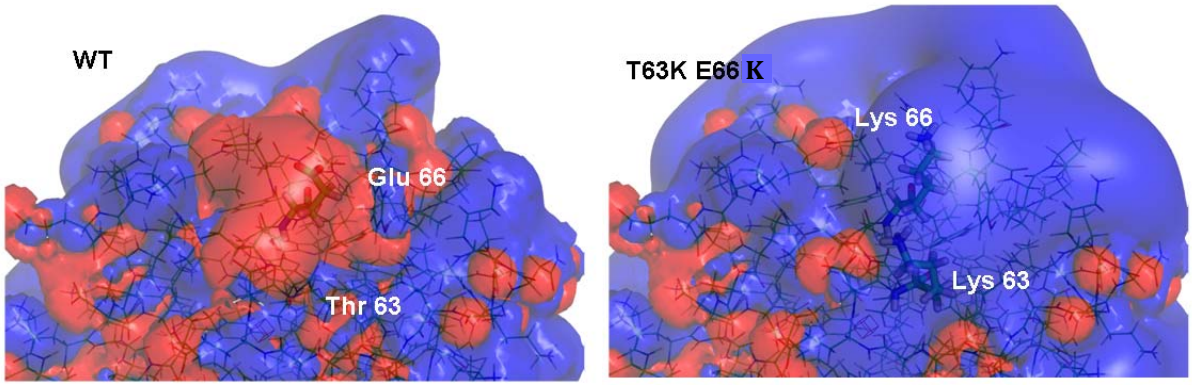

Figure 35 Surface potential representation of the area around residue 63 and 66 in human cyt c: regions where the electrostatic potential is <-1 kT are red, while those >+2 kT are blue (k, Boltzmann constant; T, absolute temperature). The wild-type and the T63K-E66K variant are represented in the left and right panels, respectively. The residues at position 63 and 66 are shown as sticks and visible in transparency. Residue labels have been added at the terminal part of the side chains, to show their orientation.

It can be seen that for the double mutant the charge distribution is significantly altered compared to the wild-type: A very large and rather uniform positive area is supposed to be formed which does not occur for the two single mutants. In the single mutant there can be still seen a sort of "negative ring" surrounding the putative pocket (Figure 34), while in the double mutants there is an ample positive area that may misguide the anion. This can be an effect of a rearrangement of the side chains and the combined effect of two positively charged residues. Apparently superoxide as a mobile, negatively charged, small radical cannot be directed anymore efficiently towards the pocket. Also in literature for double mutants of SOD in the active site channel, a non trivial additive effect due to a charge rearrangement was observed (Polticelli et al. 1995).

In conclusion the reaction rate between cyt c and superoxide can be enhanced by introducing positively charged lysines at certain positions. Structural changes represent one of the reasons for the enhanced reaction rate. When the structure is retained the charge distribution is an important factor. Two positions are found where the enhancement for the reaction rate can be explained by electrostatic guidance to this protein area: T63K and E66K. The region, defined between the 60's helix, the 70's loop and the 50's helix, is suggested to be a possible access area for superoxide. This pocket includes also three aromatic amino acids,

representing potential stepping stones for a multistep electron hopping process, which might be further supported by extra hydrogen bonds provided by the basic groups of the lysines. For the electrostatic guidance the type of amino acid used for the introduction of the additional charge is important. Arginine mutants did not result in an enhanced interaction, probably due to the different charge distribution. However, when the charge is changed in such a way that a very large area of the protein is positively charged, as in case of the double mutant T63K-E66K, then electrostatic misguiding can result in a decrease of the reaction rate. This demonstrates the importance of electrostatic effects for the reaction of superoxide as factors contributing to an efficient electron transfer. Furthermore, these investigations are also a hint for an evolutionary conserved superoxide reaction pathway which might have relevance regarding the proposed role of cyt c as ROS scavenger *in vivo* and as inducer of the apoptotic pathway (see 2.1.1.2). A future investigation of this reaction *in vivo* is desirable.

4.2 Application of human cytochrome c mutants for a superoxide biosensor

Following the initial idea that an increased reaction rate of cyt c with superoxide may enhance the sensitivity of a cyt c based superoxide sensor, horse heart cyt c, human wild type cyt c and the five most promising mutant forms of cyt c (T63K, E66K, E69K Y74K and F82K), which reveal a higher radical reaction rate constant (see 4.1.3), have been chosen to be further investigated as a recognition element in a biosensor for the detection of superoxide.

4.2.1 Electrochemical characterization of mutant electrodes

The thermodynamic and kinetic properties of the cyt c mutants selected for the sensor application have been characterized electrochemically with the proteins adsorbed on a promoter modified gold electrode. All chosen mutants can be adsorbed on the negatively charged mercaptoundecanoic acid / mercaptoundecanol (MU / MUA) layer. Figure 36 demonstrates exemplarily for some mutants that the cyclic voltammograms are similar to those achieved with the wild type, but also a slight shift of the formal potential and a decreased amount of electro-active cytochrome c in the case of F82K.

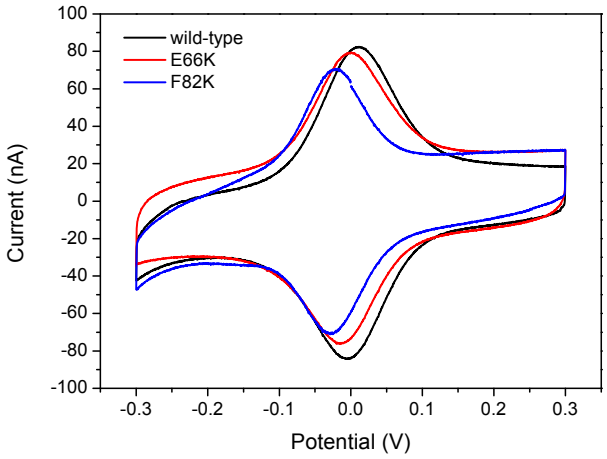

Figure 36 Cyclic voltammograms of E66K, F82K and the wild-type form of human recombinant cyt c adsorbed on a MUA/MU modified gold electrode (5mM potassium phosphate buffer pH 7 at 100mV/s).

The behavior is also studied kinetically and the values for the formal potential, the half peak potential, the surface coverage and the heterogeneous electron transfer rate constants (k_s) are presented in Table 3 (see 4.1.4.2). The rather similar redox properties and surface coverage of the proteins, in comparison with the values for the wild-type and horse heart cyt c, are promising for a sensor application. However a decrease in surface coverage was measured for

F82K and Y74K (of ca. 40% and 30% respectively), which may be due to structural changes as explained in the former section 4.1.6.

A similar trend for most of the mutants can also be observed in the k_s values and the peak shape; however F82K and Y74K vary from the other cyt c types. They have a 2.2 and 1.8 fold increased electron transfer rate and a slightly smaller half peak width (<100mV). Here the electron transfer from cyt c to the electrode seems to be facilitated (see 4.1.4.2 for further discussion). However, this is not a real advantage for a superoxide biosensor since k_s influences mainly the dynamic range, which is not critical in superoxide analysis because of the low steady-state concentrations to be detected (in the nano- and micromolar range, Ge and Lisdat 2002)

4.2.2 Sensor behavior of mutant sensor electrodes

4.2.2.1 Sensitivity

For sensor construction, all five mutants selected have been covalently attached to the MU/MUA modified electrode. The formal potential for the mutants and the wild-type protein increases just slightly after covalent immobilization (about 5 mV) compared to proteins in the adsorbed state despite for the mutant F82K. Here the formal potential decreases slightly by about 5 mV. However, these slight changes in E_f do not affect the protein's behavior as a recognition element for superoxide. Indeed, with all mutant electrodes the superoxide radical could be detected. A typical current response under constant polarization (at 150 mV) with superoxide present in solution is shown in Figure 37. Different superoxide concentrations are established by a variation of the XOD activity in the enzymatic generation system (Ge et al. 2002). The right graph in Figure 37 depicts that the current follows with the steady-state superoxide concentration in a linear manner. This holds for all investigated mutant electrodes and has been tested in the concentration range from 0.15 µM to 0.4 µM. In addition, the signal can be completely suppressed by the enzyme superoxide dismutase (SOD) which can effectively remove the radical from solution by dismutation to molecular oxygen and hydrogen peroxide. This leads to the conclusion that the sensors respond selectively to superoxide. Figure 37 compares the current signals from wild type and mutant E66K electrodes. An increase of the sensor signal for E66K for the same O_2^- concentration can be clearly noted.

The sensitivity has been calculated for each protein used for sensor construction (Figure 38). Mutant E66K shows the highest sensitivity for the oxygen radical (620 $Am^{-2}\ M^{-1}$), whereas for the other protein electrodes, no significant increase of the signal has been observed. They are all in the sensitivity range obtained for a horse heart cyt c based sensor (Ge et al. 2002). The approximately 40% increase in sensitivity found for the mutant E66K is in good agreement with

the photometrically determined enhancement of the rate constants for the cyt c radical reaction. In both investigations, the variant E66K shows the highest values.

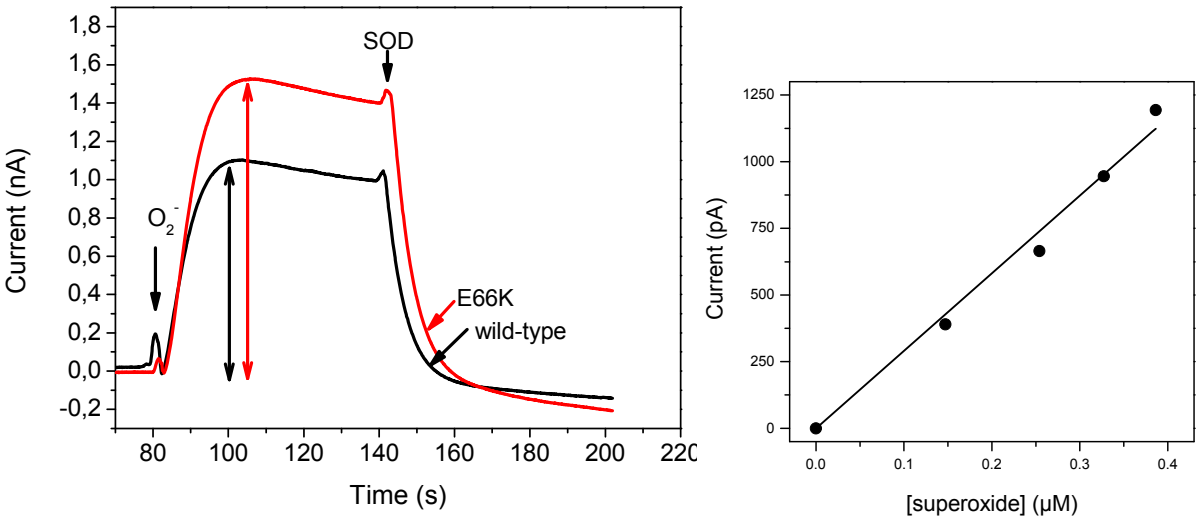

Figure 37 Amperometric measurement of superoxide using cyt c based electrodes (Au|MUA/MU|covalently fixed cyt c). Comparison of current responses of wild-type cyt c with the variant E66K after starting the production of superoxide with xanthine oxidase and later scavenging all superoxide radicals with superoxide dismutase (50 mM sodium phosphate buffer pH 7.5 at +150 mV vs. Ag/AgCl/1M KCl). Right: Linear dependence of current signal on superoxide concentration calculated according to Ge and Lisdat 2002.

However, F82K does not exhibit the same enhancement as expected from the reaction rate with superoxide in solution: It showed decreased sensitivity. This can be attributed to the fact that with this mutant a lower surface coverage after covalent immobilization is achieved compared to the other variants due to conformational changes. Since the rate constant and the surface coverage equally influence the sensitivity, this could explain the lack of sensitivity increase.

T63K, E69K and Y74K electrodes show only a slightly enhanced sensitivity, which is in accordance with the slight increase in reaction rates with superoxide, found for these proteins in solution. However, for some mutants there is no significant correlation between the rate constant found in solution and the sensitivity of the sensor electrodes. For example although the rate constant for the reaction with superoxide of T63K (11.3 M^{-1} s^{-1}) is higher than for E69K (8.8 M^{-1} s^{-1}), the sensitivity is smaller for T63K. Also wild-type human cyt c with nearly the same reaction rate (6.6 M^{-1} s^{-1}) as horse heart cyt c (6.7 M^{-1} s^{-1}) has a slightly lower sensitivity. As already mentioned above for F82K, the varying surface coverage in the range of 30% between the mutants can explain this observation. An additional point could also be the restricted mobility of cyt c after covalent immobilization of the protein and the fact that the positive charge of F82K is situated at the site facing the electrode as it can be seen in Figure 27 in 4.1.4.2 for the adsorbed state. Also in the covalently fixed mode, this site might not be accessible for superoxide

due to this restricted orientation of the covalently fixed protein at the interface in contrast to the situation in solution.

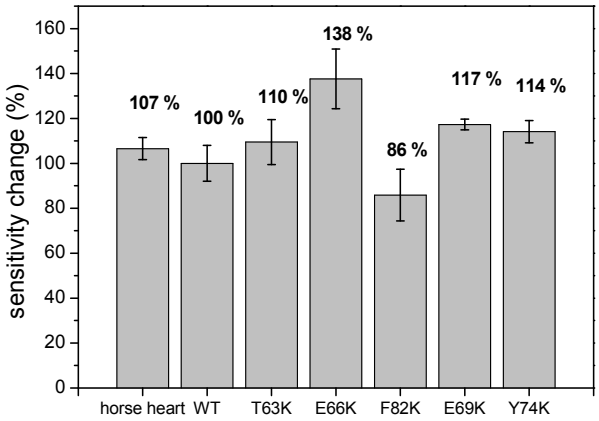

Figure 38 Relative sensitivity of mutant electrodes for superoxide compared to wild type sensor electrodes calculated from independent amperometric measurements of three electrodes (E= +150 mV vs. Ag/AgCl, enzymatic superoxide generation using XOD and hypoxanthine). Sensors were constructed by covalent attachment of human cyt c wild type and mutants on MUA/MU modified gold electrodes. The 100 % value for the wild type cyt c (WT/wild-type) corresponds to 450 A / m² M.

4.2.2.2 Stability and impact of H_2O_2 interference

From the sensitivity measurements, the mutant E66K seems to be best suited for the construction of superoxide sensor electrodes. Thus, other important sensor properties, such as stability and the influence of interferences, have been investigated for this protein electrode. It is known that cyt c immobilized on electrodes can exhibit pseudoperoxidase activity (Lei et al. 1999; Ju et al. 2002; L. Wang et al. 2008). In analogy to the natural interaction with anionic phospholipids, particularly mitochondria-specific cardiolipin (CL), cyt c undergoes structural changes and peroxidase activity increases (see 2.1.1.1). The pseudoperoxidase activity could lead to an interference of superoxide oxidation by the reduction of H_2O_2. Since H_2O_2 always coexists with O_2^-, it is important to exclude this potential interference.

At a potential of 0 V, where the pseudoperoxidase activity can be clearly characterized, the reduction current is measured in the presence of 5 mM H_2O_2. No enhancement in the H_2O_2 reduction current can be observed compared to the wild-type and horse heart protein. Furthermore, the potential of +150 mV vs. Ag/AgCl chosen for the amperometric superoxide sensor measurement is high enough to prevent the reduction of H_2O_2. This can be verified by amperometric control experiments with mutant E66K in the presence of 200 µM hydrogen peroxide. For comparative reasons the pseudoperoxidase activity has also been characterized for the mutants Y74K, F82K, E69K. These protein electrodes exhibit no enhanced activity with

the exception of the Y74K electrode. Here a two fold increase in hydrogen peroxide response could be detected (Figure 39), which is indicative of another important parameter to be considered in the design of improved recognition elements.

A similar observation was done in two recent studies of the mutant Y67H and Y67R, where the introduced histidine and arginine caused a drastic increase of catalytic peroxidase activity of yeast cyt c (Casalini et al. 2010; Ying, Z.-H. Wang, et al. 2009). A conformational transition with a weakening effect on the heme-Met80 coordination accompanied by an altering of the H-bonding network in the heme crevice was suggested. Furthermore it is assumed that these amino acids act as a general acid-base catalyst for H_2O_2. Since the mutant Y74K has an introduced basic amino acid situated in close proximity to Y67 (see Figure 32 in 4.1.6) a comparable mechanism for the enhanced pseudoperoxidase activity is likely. In addition this might be also a hint that this region is important during activation of the peroxidase activity during binding to cardiolipin. It was recently suggested that this region is part of a hydrophobic channel which could host one cardiolipin acyl chain (Sinibaldi et al. 2010).

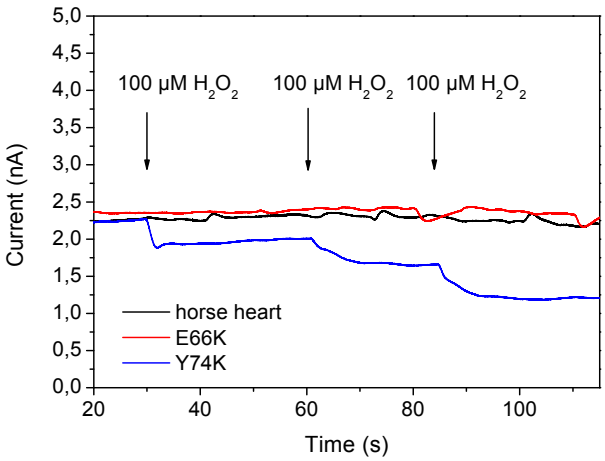

Figure 39 Amperometric measurement in the presence of up to 300µM H_2O_2 using cyt c based electrodes (Au|MUA/MU|covalently fixed cyt c). Comparison of current responses of horse heart cyt c with the variant E66K and Y74K after addition of three times 100µM H_2O_2 (50 mM sodium phosphate buffer pH 7.5 at +150 mV).

Finally, investigations on the E66K sensor electrode stability have been performed. The prepared electrodes were stored dry at 4 °C. The surface coverage and the sensor response to a fixed superoxide concentration have been tested for different time periods after the preparation (Figure 40). Since no relevant loss of surface coverage was detected and only a 30% decrease in sensitivity is found within eight weeks storage, it can be concluded that these mutant sensor electrodes can be used at least for one month after preparation without significant loss of sensitivity. For a wet storage a drastically decreased surface coverage was observed within the time period of one week.

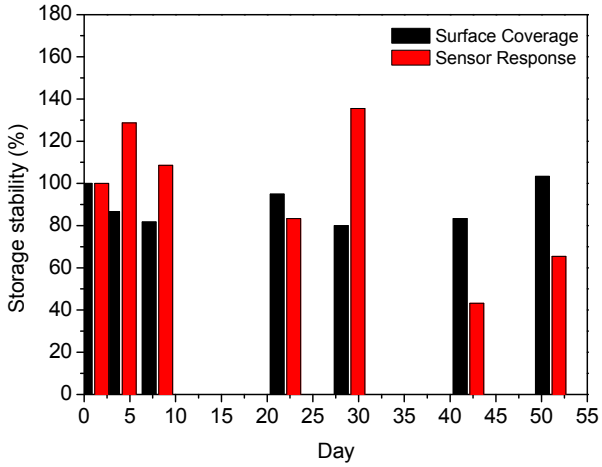

Figure 40 Storage stability of a sensor electrode with E66K. The electrode was stored dry at 4°C. The surface coverage determined by cyclic voltammetry at the first day corresponds to 6 pmol/cm² and the sensor response for 290 nM superoxide on the first day corresponds to 900 pA (E= +150 mV vs. Ag/AgCl, enzymatic superoxide generation using XOD and hypoxanthine).

In a final analysis the results presented in this section demonstrate that there are several important factors for a successful superoxide sensor construction which can be influenced by the cyt c form used. As it was the approach of this thesis the reaction rate of cyt c with superoxide can influence the sensitivity of the sensor electrode. However, there are also other properties crucial for the sensor performance as e.g. the amount of electro-active cyt c which can be covalently immobilized. A decrease here causes a drop of the current density and thus a loss of sensitivity as it is the case for several investigated mutants e.g. for F82K and Y74K. Another point is the heterogeneous electron transfer rate between the electrode and the protein. A decrease can shorten the linear dependence of the current signal on the superoxide concentration. The mutants engineered in this thesis mostly have no altered k_s value or an increased transfer rate constant and hence they have no disadvantages regarding the sensor performance. Another aspect is represented also by the cyt c's site activities for hydrogen peroxide which has to be considered. The point mutation can increase this activity, as for the mutant Y74K, and cause a decline in selectivity, which may reduce the area of application for the sensors.

In the case of the mutant E66K, an increased reaction rate with superoxide is achieved due to the extra positive charge and an electrostatic guidance without any other side effects caused by the mutation such as structural changes which lead to changes in k_s, formal potential, electrode surface coverage or peroxidase activity. Hence, with this mutant an improved superoxide sensor could be constructed.

As an outlook one can think of the design of cyt c with a higher redox potential as another approach to enhance the reaction rate. This could increase the driving force for the superoxide oxidation. However, since in this case amino acid changes close to the heme group have to be

conducted (to provide a more hydrophobic environment), there is the risk of induced larger structural changes and thereby other unfavorable properties.

4.3 Reaction of human cytochrome c mutants with other proteins in solution

In this section of the thesis the impact of the mutations in human cytochrome c towards the reaction with other proteins as sulfite oxidase and bilirubin oxidase will be investigated. In contrast to small molecules like superoxide which can also react with the heme iron, for proteins the docking to the cyt c surface is an essential step.

One has generally to distinguish between amino acids involved in the binding of the redox partner and amino acids involved in the inter and intra protein electron transfer. These amino acids can, but do not have to be identical, or electron transfer is tunneled between the redox centers.

Mutational studies of proteins are often used to understand the reaction with its partners or to figure out binding sites, and it is known that mutations of the lysines close to the heme edge in cyt c can affect the reaction with its natural reaction partners (Döpner et al. 1999; Pepelina et al. 2010). Since protein-protein interactions occur often due to electrostatic interactions it is suggested that an introduced extra positive charge in form of the amino acid lysine in human cyt c may also alter its reaction with BOD and SOX.

The electrostatic interactions between positively charged lysine residues on the surface of cyt c around the heme cavity ("front face") and negatively charged residues of amino acids on subunits of the redox partners of cytochrome c are known since decades to play a key role in the formation of complexes (Brautigan et al. 1978; Rieder et al. 1980). However, the order of importance of the cyt c lysine residues for the two complexes varies (Pepelina et al. 2010; Rieder et al. 1980), and it was shown that also hydrophobic interactions are of crucial importance for the binding of cyt c_1 of cyt c reductase and cyt c peroxidase (Bertini et al. 2006). In contrast, in Apaf-1 binding (a cytosolic apoptotic factor), it seems that cyt c uses not only this front face, but also an opposite surface centered around positions 39 and 62–65 (Yu et al. 2001; Mufazalov et al. 2009; Ow et al. 2008).

Furthermore it was demonstrated that cyt c from different species exhibits different affinities and thus also activities towards its redox partners due to the little differences in their amino acid sequences (Rhoten et al. 2002; Rodríguez-Roldán et al. 2006).

In this part of the thesis, the reactions of recombinant human cytochrome c mutants with two different enzymes, the recombinant human sulfite oxidase (SOX), a homodimeric enzyme, and the fungi bilirubin oxidase (BOD), a monomeric enzyme are investigated by cyclic voltammetry. Whereas it is well known that cytochrome c is the physiological electron acceptor of sulfite oxidase during the oxidation cycle of sulfite (see section 2.1.4), for BOD only *in vitro* experiments could show that both bilirubin and cyt c can act as electron donor for the enzyme (see section 2.1.3). The X-ray structure of the cyt b_5 domain of human SOX which binds to cyt c

under physiological conditions is solved (Rudolph et al. 2003). Similar to the case of cyt c oxidase the lysines around the cyt c heme edge are shown to be important for the reaction with SOX (Webb et al. 1980; Speck et al. 1981). This becomes obvious looking at the negative surface potentials of the cyt b5 domain of SOX in contrast to the positive ones around the heme edge of cyt c (Figure 41).

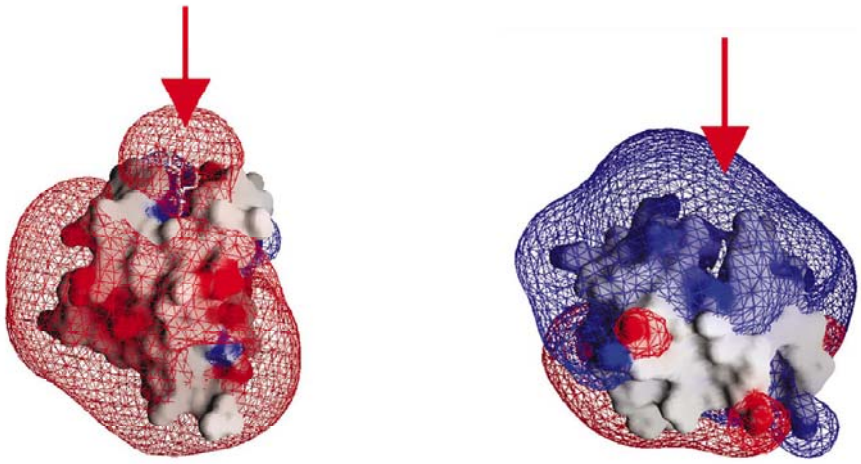

Figure 41 Electrostatic surface and isopotential contour representation of the human SOX cytochrome b_5 domain (left) and horse heart cyt c (right). Blue and red regions representing electropositive (>7kBT) and electronegative (<-7kBT) potential, respectively are mapped onto the molecular surfaces. Isopotential contours at + and - 1kBT are drawn where the blue and red contour maps represent positive and negative isopotentials. The calculation assumed an ionic strength of 100 mM. arrows point to the heme exposed edges (Rudolph et al. 2003).

The recently published crystal structure of BOD demonstrates a large structural similarity to laccase (K. Mizutani et al. 2010) and several hints exist that the electron entrance occurs near to the T1 copper site of BOD (Dronov, Kurth, Frieder W. Scheller, et al. 2007; Shleev et al. 2005; Shleev et al. 2004). However, since the PDB file of BOD (3gbd) was not available by the time of the experiments, electrostatic interactions with cyt c could only be assumed.

For these studies human wild-type cyt c and seven human cytochrome c mutants are chosen to be investigated as electron donors for BOD and as electron acceptor for human SOX in comparison with the horse heart cyt c being used in former studies with both proteins (Spricigo et al. 2008; Dronov, Kurth, Frieder W. Scheller, et al. 2007). In each mutant a single neutral or negatively charged amino acid is exchanged by a positively charged lysine. The mutation sites are surface exposed and located on one side of the molecule in respect to the heme edge (Figure 42).

The electrochemical properties of the cyt c forms such as formal redox potential and diffusion coefficient were determined (Table 2 in section 4.1.4.1). The diffusion coefficient of horse heart cyt c is found to be slightly higher than for the human wild-type ([1.7 ± 0.4] × 10^{-6} cm^2/s). This implies that the structure of horse heart cyt c is little more compact than the human wild-type one. For the human cyt c mutants no significant alteration for the determined

properties compared with the wild-type were found. Also the structural integrity was checked with ^{1}H NMR spectroscopy. For I81K the introduction of a lysine at position 81 induces chemical shift changes in all the Met80 side-chain resonances (from -0.02 to +0.04 ppm), indicating structural changes for this mutant (Appendix A14).

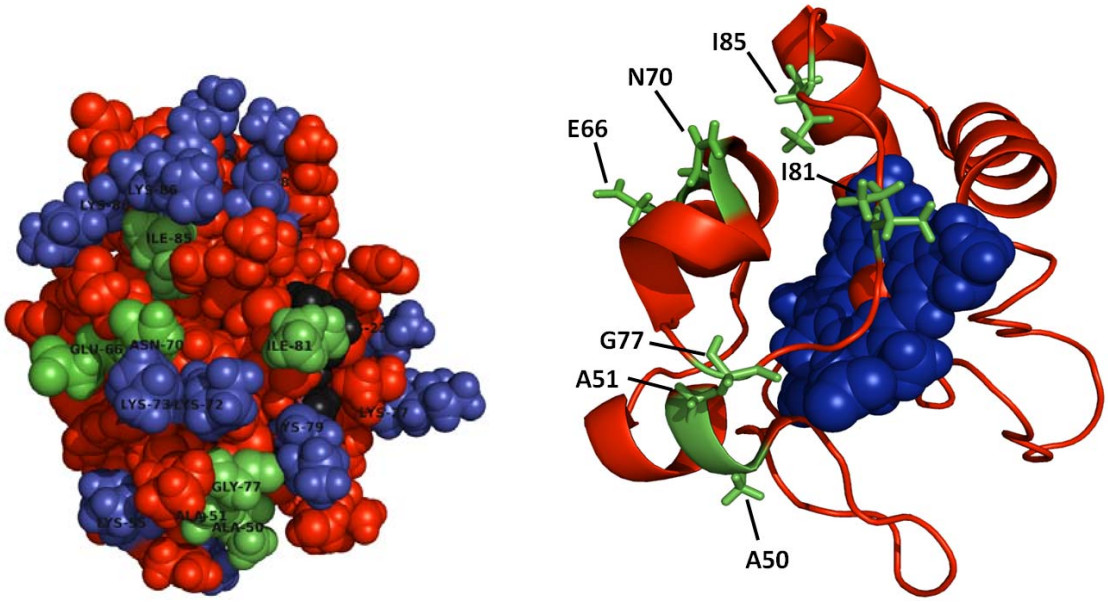

Figure 42 Left: NMR structure of human cyt c with mutation sites depicted in green. Blue spheres represent lysines present in the wild-type protein. The heme group is presented in black spheres. Right: NMR structure of human cyt c in cartoon representation with mutation sites depicted as green sticks. The heme group is presented with blue spheres with the heme iron as red sphere in the center. The images were built with the software Pymol (http://pymol.sourceforge.net) using the pdb file 1J3S.

4.3.1 The reaction with sulfite oxidase

The catalytic reaction of human SOX and cyt c in solution was investigated using cyclic voltammetry with MUA/MU modified gold electrodes. The resulting electron transfer chain is presented in Figure 43. The substrate sulfite is oxidized in two steps to sulfate. In each step the reduced molybdopterin (MPT) cofactor transfers an electron to the cyt b_5 domain (see 2.1.4 for more details). After this intraprotein electron transfer cyt c accepts the electron from cyt b_5 getting reoxidized by the electrode and as result an oxidation current appears. The continuous reoxidation of cyt c by the electrode - at potentials allowing redox conversion of cyt c - provides the regeneration of electron acceptor molecules for the reduced MPT of SOX. Thereby a typical catalytic voltammogram is formed (Figure 44). For all chosen mutant forms catalytic currents could be obtained. However, for some of the human cyt c mutants with introduced positively charged lysines different reaction rates were determined.

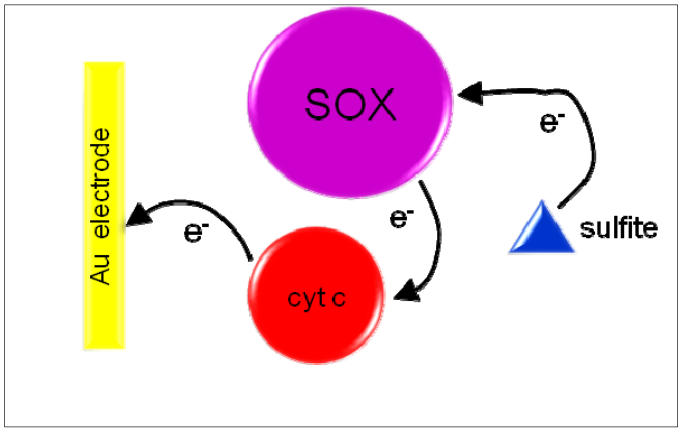

Figure 43 Simplified schematic representation of the electron transfer chain for cyt c and SOX in solution.

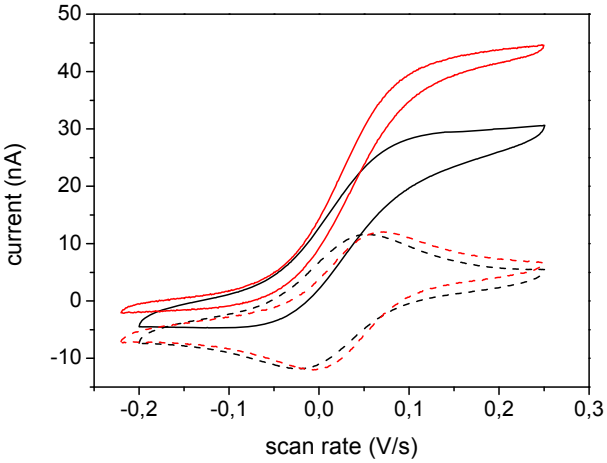

Figure 44 Cyclic voltammogram of MUA/MU modified gold electrode in air-saturated 50 mM phosphate buffer pH 8.5 in presence of 10 µM E66K (red) or N70K (black) cyt c and 2 mM sulfite (saturation), scan rate 8 mV/s, dashed line: without SOX, straight line: with 400nM SOX.

The limiting current, corresponding to the plateau of the voltammogram in Figure 44, is independent of further additions of sulfite. This indicates that the reaction of SOX with sulfite is a kinetically fast step, faster than the rates of reoxidation of cyt c by the electrode or the electron transfer between cyt c and the reduced enzyme.

One can already see that under the same conditions two human cyt c mutants N70K and E66K exhibit different catalytic plateau currents. To quantify the differences for the homogeneous electron transfer reaction between human SOX and the different cyt c forms the second order reaction rate constant k is determined using the method of Nicholson and Shain (Nicholson et al. 1964; Antiochia et al. 2001). Initially, the pseudo first-order kinetic constant k_{cat} is calculated by quantifying the ratio of the catalytic currents (I_{cat}) and the diffusion-limited currents (I_{diff} without SOX) at various scan rates (ν) for different SOX concentrations. This can be done according to the relation given in equation (1).

$$\lambda = 0.1992\ (I_{cat}/I_{diff})^2 = k_{cat}\ (\zeta RT/nF)\ 1/\nu \qquad (1)$$

This simplified relation can be used only if the ratio I_{cat}/I_{diff} is ≥ 1.7. ζ is the ratio of the stoichiometric coefficients of the reaction between the mediator (here cyt c) and the enzyme SOX. ζ is in the case of SOX equal to 2 since two molecules of cyt c are reduced during oxidation of one molecule sulfite (see 2.1.4).
Plotting k_{cat} versus the SOX concentration, the reaction rate constant k can be derived from the slope of the straight line using equation (2).

$$k_{cat} = k\ [SOX] \qquad (2)$$

The resulting rate constants are presented in Figure 45. For horse heart cyt c a value of 0.7 ± 0.2 $\mu M^{-1}s^{-1}$ is determined. For the same experimental conditions this value was found earlier to be 4.47 ± 0.13 $\mu M^{-1}s^{-1}$ (Spricigo et al. 2008). Moreover, in another work at pH below the optimum with chicken SOX the value 2.53 ± 0.24 $\mu M^{-1}s^{-1}$ was determined (Ferapontova et al. 2003). In both works an incorrect version of formula (1) was used, resulting in the higher apparent values: the factor 0.1992 as well as the parameter ζ were not applied. After correction of these literature values by applying the missing factors, a similar magnitude as in this thesis is reached (0.5 and 0.12 $\mu M^{-1}s^{-1}$, respectively). Another work stated a value in the range of 0.6 $\mu M^{-1}s^{-1}$ under similar conditions in solution, but with a different experimental approach (Wherland et al. 1976).

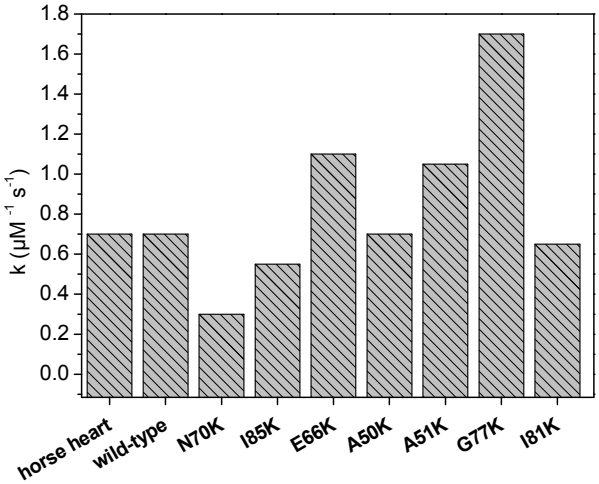

Figure 45 Second order reaction rate constants for the reaction of cytochrome c (mutants) with SOX in solution, calculated according to (Nicholson et al. 1964) with MUA/MU modified gold electrodes in air-saturated 50 mM phosphate buffer pH 7.0 in the presence of 10 µM cyt c and 50-700 nM BOD. The experimental error was in the range of ± 0.2 $\mu M^{-1}\ s^{-1}$.

As far as known, for the first time the second order reaction rate constant for human SOX with human cyt c was determined here in this thesis. Although the sequence homology between horse heart and human cyt c is only 78 % no difference in the rate constants could be observed, indicating no major alterations for the interaction site. Moreover, the unchanged reaction rates suit to the known importance of electrostatic interactions between SOX and cyt c, since the sequence differences mostly account to slight changes in hydrophobicity of the cyt c surface.

However, some human cyt c mutants have different reaction rate constants compared with the wild-type. For N70K a clearly decreased rate constant is found. Here the affinity seems to be negatively affected. N70 is situated very close to K72 (Figure 42). This lysine was already shown to be important for the binding of horse heart cyt c and SOX (Speck et al. 1981; Webb et al. 1980). N70K may cause electrostatic repulsion to K72 and thereby alter the orientation of K72. The negative effect on the reaction rate of N70K could also be connected to a change of the dipole moment of cyt c and thereby, like it was shown for chemically modified horse cyt c and the reaction with beef liver SOX, can cause an unfavorable orientation during interaction (Speck et al. 1981).

G77K shows the highest reaction rate constant compared to the wild-type. This mutation site is located close to K79, whose positive charge was shown to be important for the affinity of the two proteins (Webb et al. 1980). Hence, for both mutants G77K and N70K - with the most pronounced increasing and decreasing effect respectively - the affected mutation site is located close to a lysine residue putative important for the interaction with SOX in the wild-type protein.

Another possible explanation for the increased and decreased reaction rate constants is connected to the intraprotein ET: It was shown that in the reduction half cycle the intraprotein ET is the limiting step probably due to the conformational change which is necessary to bring the heme b_5 domain close to the MPT domain to conduct reduction of heme b_5 (C. Feng et al. 2007). This can mean that a changed affinity of the heme b_5 domain towards cyt c influences also the binding and reduction of the heme b_5 domain towards the MPT cofactor. Thus contrary to the explanation above if the dissociation of ferri-cyt c from ferri-heme b_5 is impeded – perhaps due to the increased electrostatic interaction e.g. for N70K – the intraprotein ET which creates the reduced heme b_5 may also be impeded. A facilitated dissociation could cause the opposite effect being a reason for the increased rate constant found for G77K.

4.3.2 The reaction with bilirubin oxidase

Cyclic voltammetry was also used to examine the catalytic reaction of BOD and cyt c in solution. For the first time it could be shown that also human cyt c reacts with BOD although the sequence has only 78 % homology with the horse form of cyt c used in former studies (Dronov,

Kurth, Frieder W. Scheller, et al. 2007). A representative cyclic voltammogram of the catalytic reaction of the mutant N70K and horse heart cyt c in comparison is shown in Figure 46. The electron pathway of the system is schematically presented in Figure 47 and can be described as follows: cyt c is reduced at the MUA/MU modified gold electrode, then donating its electron most probably to the T1 site copper ion, where normally bilirubin as natural substrate gets oxidized. Then an intramolecular electron transfer to the T2/T3 trinuclear cluster takes place. Here, four electrons are subsequently transferred to molecular oxygen (S Tsujimura et al. 2005; Shimizu et al. 1999; F. Xu et al. 1996). Since cyt c is reoxidized by BOD, there is a regeneration of cyt c newly available for the reduction at the gold electrode. The different magnitude of the catalytic reduction current (Figure 46) for the same concentrations indicates that the reaction between N70K and BOD seems to be less effective than for horse cyt c.

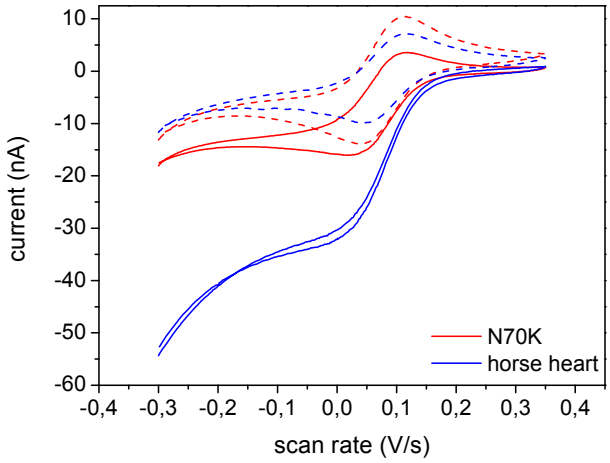

Figure 46 Cyclic voltammogram of MUA/MU modified gold electrode in air-saturated 50 mM phosphate buffer pH 7.0 in presence of 10 µM horse heart or N70K cyt c, scan rate 4 mV/s, dashed line: without BOD, straight line: with 200nM BOD

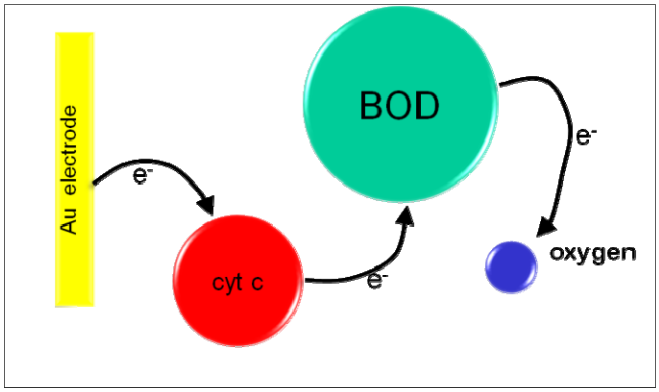

Figure 47 Schematic representation of the electron transfer chain for cyt c and BOD in solution

To quantify the differences for the homogeneous electron transfer reaction between BOD and cyt c the second order reaction rate constant k was determined using the method of Nicholson and Shain (Nicholson et al. 1964). First the pseudo first-order kinetic constant k_{cat} is calculated by quantifying the ratio of the catalytic currents (I_{cat}) and the diffusion limited currents (I_{diff} without BOD) at various scan rates (ν) and for different BOD concentrations. The same relations as given in equation (1) and (2) in section 4.3.1 were used and a stoichiometric factor ζ of 4 was applied. The different second order reaction rate constants k for horse heart cyt c, human wild-type cyt c and their mutants are presented in Figure 48.

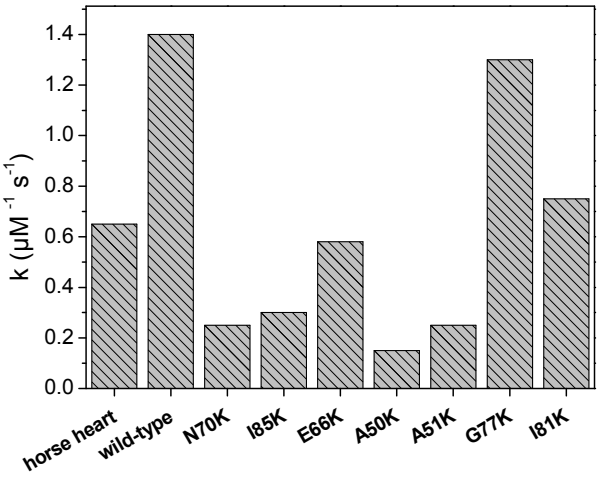

Figure 48 Second order reaction rate constants for the reaction of cytochrome c (mutants) with BOD in solution, calculated according to (Nicholson et al. 1964) with MUA/MU modified gold electrodes in air-saturated 50 mM phosphate buffer pH 7.0 in the presence of 10 µM cyt c and 50-700 nM BOD. The experimental error was in the range of ± 0.1 $\mu M^{-1} s^{-1}$.

In general, taking the reaction rate for the horse heart cyt c as a reference, the reaction rate constant for the reaction with BOD was found to be similar to SOX, although the latter is an established physiological reaction, whereas for the former reaction no physiological importance was known until now. However, the reaction of SOX with cyt c might be limited due to a conformational change of the cyt c reducing heme b_5 domain of SOX to switch between intra- and intermolecular ET. No conformational change is known to occur during the intra- and intermolecular ET in BOD.

It can be also seen that in contrast to SOX there is already a two-fold difference between horse heart cyt and the human wild-type reaction with BOD. The higher reaction rate found for the human wild-type might originate from a slightly different structure, caused by the twelve amino acids differing between both species. The evolutionary exchanged amino acids are mainly situated around the heme crevice, where the possible interaction area is also located. This area of the human protein is more hydrophobic compared to the horse form (see 2.1.1.3). The

increase in the surface hydrophobicity of the human cyt c may facilitate hydrophobic interactions with the surface of BOD causing a higher affinity. If one would additionally consider the higher diffusion coefficient of horse heart cyt c, conclusion can be made that proteins' structure is more compact, having less BOD interaction sites exposed than that of the human cyt c. Rodríguez-Roldán et al. have recently reported on differences in the interaction of cyt c oxidase with human cyt c compared to *Arabidopsis* and horse cyt c: the second order rate constant for the human form is increased by 76 % compared to the horse cyt c form (Rodríguez-Roldán et al. 2006).

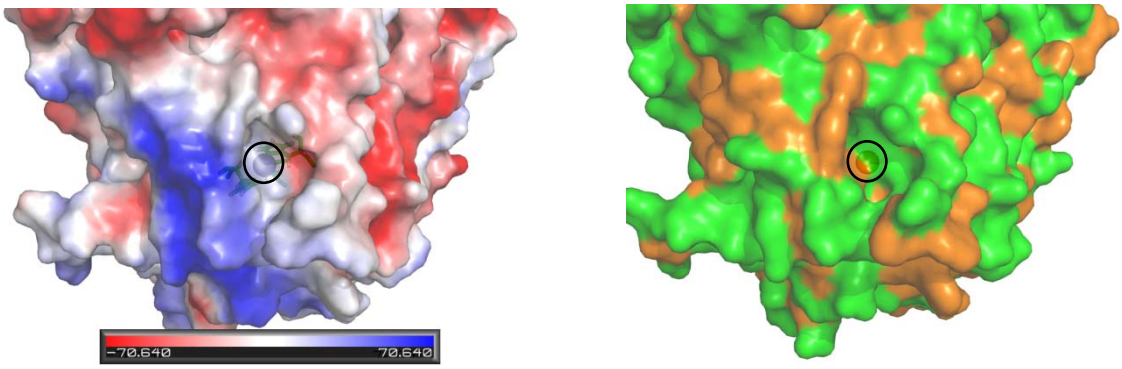

Figure 49 Surface of BOD around the T1 copper ion (marked with a black circle). Left: presentation of surface charges (blue – positive patches, red – negative patches). Note, this is no presentations of profound electrostatic calculation of the surface potential. Right: presentation of hydrophilic and hydrophobic surface aera (green – hydrophilic patches; orange – hydrophobic patches. Image build with Pymol.

None of the mutants have a higher reaction rate constant than the wild-type. The rate constant of G77K reaches the same level as the wild type, probably because this mutation site is located in close proximity to the heme edge (Figure 42). Since all other mutants have a decreased rate constant one might conclude that either the cyt c interaction site at BOD is more positively charged causing a repulsion effect attributed to the extra positive charge at cyt c or the interaction takes place at another cyt c region so that the extra positive charge would orient the molecule in an unfavorable way. The hydrophobic interactions mentioned before may also be disturbed due to the extra positive charge. The recently available pdb structure file of BOD gives the possibility to analyze the amino acid environment of the T1 copper ion. As it can be seen in Figure 49 there are positively and negatively charged patches around the copper ion. The positive patch could be responsible for the possible electrostatic repulsion with the lysine mutants. However, in the right depiction of Figure 49 also hydrophobic patches are visible; hence, a possible disturbance of hydrophobic interaction cannot be fully excluded.

For the mutant G77K another phenomenon has been observed: the catalytic current in the cyclic voltammogram with both proteins in solution increased with time (Figure 50). This effect

could also be observed with I81K. After mixing the solution with the pipette, the current went back to the magnitude detected at the beginning, afterwards started increasing again with time. It can be explained as a kind of complex formation between the cyt c molecule and BOD with time, facilitating the electron transfer to BOD. In the period between two voltammetric cycles no potential was applied, disregarding the potential-induced effect.

Further NMR or SPR investigations could help to understand the different interaction behavior of the cyt c mutants with BOD. The possible effect of an altered reaction rate in a multilayer assembly is analyzed in the next section of this thesis.

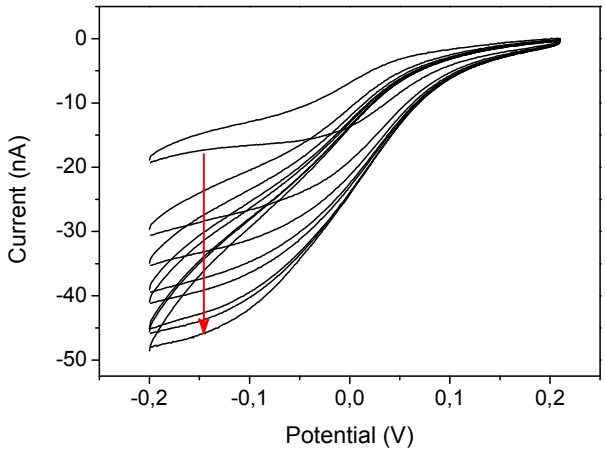

Figure 50 Cyclic voltammograms with MUA/MU modified gold electrodes in air-saturated 50 mM phosphate buffer pH 7.0 in the presence of 10 µM G77K and 250 nM BOD at a scan rate of 6 mV/s. The arrow indicates the time range of 45 min from the first scan to the last scan

4.4 Multilayer electrodes with human cytochrome c mutants and bilirubin oxidase

In this section some of the human cyt c forms are examined in the immobilized state as parts of a multilayer assembly with and without a second redox protein. Bi-protein multilayer assemblies were already successfully constructed (Dronov, Kurth, Möhwald, Frieder W. Scheller, and Lisdat 2008; Dronov, Kurth, Möhwald, Roberto Spricigo, Leimkühler, et al. 2008b; Spricigo et al. 2008) with both protein couples investigated in this thesis (cyt c / SOX and cyt c / BOD). The bi-protein multilayer system with cyt c and BOD is applied in this section using wild-type and mutant forms of cyt c. The selection of different cyt c forms is motivated by different rate constants determined in solution (see 4.3.2). Together with G77K which exhibits a reaction rate constant similar to the wild-type, also N70K with a large decrease of the reaction rate constant was chosen along with horse heart cyt c and human wild-type cyt c for comparative reasons to be investigated as electron donor protein in a layered architecture with BOD.

BOD has already been successfully applied in a multilayer assembly on gold to form a bi-protein artificial signal chain as schematically shown in Figure 51 (Dronov, Kurth, Möhwald, Frieder W. Scheller, and Lisdat 2008). In this bi-protein electrode electrons are transferred from the gold electrode to the cyt c monolayer, afterwards via the cyt c molecules in different layers to BOD, where finally the four electron reduction of oxygen takes place. It could be shown, that the oxygen reduction at the enzyme becomes the rate-determining step at low scan rates. However, it seems that at higher scan rates the supply of electrons to the enzyme becomes important. The altered BOD-cyt c reaction rate of the horse, human and the engineered cyt c forms provides the possibility for a closer examination of this aspect.

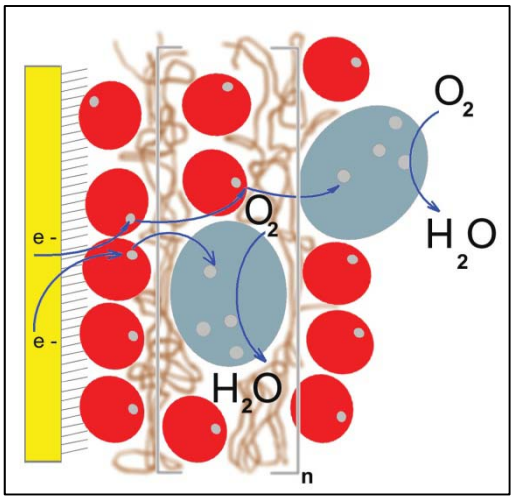

Figure 51 Schematic illustration of the redox chain in cyt.*c*/BOD multilayer electrodes (Lisdat et al. 2009). Red circles = cyt c protein, blue shapes = BOD enzyme, arrows indicate electron transfer pathways between cyt.*c* and BOD within the polyelectrolyte network and the four-electron oxygen reduction process

4.4.1 Multilayers of human cytochrome c mutants and PASA

In a first approach multilayer systems consisting only of different cyt c forms were investigated (schematically shown in Figure 52). The ability of multilayer formation with sulfonated polyaniline (PASA) was studied and the electrochemical properties were examined.

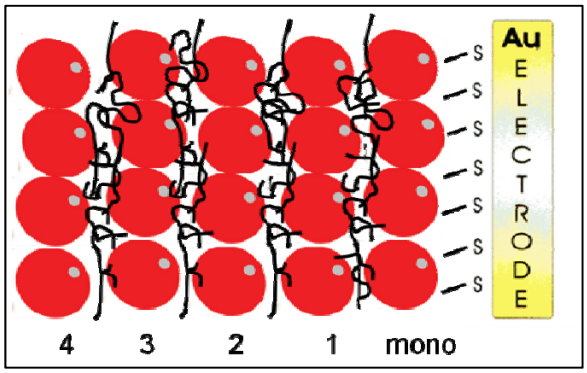

Figure 52 Schematic representation of a 4-bilayer SAM modified electrode with cyt c (red circles) and PASA (black coiled lines).

4.4.1.1 Study of the multilayer formation by SPR

The formation process of the different assemblies of cyt c and the polyelectrolyte was examined by surface plasmon resonance (SPR) spectroscopy. Here, cyt c and PASA were deposited on a planar MUA/MU modified SPR-chip in a flow system to study the mass adsorption during the built-up. The formation process for a four bi-layer electrode is given in Figure 53. The SPR sensograms characterize the multilayer formation of the four different cyt c forms investigated. The human and horse wild-type proteins show rather similar mass deposition during the multiple adsorption steps. However, the mutant N70K exhibits a slightly enhanced immobilization, whereas for the G77K mutant the assembly is rather weak. The different charge distribution on the protein surface can alter the immobilization with the sulfonated polyaniline. However, the drastic decrease in adsorption of G77K compared to the other proteins cannot be fully understood since ^{1}H NMR investigations reveal a rather undisturbed overall structure (Appendix A14). Despite G77K, all sensograms show an exponential increase of the deposited mass during the multilayer assembly. This was already observed in former studies and is related to partial interpenetration of the layers and an increased surface roughness (Dronov, Kurth, Möhwald, Frieder W Scheller, Friedmann, et al. 2008a).

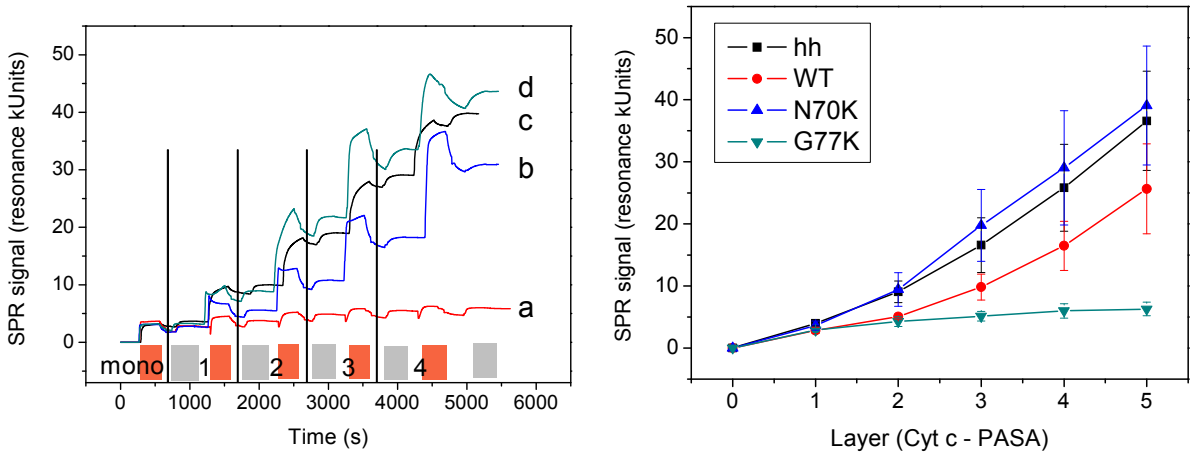

Figure 53 Left: SPR experiment showing the formation of the cyt c-PASA assembly for four bi-layers on a gold chip modified with MUA/MU, the red bar indicates the time of cyt c flow and the grey bar the time of PASA flow over the chip (a – G77K, b – wild-type, c – horse heart, d – N70K). Right: Mean SPR signal for the different cyt c forms for each layer of cyt c and PASA calculated from three independent measurements (Layer 0 for cyt c corresponds to a cyt c monolayer).

4.4.1.2 Electrochemical behavior

Since the SPR experiments reflect only the amount of immobilized cyt c molecules, the functional properties are analyzed by cyclic voltammetry. For all human cyt c forms electro-active multilayer electrodes could be constructed. Representative cyclic voltammograms measured with a monolayer electrode and after the assembly of four bi-layers of the human wild-type and PASA are given in Figure 54, left. One can see that both the oxidation and reduction peaks increase with the number of layers. This means that even the cyt c molecules in the outer layers are in contact with the electrode. Several electron transfer steps have to be considered here (Figure 54, left): the electron transfer from the gold electrode via the MUA/MU SAM-layer to the cyt c monolayer and then to the cyt c molecules of the subsequent layers. The latter step can be either realized by an inter-protein electron transfer only between the cyt c molecules, with PASA being just a stabilizing compound or by PASA being an active part in the electron transfer chain, conducting the electrons from one cyt c molecule to another. Several arguments have been collected to support the idea of electron exchange between the cyt c molecules as a dominating mechanism (Lisdat et al. 2009). A careful examination of the transfer steps has been performed by a kinetic analysis with a systematic scan rate variation for all multilayer electrodes with the four different proteins. The resulting cyclic voltammograms for horse heart cyt c and the mutant N70K for four different scan rates are presented in Figure 55 a) and c). For the mutant N70K the decrease of the voltammetric peaks with decreasing scan rate is much smaller than for horse heart cyt c. The difference becomes even more obvious after normalization of the current values in relation to the scan rate is performed. This can be done,

since there is a linear relation of the current and the scan rate for immobilized species (Wang 2000). The cyclic voltammograms normalized in this way are shown in Figure 55 b) and d).

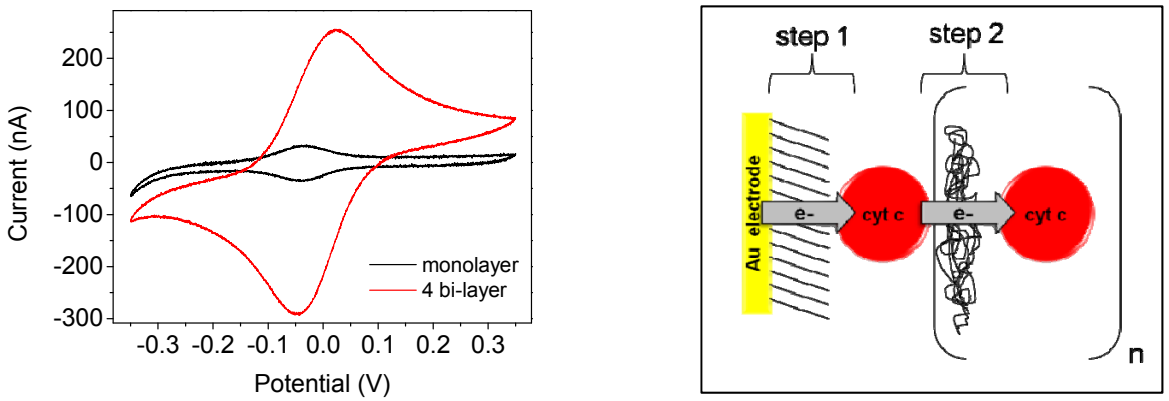

Figure 54 Left: Cyclic voltammograms of a human wild-type mono-layer MUA/MU modified gold electrode and of a 4 bi-layer electrode with cyt c and PASA in each layer, scan rate 100 mV/s. Right: Schematic representation of the electron transfer steps in a Au-SAM-cyt c-(PASA-cyt c)$_n$ multilayer coated electrode.

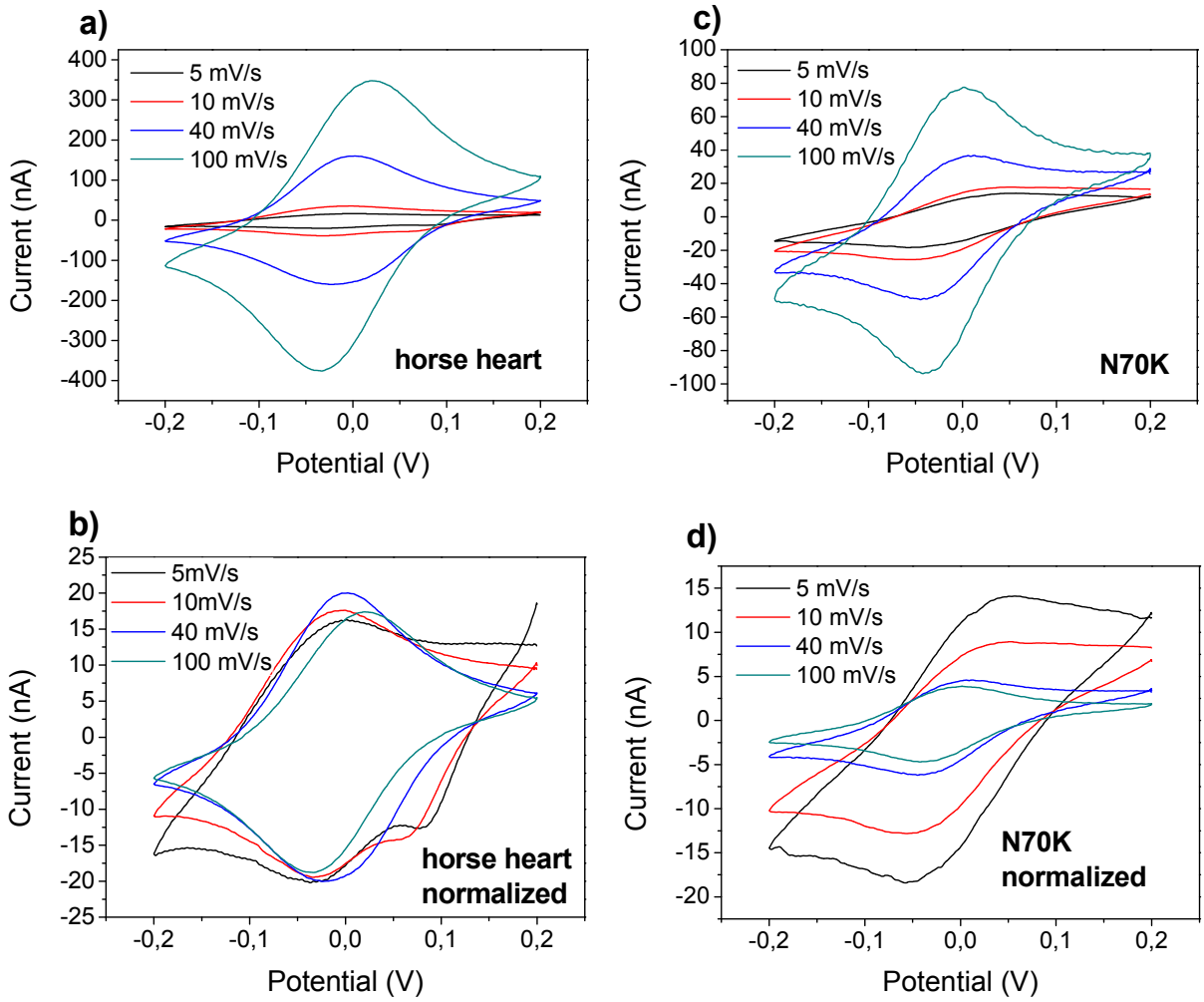

Figure 55 Cyclic voltammetry of Au-MUA/MU-cyt c-(PASA-cyt c)$_4$ multilayer coated electrodes for horse heart cyt c (left) and N70K (right) measured at different scan rates. The current values of the voltammograms b) and d) are normalized to 5 mV/s by dividing the values by the factor [(actual scan rate) / (5 mV/s)].

Integration of voltammograms' peak areas for all mutants gives the electro-active surface coverage Γ at different scan rates and is depicted in Figure 56. This specifies once more the different electrochemical behavior of the protein multilayers. The horse heart cyt c multilayer electrode exhibits the already described behavior (Moritz Karl Beissenhirtz et al. 2004): up to 80 mV/s the amount of electrode-addressable cyt c remains stable and then decreases slightly. This suggests that beyond 80 mV/s a scan rate is reached which is in the range of the cyt c – cyt c electron transfer rate (step 2 in the right scheme of Figure 54), so that not all cyt c molecules immobilized in the multilayer assembly can be oxidized or reduced within the time period of a voltammetric sweep. For the human wild-type cyt c electrode, although the behavior at 80-100 mV/s is rather similar to that of horse cyt c, the electro-active amount further increases at slow scan rates. This is indicative of a slower self-exchange rate of the immobilized protein. For the mutant N70K this effect is even more pronounced. At a scan rate of 80 mV/s only a small amount of the cyt c molecules can be detected. The cyt c molecules embedded into the layers become only visible at very low scan rates.

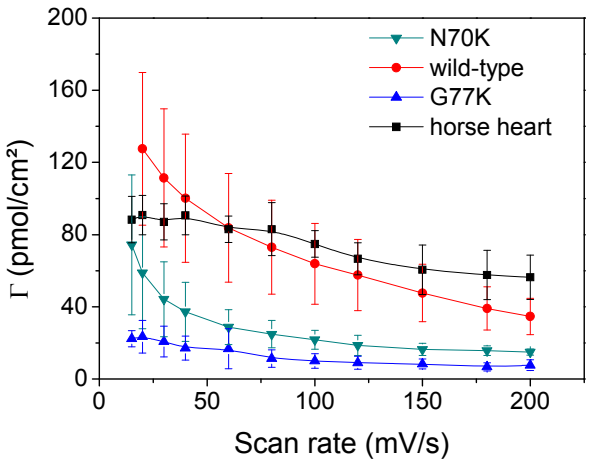

Figure 56 Electro-active surface coverage Γ for the four different cyt c multilayer electrodes at different scan rates.

To rule out that the electron transfer from the electrode to the monolayer (step 1 in the right scheme of Figure 54) is the limiting step the k_s values of the cyt c monolayer electrodes were determined (horse heart, wild-type and N70K). No significant decrease has been observed (55 ± 5; 64±6 and 45 ± 3 s^{-1} respectively). The slight decrease for N70K cannot cause the drastic decrease of contactable cyt c molecules at higher scan rate.

The experiments with the G77K mutant reflect the results of the SPR investigations. Much less protein can be adsorbed in the multilayer structure and thus detected electrochemically. However, the electro-active amount is again decreasing with increasing scan rate, with a similar

relative change compared to the human wild type, indicating also a decreased self-exchange rate for this mutant.

The slight decrease of the self-exchange rate of the human wild-type protein compared with horse heart cyt can be caused by a more compact structure of the latter one, caused by the higher diffusion coefficient value. A faster diffusion would enhance the probability of favorable orientation of the cyt c molecules to conduct the electron transfer. Additionally, a more compact structure and a smaller radius can contribute to a closer distance of the heme exposed "faces" of cyt c and thereby accelerate the electron transfer according to the Marcus theory (Marcus et al. 1985). This was also assumed by comparison of the self-exchange rate of different cytochromes (Dixon et al. 1989). Furthermore, 7 of the 12 amino acids being different between horse heart cyt and human cyt c are situated on the front heme "face". This can also affect the protein interaction area and thereby the electron transfer rate.

The decreased self exchange rate for the two mutant proteins can be understood as an increase of electrostatic repulsions between two cyt c molecules due to the extra positive charge since there are studies demonstrating that the protein—protein contact region is centered on the heme crevice (Pielak et al. 1987). For the two mutants investigated here the mutation sites are closely situated to the heme edge. In an earlier study the importance of surface charges for the self exchange rate has been shown by chemically modified single lysine side chains concentrated around the heme crevice as well as by binding anions at specific sites near the partially exposed heme edge (D.W. Concar et al. 1986).

It might seem uncommon that these single mutations or sequence differences between horse and human cyt c cause a remarkable difference, but if one takes the self-exchange rate constant for structurally very similar cytochromes c into account, a span over six orders of magnitudes can be observed (Simonneaux et al. 2005). However, to prove the assumptions for the mutants prepared here the cyt c self-exchange rate remains to be determined.

The dependence of the formal potential and the peak separation on the scan rate can be found in Table 5. The peak separation increases for all protein electrodes with increasing scan rate. However for the mutant N70K the increase at low scan rates is much steeper compared with the other multilayer electrodes. This observation supports once more the reduced effective electron transfer within the N70K multilayer assembly.

A slight drift for the formal potential can be observed which reflects the not fully reversible behavior of the system. The formal potentials of the multilayer electrodes are varying only slightly. By evaluating the peak shape of the normalized cyclic voltammograms at small scan rates (Figure 55) one observes an additional voltametric peak at about + 75 mV for the horse cyt c-containing assemblies. This can be attributed to the reduction of PASA as it has been shown before (Dronov, Kurth, Möhwald, Frieder W Scheller, Friedmann, et al. 2008a). For the

electrodes containing the human form this is much weaker and cannot be observed for the two mutants (Figure 57).

Table 5 Formal potential E_f and peak separation ΔE_p for the cyt c multilayer assembly with the four different cyt c forms at various scan rates (results from three independent electrodes)

scan rate (mV/s)	E_f (mV) horse heart	E_f (mV) human wild-type	E_f (mV) G77K	E_f (mV) N70K
20	-12	-16	-9	-8
40	-5	-15	-12	-10
80	-6	-18	-12	-16
scan rate (mV/s)	**ΔE_p (mV) horse heart**	**ΔE_p (mV) human wild-type**	**ΔE_p mV) G77K**	**ΔE_p (mV) N70K**
20	7	23	32	59
40	15	36	40	59
80	45	60	51	46

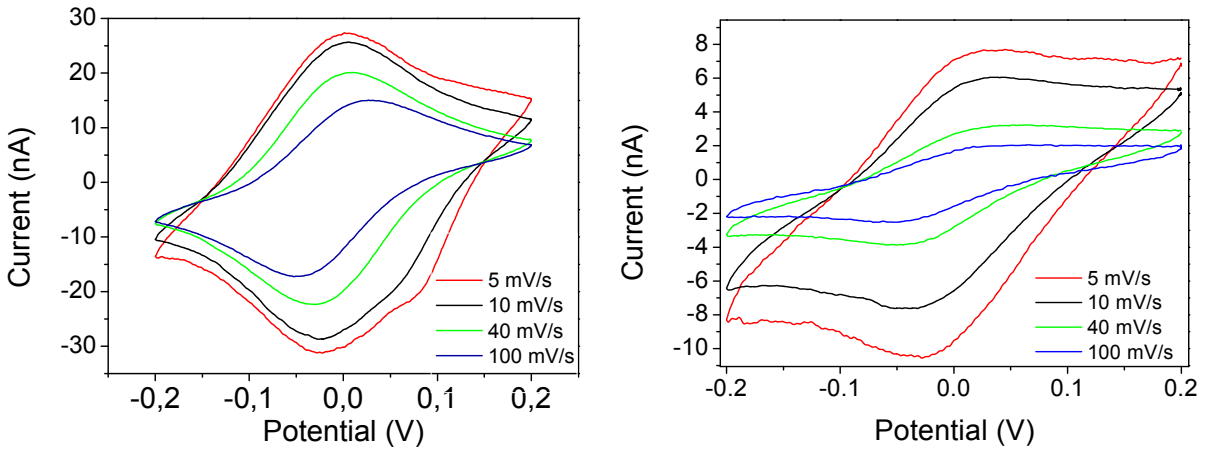

Figure 57 Cyclic voltammetry of Au-MUA/MU-cyt c-(PASA-cyt c)$_4$ multilayer coated electrodes for human wild-type (left) and G77K (right) measured at different scan rates. The current values of the voltammograms are normalized to 5 mV/s by dividing the values by the factor [(actual scan rate) / (5 mV/s)].

Overall the investigations show, that the different cyt c proteins exhibit not only a different adsorption behavior during the multilayer assembly but also a different kinetic electrochemical behavior with a limiting inter-protein electron transfer. However, electrochemically active multilayer electrodes can be constructed not only with horse heart cyt c but also with at least two human forms of the redox protein.

4.4.2 Multilayers of different cytochrome c forms with BOD and PASA

In order to build up new enzyme containing assemblies with the four different cyt c proteins the cyt c monolayer electrodes were incubated alternating in solutions of PASA and a cyt.c/BOD mixture allowing an immobilization of BOD in multiple layers (Dronov, Kurth, Möhwald, Frieder W. Scheller, and Lisdat 2008). The resulting multilayer electrode is schematically shown in Figure 51. The relevant electron transfer steps are depicted in the scheme of Figure 58. Two additional steps have to be considered: the electron transfer from cyt c to the enzyme BOD (step 3) and from BOD to molecular oxygen (step 4).

With all four constructed cyt c-BOD multilayer electrodes a catalytic current can be observed at low scan rates (Figure 59). Hence a successful electron transfer from the electrode via cyt c and BOD to oxygen is achieved. However, both mutant multilayer electrodes show a significantly smaller catalytic activity to oxygen reduction compared to the human and horse form. To evaluate the behavior in more detail a scan rate variation is also conducted here as it has been done for the layered electrodes without BOD.

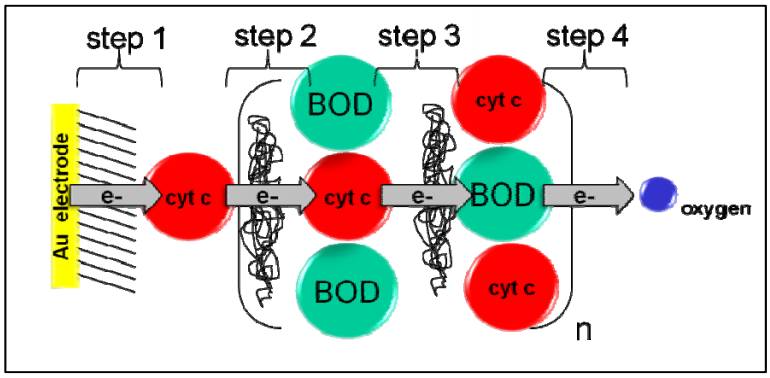

Figure 58 Schematic representation of a Au-MUA/MU-cyt c-(PASA-cyt c/BOD)$_n$ multilayer coated electrode (left) and the relevant electron transfer steps (right)

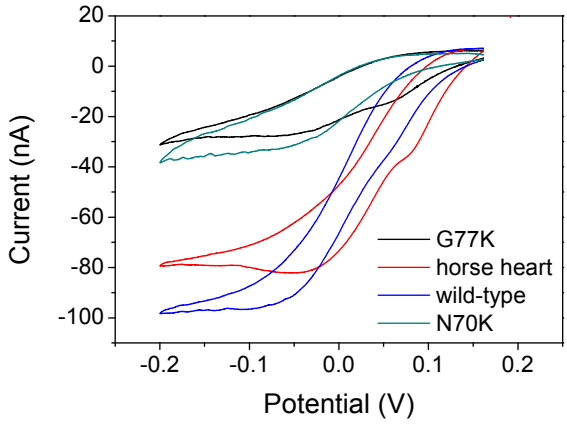

Figure 59 Cyclic voltammetry of Au-MUA/MU-cyt c-(PASA-cyt c/BOD)$_4$ multilayer electrodes, scan rate 2.5 mV/s

Cyclic voltammograms at three different scan rates for the four different cyt c forms normalized to 5 mV/s are presented in Figure 60. Beside the different magnitude of the reduction current at 5 mV/s it is also obvious that at higher scan rates the catalytic current disappears. Although this effect appears for all four cyt c forms, a difference in behavior is observable. For instance, at 40 mV/s for the horse heart electrode still a large impact of the catalytic reaction on the cyclic voltammogram can be seen, whereas for N70K the catalytic current disappears at this scan rate.

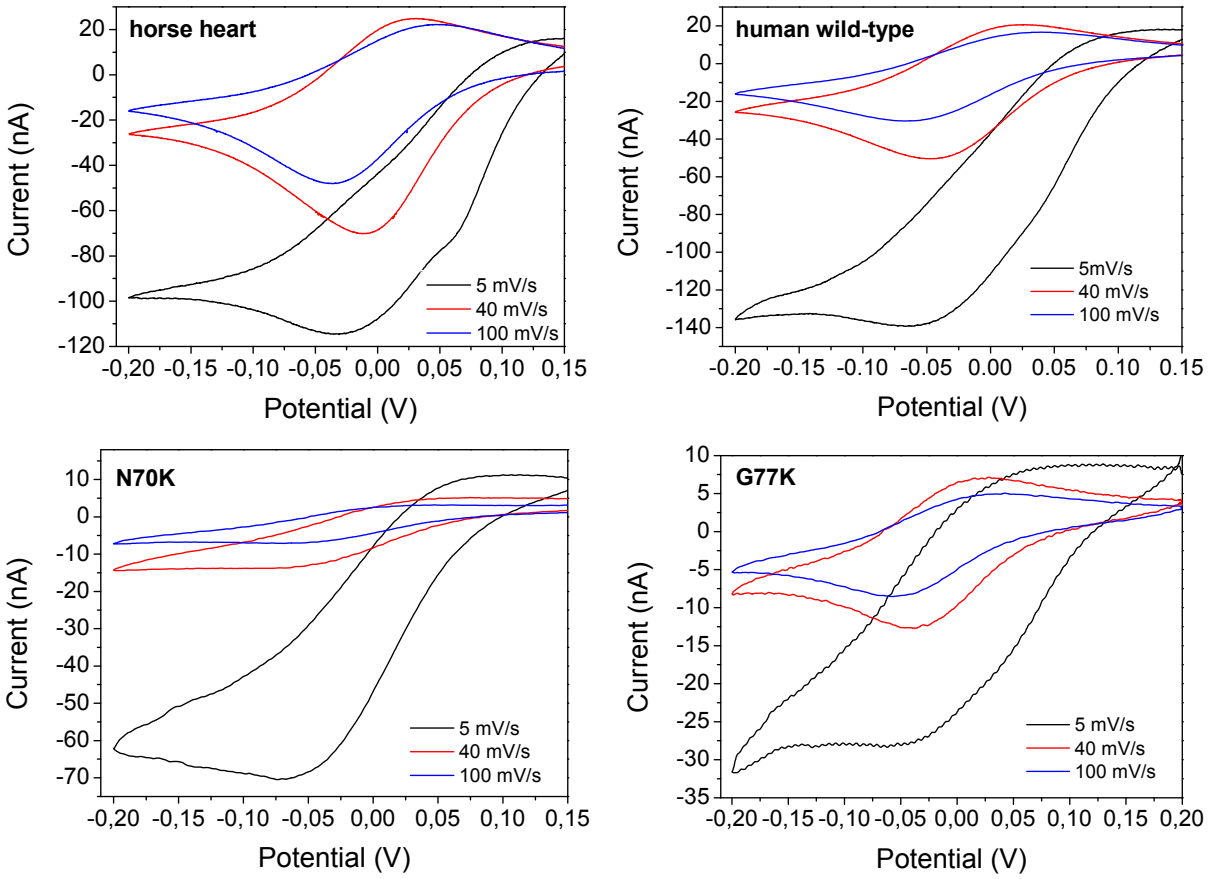

Figure 60 Cyclic voltammetry of Au-MUA/MU-cyt c-(PASA-cyt c/BOD)$_4$ multilayer coated electrodes measured at different scan rates. The current values are normalized to 5 mV/s by dividing the values by the factor [(actual scan rate) / (5 mV/s)].

Since the catalytic currents at low scan rate follow the oxygen concentration, as it has already been shown with horse heart/BOD multilayers in a previous study (Dronov, Kurth, Möhwald, Frieder W. Scheller, and Lisdat 2008), the oxygen conversion of BOD is the limiting step in the signal chain. However, at higher scan rates the catalytic current disappears and the system behaves similar to a multilayer assembly with only cyt c, because the scan rate is here too high to allow a transfer of the electrons to the BOD. Since the reaction rate for the immobilized protein is not known, the limiting process cannot be unambiguously identified, but

the decrease in electro-active amount of the only cyt c containing system indicates that cyt c - cyt c electron transfer (step 2) is the rate-limiting step.

A deeper understanding of the kinetics of the electron transfer processes is provided by the evaluation of the different normalized peak current values for both the reduction and oxidation presented in Figure 61. The increasing reduction current with decreasing scan rate clearly demonstrates the catalytic process at low scan rates. At higher scan rates the catalytic current disappears. However the current does not remain at a certain level, but shows the tendency of further decrease. This behavior is less pronounced for the horse cyt c. This is in agreement with the behavior of multilayers consisting only of cyt c as analyzed before. Here the amount of electrode addressable horse cyt c decreases less steeply than for the other multilayer electrodes.

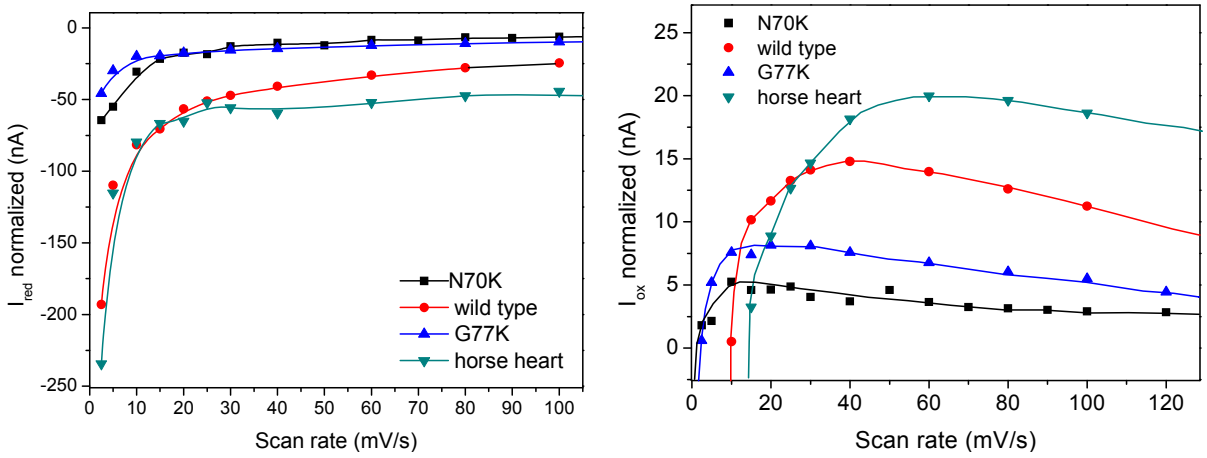

Figure 61 Normalized cathodic (I_{red}, left) and anodic (I_{ox}, right) peak current values of Au-MUA/MU-cyt c-(PASA-cyt c/BOD)$_4$ multilayer coated electrodes measured at different scan rates. Current values are derived from three independent electrodes.

Regarding the efficiency of the multilayer electrode the currents for the wild-type and horse heart/BOD multilayers do not differ significantly, although the reaction rate constant of the human form was determined to be higher. This is probably due to the slightly decreased cyt c self exchange rate of human cyt c. The G77K/BOD multilayer electrode showed a clearly decreased efficiency compared to all other electrodes. To a large extent this is because only a small amount of cyt c could be adsorbed, and also the decreased self-exchange rate contributes to the behavior. Similarly, the N70K/BOD multilayer electrode exhibits a decreased efficiency with respect to the human and horse heart cyt c. However, here the immobilization process was not hindered (see 4.4.1.1). Thus for this mutant/BOD electrode step 2 and step 3 are limiting the catalytic current: The rate constant for the reaction with BOD is decreased and already at rather low scan rates the range of the cyt c self exchange rate is reached. This is the reason why we only see a small reduction peak current in Figure 61 (left). However it has to be noted, that the

amount of BOD molecules embedded within the layers cannot be given exactly. We assume that the amount of BOD immobilized goes with the amount of cyt c adsorbed without the presence of BOD.

Also the normalized oxidation peak currents plotted against the scan rate, presented in the right diagram of Figure 61, reflect the described behavior well. It can be seen that for all mutants at low scan rates the cyt c oxidation current disappears. At higher scan rates the cyt c redox peak becomes visible and so the peak current increases. However, the oxidation current does not remain at a certain level since with further enhanced scan rates the electrode addressable amount of cyt c decreases as described before, and so does the oxidation peak current. The different magnitudes of the maximum oxidation peaks reflect therefore the order of differences found for the cyt c self exchange rate.

5 SUMMARY

The small redox protein cyt c covers a large research area since many decades. At present time it is popular mainly from two points of view: newly discovered functionality beyond the role as an electron transfer carrier in the respiratory chain is raising a lot of interest. Besides, it represents also a favorite component in bioelectronic systems, since the protein is stable and its electron transfer properties are easy to study. Both recombinant expression and protein engineering offer the possibility to investigate the functionality of the rarely available human form of cyt c and moreover specially designed mutant forms of cyt c.

The aim of this thesis is the design, expression and purification of human cytochrome c mutants and their characterization with regard to electrochemical and structural properties as well as with respect to the reaction with the superoxide radical and the selected proteins sulfite oxidase from human and fungi bilirubin oxidase. All three interaction partners are studied here for the first time with human cyt c and with mutant forms of cyt c.

A further aim is the incorporation of the different cyt c forms in two bioelectronic systems: an electrochemical superoxide biosensor with an enhanced sensitivity and a protein multilayer assembly with and without bilirubin oxidase on electrodes.

The first part of the thesis is dedicated to the design, expression and characterization of the mutants. A focus is here the electrochemical characterization of the protein in solution and immobilized on electrodes. Further the reaction of these mutants with superoxide was investigated and the possible reaction mechanisms are discussed.

The selection of mutation sites was mainly driven by the chance to increase the reaction rate with the negatively charged radical superoxide via an enhanced electrostatic guidance by exchanging neutral and negatively charged amino acids by positively charged amino acids. In three mutation rounds in total sixteen single lysine, two single arginine and two double lysine human cyt c mutants were successfully designed, expressed and purified. All engineered cyt c forms were further characterized thoroughly. Significant differences in the reaction rate with superoxide, the formal potential, the diffusion constant, the behavior at SAM coated electrodes and in the UV-Vis spectra were found for several human cyt c mutants. Six of the twenty mutants were not affected with respect to the properties investigated (A50K, D62K, E69K, N70K, G77K and V83K). For five mutants structural changes were observed (Y46K, Y74K, I81K, F82K and E66K-F82K) which account for some of the changed properties. This underlines that also single charge-changing point mutations located rather on the surface of cyt c can have a considerable impact on the structure and/or properties of the redox protein. However, despite the diffusion coefficient no changed properties were found between the horse heart and the human wild-type

protein. Since the sequence differences between both forms affect mostly the hydrophobicity of the cyt c molecule it can be concluded that this is not an important factor for the other investigated properties (reaction with superoxide, formal potential, diffusion constant, behavior at SAM coated electrodes and position of UV-Vis spectra peaks).

The reaction rate constant with superoxide was found to be increased for four single lysine mutants (T63K, E66K, Y74K and F82K) and decreased for six mutants (Y46K, A51K, I57K, I85K and both double mutants). Hence, it could be shown – as it was expected – that the reaction rate between cyt c and superoxide can be enhanced by introducing positively charged lysines. Structural changes are one reason for the enhanced reaction rate as in the case of F82K and Y74K. However, for the two mutants Y46K and I57K the mutations caused a decrease in formal redox potential which clearly can be connected to the decreased rate constant found for both mutants, since the driving force of the reaction is diminished. When the structure is retained the charge distribution is an important factor. Two positions are found where the enhancement for the reaction rate can be explained by electrostatic guidance to this protein area: T63K and E66K. The region, defined between the 60's helix, the 70's loop and the 50's helix, is suggested to be a possible access area for superoxide. This pocket includes also three aromatic amino acids, representing potential stepping stones for an electron hopping process.

For the electrostatic guidance the type of amino acid used for the introduction of the additional charge was found to be important. Arginine mutants did not result in an enhanced interaction, probably due to the different charge distribution. However, when the charge is changed in such a way that a very large area of the protein becomes positively charged, as in case of the double mutant T63K-E66K, electrostatic misguiding can result in a decrease of the reaction rate. This demonstrates that for the reaction of superoxide electrostatic effects are important factors contributing to an efficient electron transfer. Further, these investigations are also a hint for an evolutionary conserved superoxide reaction pathway which might have relevance regarding the proposed role of cyt c as ROS scavenger *in vivo* and as inducer of the apoptotic pathway.

In the second part of the work an amperometric superoxide biosensor with selected human cytochrome c mutants was constructed and the performance of the sensor electrodes was studied. The human wild-type and four of the five mutant electrodes could be applied successfully for the detection of the superoxide radical.

Several important factors for the successful superoxide sensor construction could be identified which can be influenced by the cyt c form used: As it was one aim of this thesis the reaction rate of cyt c with superoxide can influence the sensitivity of the sensor electrode. However there are also other properties as e.g. the amount of electro-active cyt c which can be

covalently immobilized. A decrease here causes a drop of the current density and thus a loss of sensitivity as it is the case for several investigated mutants e.g. for F82K and Y74K. Another point is the heterogeneous electron transfer rate between the electrode and the protein. A decrease can shorten the linear dependence of the current signal on the superoxide concentration. The mutants engineered in this thesis mostly have no altered k_s value or an increased transfer rate constant and hence they have no limitations regarding the sensor performance. Another aspect is represented also by the cyt c's site activities for hydrogen peroxide which have to be considered. The point mutation can increase this activity, as for the mutant Y74K, and cause a decline in selectivity, which may reduce the area of application for the sensors.

In case of the mutant E66K, an increased reaction rate with superoxide is achieved due to the extra positive charge and an electrostatic guidance without any other side effects caused by the mutation. Thus no structural changes, no changes in heterogeneous ET rate, formal potential, and electrode surface coverage or peroxidase activity was observed. Hence, with this mutant an improved superoxide sensor with a by 30 % increased sensitivity compared to former sensor electrodes with horse heart cyt c could be constructed.

In the third part of the thesis the reaction of horse heart cyt c, the human wild-type and seven human cyt c mutants with the two proteins sulfite oxidase and bilirubin oxidase was studied electrochemically and the influence of the mutations on the electron transfer reactions was discussed.

In general taking the reaction rate for the horse heart cyt c as a reference the reaction rate constant for the reaction with BOD was found to be similar to that of SOX although the latter reaction is a proven physiological reaction and for the former until now no physiological importance is known.

For the first time the second order reaction rate constant for human SOX with a cyt c form of the same species could be determined in this thesis. Although the sequence homology between horse heart and human cyt c is only 78% no difference for the rate constants could be observed, indicating no major alterations of the interaction site. The unchanged reaction rates moreover are consistent to the known importance of electrostatic interactions between SOX and cyt c, since the sequence differences account mostly to slight changes in hydrophobicity of the cyt c surface. For all mutant forms catalytic currents could be obtained. However, for some of the mutant forms of human cyt c with introduced positively charged lysines different reaction rates were determined. G77K and N70K have the most pronounced increasing and decreasing effect, respectively. In both cases the affected mutation site is located close to a lysine residue putatively important for the interaction with SOX in the wild-type protein.

In contrast to SOX the reaction between BOD and cyt c differs for the human and horse heart form. This suggests that either also hydrophobic interactions play a role for the reaction between both proteins - since the increased reaction rate for the human form correlates with an increased hydrophobicity - or that the rate is influenced by a putatively changed compactness of the molecule indicated by the different diffusion coefficient. Nevertheless also the mutant forms with additional positive charges have an effect on the reaction rate, indicating also an impact of electrostatic interactions. However, in contrast to the reaction with SOX, only a decreasing effect of the mutations was observed.

Finally protein multilayer electrodes with different cyt form including the mutant forms G77K and N70K which exhibit different reaction rates towards BOD were investigated and BOD together with the wild-type and engineered cyt c was embedded in the multilayer assembly. The relevant electron transfer steps and the kinetic behavior of the multilayer electrodes are investigated since the functionality of electroactive multilayer assemblies with incorporated redox proteins is often limited by the electron transfer abilities of the proteins within the multilayer. The formation via the layer-by-layer technique and the kinetic behavior of the mono and bi-protein multilayer system are studied by SPR and cyclic voltammetry.

It could be demonstrated that electroactive mono-protein multilayers can be constructed also with other cyt c forms than horse heart cyt c. Hence, the assembly is not limited to this protein. However, it was observed that the amount of protein deposited by the layer-by-layer approach can be negatively influenced by a mutation as in the case of the mutant G77K and thus can limit the current density. The distinct kinetic behavior of the multilayer system with different cyt c forms indicates strongly that a decreased cyt c self exchange rate – as for the N70K electrode – can be also a limiting factor. This corroborates a dominating role of the redox protein for the electron transfer through the system.

Also multilayer electrodes with BOD and different forms of cyt c show a diverse catalytic behavior for the signal chain from the electrode via cyt c to BOD and molecular oxygen. The G77K/BOD electrode shows the smallest catalytic current, mainly owing to small amount of protein which could be adsorbed on the electrodes. Kinetic studies suggest a limitation of the catalytic current if the cyt c self exchange rate is decreased compared to the horse heart cyt c/ BOD multilayer electrode such as in the case of N70K .

Overall three different parameters were identified here which influence the behavior of the BOD/cyt c multilayers: the amount of molecules per layer which can be immobilized on the electrodes, the cyt c self-exchange rate and the rate constant for the reaction with BOD.

In conclusion this thesis shows that protein engineering is a helpful instrument to study protein reactions as well as electron transfer mechanisms of complex bioelectronic systems (such as bi-protein multilayers). Furthermore, the possibility to design tailored recognition elements for the construction of biosensors with an improved performance is demonstrated.

REFERENCES

Abreu, I. a, and Cabelli, Diane E (2010). Superoxide dismutases-a review of the metal-associated mechanistic variations. Biochimica et biophysica acta 1804, 263-74.

Allen, J. W. a, Daltrop, O., Stevens, J. M., and Ferguson, S. J. (2003). C-type cytochromes: diverse structures and biogenesis systems pose evolutionary problems. Philosophical transactions of the Royal Society of London. Series B, Biological sciences 358, 255-66.

Alvarez-Paggi, D., Martín, D. F., DeBiase, P. M., Hildebrandt, Peter, Martí, M. a, and Murgida, D. H. (2010). Molecular basis of coupled protein and electron transfer dynamics of cytochrome c in biomimetic complexes. Journal of the American Chemical Society 132, 5769-78.

Andolfi, L., Cannistraro, S., Canters, G. W., Facci, P., Ficca, A. G., Van Amsterdam, I. M. C., and Verbeet, M. P. (2002). A poplar plastocyanin mutant suitable for adsorption onto gold surface via disulfide bridge. Archives of biochemistry and biophysics 399, 81-8.

Andreescu, S., Barthelmebs, L., and Marty, J. (2002). acetylcholinesterase on screen-printed electrodes: comparative study between three immobilization methods and applications to the detection of organophosphorus. Analytica Chimica Acta 464, 171-180.

Antiochia, R., Lavagnini, I., and Magno, F. (2001). A general method for the electrochemical evaluation of the bimolecular rate constant in enzyme catalyzed reaction kinetics. Electroanalysis 13, 601-602.

Aon, M. A., Cortassa, S., and O□Rourke, B. (2010). Redox-optimized ROS balance: A unifying hypothesis. Biochimica et biophysica acta.

Ariga, K., and Nakanishi, T., T (2006). Immobilization of biomaterials to nano-assembled films (self-assembled monolayers, Langmuir-Blodgett films, and layer-by-layer assemblies) and their related. Journal of nanoscience and nanotechnology 6, 2278-2301.

Arnold, S., Fenga, Z. Q., Kakiuchia, T., Knoll, W., and Katsumi, N. (1997). Investigation of the electrode reaction of cytochrome c through mixed self-assembled monolayers of alkanethiols on gold(111) surfaces. Journal of Electroanalytical Chemistry 438, 91-97.

Arslan, E., Schulz, H., Zufferey, R., Künzler, P., and Thöny-Meyer, L. (1998). Overproduction of the Bradyrhizobium japonicum c-type cytochrome subunits of the cbb3 oxidase in Escherichia coli. Biochemical and biophysical research communications 251, 744-7.

Avila, A., Gregory, B. W., Niki, Katsumi, and Cotton, T. M. (2000). An Electrochemical Approach to Investigate Gated Electron Transfer Using a Physiological Model System: Cytochrome c Immobilized on Carboxylic Acid-Terminated Alkanethiol Self-Assembled Monolayers on Gold Electrodes. The Journal of Physical Chemistry B 104, 2759-2766.

Baddam, S., and Bowler, B. E. (2005). Conformationally gated electron transfer in iso-1-cytochrome c: engineering the rate of a conformational switch. Journal of the American Chemical Society 127, 9702-3.

Balkenhohl, T., Adelt, S., Dronov, R., and Lisdat, F. (2008). Oxygen-reducing electrodes based on layer-by-layer assemblies of cytochrome c and laccasse. Electrochemistry Communications 10, 914-917.

Banci, L., Bertini, I., Rosato, A., and Varani, G. (1999). Mitochondrial cytochromes c: a comparative analysis. Journal of Biological Inorganic Chemistry 4, 824–837.

Bard, A. J., and Faulkner, L. R. (1980). Electrochemical Methods, Fundamentals and Applications (New York: John Wiley and Sons,).

Bartosz, G. (2009). Reactive oxygen species: destroyers or messengers? Biochemical pharmacology 77, 1303-15.

Basova, L. V. et al. (2007). Cardiolipin switch in mitochondria: shutting off the reduction of cytochrome c and turning on the peroxidase activity. Biochemistry 46, 3423-34.

Battistuzzi, G., Borsari, M., Bortolotti, C. A., Di Rocco, G., Ranieri, A., and Sola, M. (2007). Effects of mutational (Lys to Ala) surface charge changes on the redox properties of electrode-immobilized cytochrome c. The journal of physical chemistry. B 111, 10281-7.

Bayir, H., and Kagan, V. E. (2008). Bench-to-bedside review: Mitochondrial injury, oxidative stress and apoptosis--there is nothing more practical than a good theory. Critical care (London, England) 12, 206.

Becker, L. B., Hoek, T. L. vanden, Shao, Z. H., Li, C. Q., and Schumacker, P. T. (1999). Generation of superoxide in cardiomyocytes during ischemia before reperfusion. The American journal of physiology 277, H2240-6.

Behar, D., Czapski, G., Rabani, J., Dorfman, L. M., and Schwarz, H. A. (1970). Acid dissociation constant and decay kinetics of the perhydroxyl radical. The Journal of Physical Chemistry 74, 3209–3213.

Beissenhirtz, M.K., Kwan, R. C. H., Ko, K., Renneberg, R., Scheller, F., and Lisdat, F. (2004). Comparing an in vitro electrochemical measurement of superoxide scavenging activity with an in vivo assessment of antioxidant potential in Chinese tonifying herbs. Phytotherapy Research 18, 149–153.

Beissenhirtz, M.K., Scheller, F.W., and Lisdat, F. (2004). A superoxide sensor based on a multilayer cytochrome c electrode. Anal. Chem 76, 4665–4671.

Beissenhirtz, Moritz Karl, Kafka, J., Schäfer, D., Wolny, M., and Lisdat, F. (2005). Electrochemical Quartz Crystal Microbalance Studies on Cytochrome c/Polyelectrolyte Multilayer Assemblies on Gold Electrodes. Electroanalysis 17, 1931-1937.

Beissenhirtz, Moritz Karl, Scheller, Frieder W., and Lisdat, F. (2003). Immobilized cytochrome c sensor in organic/aqueous media for the characterization of hydrophilic and hydrophobic antioxidants. Electroanalysis 15, 1425-1435.

Beissenhirtz, Moritz Karl, Scheller, Frieder W., Stöcklein, W. F. M., Kurth, D. G., Möhwald, H., and Lisdat, F. (2004). Electroactive cytochrome c multilayers within a polyelectrolyte assembly. Angewandte Chemie (International ed. in English) 43, 4357-60.

Beissenhirtz, Moritz Karl, Scheller, Frieder W., Viezzoli, Maria Silvia, and Lisdat, F. (2006). Engineered superoxide dismutase monomers for superoxide biosensor applications. Analytical Chemistry 78, 928-935.

Berners-Price, S. J., Bertini, I., Gray, H. B., Spyroulias, G. A., and Turano, P. (2004). The stability of the cytochrome c scaffold as revealed by NMR spectroscopy. Journal of Inorganic Biochemistry 98, 814.

Bertini, I., Cavallaro, G., and Rosato, Antonio (2006). Cytochrome c: occurrence and functions. Chem. Rev 106, 90–115.

Bertini, I., Luchinat, C., Parigi, G., and Walker, F A (1999). Heme methyl H-1 chemical shifts as structural parameters in some low-spin ferriheme proteins. Journal of Biological Inorganic Chemistry 4, 515-519.

Bokov, A., Chaudhuri, A., and Richardson, A. (2004). The role of oxidative damage and stress in aging. Mechanisms of ageing and development 125, 811-26.

Bonk, S. M., and Lisdat, F. (2009). Layer-by-layer assembly of electro-active gold nanoparticle/cytochrome c multilayers. Biosensors & bioelectronics 25, 739-44.

Borgmann, S. (2009). Electrochemical quantification of reactive oxygen and nitrogen : challenges and opportunities. Analytical and Bioanalytical Chemistry, 95-105.

Brautigan, D., Ferguson-Miller, S, and Margoliash, E. (1978). Definition of cytochrome c binding domains by chemical modification. J. Biol. Chem, 130-139.

Brown, G. C., and Borutaite, V. (2008). Regulation of apoptosis by the redox state of cytochrome c. Biochimica et biophysica acta 1777, 877-81.

Bushnell, G. W., Louie, G. V., and Brayer, G. D. (1990). High-resolution three-dimensional structure of horse heart cytochrome c. Journal of molecular biology 214, 585-95.

Butler, J., Davies, D., and Sykes, A., WH (1981). Use of singly modified cytochrome c derivatives to determine the site for electron transfer in reactions with inorganic complexes. Journal of the VII, 469-471.

Butler, J., and Halliwell, B. (1982). Reaction of iron-EDTA chelates with the superoxide radical. Archives of biochemistry and biophysics 218, 174-8.

Butler, J., Jayson, G., and Swallow, A. (1975). The reaction between the superoxide anion radical and cytochrome c. Biochimica et Biophysica Acta (BBA)-Bioenergetics 408, 215–222.

Butler, J., Koppenol, W. H., and Margoliash, E. (1982). Kinetics and mechanism of the reduction of ferricytochrome c by the superoxide anion. Journal of Biological Chemistry 257, 10747.

Buttemeyer, R., Philipp, A. W., Mall, J. W., Ge, B., Scheller, Frieder W., and Lisdat, F. (2002). In vivo measurement of oxygen-derived free radicals during reperfusion injury. Microsurgery 22, 108-113.

Calvo, E. J., Etchenique, R., Pietrasanta, L., Wolosiuk, A., and Danilowicz, C. (2001). Layer-By-Layer Self-Assembly of Glucose Oxidase and Os(Bpy) 2 ClPyCH 2 NH−poly(Allylamine) Bioelectrode. Analytical Chemistry 73, 1161-1168.

Calvo, E. J., Flexer, V., Tagliazucchi, M., and Scodeller, P. (2010). Effects of the nature and charge of the topmost layer in layer by layer self assembled amperometric enzyme electrodes. Physical chemistry chemical physics : PCCP.

Campanella, L., Bonanni, A., Favero, G., and Tomassetti, M. (2003). Determination of antioxidant properties of aromatic herbs, olives and fresh fruit using an enzymatic sensor. Analytical and Bioanalytical Chemistry 375, 1011-1016.

Campàs, M., Prieto-Simón, B., and Marty, J.-louis (2009). A review of the use of genetically engineered enzymes in electrochemical biosensors. Seminars in cell & developmental biology 20, 3-9.

Caroppi, P., Sinibaldi, F., Fiorucci, L., and Santucci, R. (2009). Apoptosis and Human Diseases: Mitochondrion Damage and Lethal Role of Released Cytochrome c as Proapoptotic Protein. CURRENT MEDICINAL CHEMISTRY 16, 4058-4065.

Caruana, D. J., and Howorka, S. (2010). Biosensors and biofuel cells with engineered proteins. Molecular bioSystems 6, 1548-56.

Caruso, F., Niikura, K., Furlong, D. N., and Okahata, Y. (1997). 2. Assembly of Alternating Polyelectrolyte and Protein Multilayer Films for Immunosensing. Langmuir 13, 3427-3433.

Casalini, S., Battistuzzi, G., Borsari, M., Bortolotti, C. A., Di Rocco, G., Ranieri, A., and Sola, M. (2010). Electron transfer properties and hydrogen peroxide electrocatalysis of cytochrome c variants at positions 67 and 80. The journal of physical chemistry. B 114, 1698-706.

Casalini, S., Battistuzzi, G., Borsari, M., Bortolotti, C. A., Ranieri, A., and Sola, M. (2008). Electron transfer and electrocatalytic properties of the immobilized methionine80alanine cytochrome c variant. The journal of physical chemistry. B 112, 1555-63.

Casalini, S., Battistuzzi, G., Borsari, M., Ranieri, A., and Sola, M. (2008). Catalytic reduction of dioxygen and nitrite ion at a Met80Ala cytochrome c-functionalized electrode. Journal of the American Chemical Society 130, 15099-104.

Chambers, J. P., Arulanandam, B. P., Matta, L. L., Weis, A., and Valdes, J. J. (2008). Biosensor recognition elements. Current Issues in Molecular Biology 10, 1-12.

Chen, L.-Q., Zhang, X.-E., Xie, W.-H., Zhou, Y.-F., Zhang, Z.-P., and Cass, A. E. G. (2002). Genetic modification of glucose oxidase for improving performance of an amperometric glucose biosensor. Biosensors & bioelectronics 17, 851-7.

Chen, R., Warden, J. T., and Stenken, J. A. (2004). Microdialysis sampling combined with electron spin resonance for superoxide radical detection in microliter samples. Analytical chemistry 76, 4734-40.

Chen, X., Zhang, Laibin, Zhang, Liang, Wang, Jun, Liu, Haiying, and Bu, Y. (2009). Proton-regulated electron transfers from tyrosine to tryptophan in proteins: through-bond mechanism versus long-range hopping mechanism. The journal of physical chemistry. B 113, 16681-8.

Concar, D.W., Hill, H. A. O., Moore, G. R., Whitford, D., and Williams, R.J.P. (1986). The modulation of cytochrome c electron self-exchange by site-specific chemical modification and anion binding. FEBS letters 206, 15–19.

Cordes, M., and Giese, B. (2009). Electron transfer in peptides and proteins. Chemical Society reviews 38, 892-901.

Cracknell, J. A., Vincent, K. A., and Armstrong, F. A. (2008). Enzymes as working or inspirational electrocatalysts for fuel cells and electrolysis. Chemical reviews 108, 2439-61.

Craig, M., and Slauch, J. M. (2009). Phagocytic superoxide specifically damages an extracytoplasmic target to inhibit or kill Salmonella. PloS one 4, e4975.

Cudd, A., and Fridovich, I. (1982). Parallel electrostatic effects in the interactions of superoxide with cytochrome c and with superoxide dismutase. FEBS letters 144, 181-182.

Davis, K. L., Drews, B. J., Yue, H., Waldeck, D.H., Knorr, K., and Clark, R. a (2008). Electron-Transfer Kinetics of Covalently Attached Cytochrome c/SAM/Au Electrode Assemblies. Journal of Physical Chemistry C 112, 6571-6576.

De Biase, P. M., Paggi, D. A., Doctorovich, F., Hildebrandt, Peter, Estrin, D. a, Murgida, D. H., and Marti, M. a (2009). Molecular basis for the electric field modulation of cytochrome C structure and function. Journal of the American Chemical Society 131, 16248-56.

Decher, G., Eckle, M., Schmitt, Johannes, and Struth, B. (1998). Layer-by-layer assembled multicomposite films. Current Opinion in Colloid & Interface Science 3, 32-39.

Decher, G., Hong, J., and Schmitt, J (1992). Buildup of ultrathin multilayer films by a self-assembly process: III. Consecutively alternating adsorption of anionic and cationic polyelectrolytes on charged surfaces. Thin solid films 210-211, 831-835.

Deng, Z., Rui, Q., Yin, X., Liu, H. Q., and Tian, Y. (2008). In vivo detection of superoxide anion in bean sprout based on ZnO nanodisks with facilitated activity for direct electron transfer of superoxide dismutase. Analytical Chemistry 80, 5839-5846.

Descroix, S., and Bedioui, F. (2001). Evaluation of the selectivity of overoxidized polypyrrole/superoxide dismutase based microsensor for the electrochemical measurement of superoxide anion in solution. Electroanalysis 13, 524-528.

Devic, E., Li, D., Dauta, A., Henriksen, P., Codd, G. A., Marty, J.-L., and Fournier, D. (2002). Detection of Anatoxin-a(s) in Environmental Samples of Cyanobacteria by Using a Biosensor with Engineered Acetylcholinesterases. Applied and Environmental Microbiology 68, 4102-4106.

Di, J. W., Bi, S. P., and Zhang, M. (2004). Third-generation superoxide anion sensor based on superoxide dismutase directly immobilized by sol-gel thin film on gold electrode. Biosensors & Bioelectronics 19, 1479-1486.

Dickerson, R., Takano, T., and Eisenberg, D., OB (1971). Ferricytochrome c. I. General features of the horse and bonito proteins at 2.8 A resolution. The Journal of, 1511-1535.

Dixon, D. W., Hong, X., and Woehler, S. E. (1989). Electrostatic and steric control of electron self-exchange in cytochromes c, c551, and b5. Biophysical journal 56, 339-51.

Dronov, R., Kurth, D. G., Möhwald, H., Scheller, Frieder W, Friedmann, J., Pum, D., Sleytr, U. B., and Lisdat, F. (2008a). Self-assembly of S-layer-enveloped cytochrome c polyelectrolyte multilayers. Langmuir : the ACS journal of surfaces and colloids 24, 8779-84.

Dronov, R., Kurth, D. G., Möhwald, H., Scheller, Frieder W., and Lisdat, F. (2007). A self-assembled cytochrome c/xanthine oxidase multilayer arrangement on gold. Electrochimica Acta 53, 1107-1113.

Dronov, R., Kurth, D. G., Möhwald, H., Scheller, Frieder W., and Lisdat, F. (2008). Communication in a protein stack: electron transfer between cytochrome c and bilirubin oxidase within a polyelectrolyte multilayer. Angewandte Chemie (International ed. in English) 47, 3000-3.

Dronov, R., Kurth, D. G., Möhwald, H., Spricigo, R., Leimkühler, S., Wollenberger, U., Rajagopalan, K V, Scheller, Frieder W., and Lisdat, F. (2008b). Layer-by-layer arrangement by protein-protein interaction of sulfite oxidase and cytochrome c catalyzing oxidation of sulfite. Journal of the American Chemical Society 130, 1122-3.

Dronov, R., Kurth, D. G., Scheller, Frieder W., and Lisdat, F. (2007). Direct and cytochrome c mediated electrochemistry of bilirubin oxidase on gold. Electroanalysis 19, 1642-1646.

Döpner, S., Hildebrandt, P, Rosell, F. I., Mauk, A. G., Walter, M. von, Buse, G., and Soulimane, T. (1999). The structural and functional role of lysine residues in the binding domain of cytochrome c in the electron transfer to cytochrome c oxidase. European journal of biochemistry / FEBS 261, 379-91.

Endo, K., Miyasaka, T., Mochizuki, S., Aoyagi, S., Himi, N., Asahara, H., Tsujioka, K., and Sakai, K. (2002). Development of a superoxide sensor by immobilization of superoxide dismutase. Sensors and Actuators B: Chemical 83, 30–34.

Feng, C., Tollin, G., and Enemark, J. H. (2007). Sulfite oxidizing enzymes. Biochimica et Biophysica Acta (BBA) - Proteins & Proteomics 1774, 527-539.

Feng, Z., Imabayashi, S., Kakiuchi, T., and Niki, K (1997). Long-range electron-transfer reaction rates to cytochrome c across long-and short-chain alkanethiol self-assembled monolayers: Electroreflectance studies. Journal of the Chemical 93, 1367-1370.

Ferapontova, E., Grigorenko, V., and Egorov, A., T (2001). Mediatorless biosensor for H2O2 based on recombinant forms of horseradish peroxidase directly adsorbed on polycrystalline gold. Biosensors and 16, 147-157.

Ferapontova, E., Ruzgas, Tautgirdas, and Gorton, Lo (2003). Direct electron transfer of heme-and molybdopterin cofactor-containing chicken liver sulfite oxidase on alkanethiol-modified gold electrodes. Anal. Chem 75, 4841-4850.

Ferri, S., and Sode, K. (2010). Amino acid substitution at the substrate-binding subsite alters the specificity of the Phanerochaete chrysosporium cellobiose dehydrogenase. Biochemical and Biophysical Research Communications 391, 1246-1250.

Fink, B., Laude, K., McCann, L., Doughan, A., Harrison, D. G., and Dikalov, S. (2004). Detection of intracellular superoxide formation in endothelial cells and intact tissues using dihydroethidium and an HPLC-based assay. American journal of physiology. Cell physiology 287, C895-902.

Fisher, C. L., Cabelli, D E, Tainer, J. a, Hallewell, R. a, and Getzoff, E. D. (1994). The role of arginine 143 in the electrostatics and mechanism of Cu,Zn superoxide dismutase: computational and experimental evaluation by mutational analysis. Proteins 19, 24-34.

Folcarelli, S., Venerini, F., Battistoni, A., O□Neill, P., Rotilio, Giuseppe, and Desideri, Alessandro (1999). Toward the Engineering of a Super Efficient Enzyme. Biochemical and biophysical research communications 256, 425–428.

Frasca, S., Graberg, T. von, Feng, J.-J., Thomas, A., Smarsly, B. M., Weidinger, I. M., Scheller, Frieder W., Hildebrandt, Peter, and Wollenberger, U. (2010). Mesoporous Indium Tin Oxide as a Novel Platform for Bioelectronics. ChemCatChem 2, 839-845.

Fridovich, I. (1972). Superoxide radical and superoxide dismutase. Accounts of Chemical Research 5, 321-326.

Fridovich, I. (1978). Superoxide radicals, superoxide dismutases and the aerobic lifestyle. Photochemistry and Photobiology 28, 733-741.

García-Heredia, J. M., Díaz-Moreno, I., Nieto, P. M., Orzáez, M., Kocanis, S., Teixeira, M., Pérez-Payá, E., Díaz-Quintana, A., and De la Rosa, M. a (2010). Nitration of tyrosine 74 prevents human cytochrome c to play a key role in apoptosis signaling by blocking caspase-9 activation. Biochimica et biophysica acta 1797, 981-993.

Garrett, R. M., Johnson, J L, Graf, T. N., Feigenbaum, a, and Rajagopalan, K V (1998). Human sulfite oxidase R160Q: identification of the mutation in a sulfite oxidase-deficient patient and expression and characterization of the mutant enzyme. Proceedings of the National Academy of Sciences of the United States of America 95, 6394-8.

Ge, B., and Lisdat, F. (2002). Superoxide sensor based on cytochrome c immobilized on mixed-thiol SAM with a new calibration method. Analytica Chimica Acta 454, 53–64.

Ge, B., Scheller, Frieder W., and Lisdat, F. (2003). Electrochemistry of immobilized CuZnSOD and FeSOD and their interaction with superoxide radicals. Biosensors and Bioelectronics 18, 295-302.

Getzoff, E. D., Cabelli, D.E., Fisher, C. L., Parge, H. E., Viezzoli, M.S., Banci, L., and Hallewell, R. A. (1992). Faster superoxide dismutase mutants designed by enhancing electrostatic guidance. Nature 358, 347-351.

Getzoff, E. D., Tainer, J. A., Weiner, P. K., Kollman, P. A., Richardson, J. S., and Richardson, D. C. (1983). Electrostatic recognition between superoxide and copper, zinc superoxide dismutase. Nature 306, 287-290.

Giannattasio, S., Atlante, A., Antonacci, L., Guaragnella, N., Lattanzio, P., Passarella, S., and Marra, E. (2008). Cytochrome c is released from coupled mitochondria of yeast en route to acetic acid-induced programmed cell death and can work as an electron donor and a ROS scavenger. FEBS letters 582, 1519-25.

Giorgio, M. et al. (2005). Electron transfer between cytochrome c and p66Shc generates reactive oxygen species that trigger mitochondrial apoptosis. Cell 122, 221-33.

Gobi, K. V., and Mizutani, F. (2000). Efficient mediatorless superoxide sensors using cytochrome c-modified electrodes: surface nano-organization for selectivity and controlled peroxidase activity. Journal of Electroanalytical Chemistry 484, 172-181.

Gonzalvez, F., and Gottlieb, E. (2007). Cardiolipin: setting the beat of apoptosis. Apoptosis : an international journal on programmed cell death 12, 877-85.

Greene, R. M., Betz, S. F., Hilgen-Willis, S., Auld, D. S., Fencl, J. B., and Pielak, G. J. (1993). Changes in global stability and local structure of cytochrome c upon substituting phenylalanine-82 with tyrosine. Journal of inorganic biochemistry 51, 663–676.

Gunner, M. R. &, and Honig, B. (1991). Electrostatic control of midpoint potentials in the cytochrome subunit of the Rhodopseudomonas viridis reaction center. Proc. Natl. Acad. Sci. USA 88, 9151-9155.

Gupte, S. S., and Hackenbrock, C. R. (1988). Multidimensional diffusion modes and collision frequencies of cytochrome c with its redox partners. The Journal of biological chemistry 263, 5241-7.

Hart, J. P., Abass, A. K., and Cowell, D. (2002). Development of disposable amperometric sulfur dioxide biosensors based on screen printed electrodes. Biosensors & bioelectronics 17, 389-94.

Henderson, J. R., Swalwell, H., Boulton, S., Manning, Philip, McNeil, C. J., and Birch-Machin, M. a (2009). Direct, real-time monitoring of superoxide generation in isolated mitochondria. Free radical research 43, 796-802.

Hille, R. (2006). Structure and Function of Xanthine Oxidoreductase. European Journal of Inorganic Chemistry 2006, 1913-1926.

Hwang, T. (1995). Water Suppression That Works. Excitation Sculpting Using Arbitrary Wave-Forms and Pulsed-Field Gradients. Journal of Magnetic Resonance, Series A 112, 275-279.

Ignatov, S., Shishniashvili, D., Ge, B., Scheller, Frieder W., and Lisdat, F. (2002). Amperometric biosensor based on a functionalized gold electrode for the detection of antioxidants. Biosensors & Bioelectronics 17, 191-199.

Imlay, J. a (2008). Cellular defenses against superoxide and hydrogen peroxide. Annual review of biochemistry 77, 755-76.

Inglis, S. C., Guillemette, J. G., Johnson, J. A., and Smith, M. (1991). Analysis of the invariant Phe82 residue of yeast iso-1-cytochrome c by site-directed mutagenesis using a phagemid yeast shuttle vector. Protein Engineering 4, 569-574.

Jeng, W.-Y., Chen, C. Y., Chang, H. C., and Chuang, W. J. (2002). Expression and characterization of recombinant human cytochrome c in E. coli. Journal of bioenergetics and biomembranes 34, 423–431.

Johnson, Jean L (2003). Prenatal diagnosis of molybdenum cofactor deficiency and isolated sulfite oxidase deficiency. Prenatal diagnosis 23, 6-8.

Jones, D. P. (2006). Redefining oxidative stress. Antioxidants & redox signaling 8, 1865–1879.

Ju, H., Liu, S., Ge, B., Lisdat, F., and Scheller, Frieder W. (2002). Electrochemistry of cytochrome c immobilized on colloidal gold modified carbon paste electrodes and its electrocatalytic activity. Electroanalysis 14, 141–147.

Kagan, V. E. et al. (2005). Cytochrome c acts as a cardiolipin oxygenase required for release of proapoptotic factors. Nature chemical biology 1, 223-32.

Kapp, A., Beissenhirtz, Moritz Karl, Geyer, F., Scheller, Frieder W., Viezzoli, Maria Silvia, and Lisdat, F. (2006). Electrochemical and sensorial behavior of SOD mutants immobilized on gold electrodes in aqueous/organic solvent mixtures. Electroanalysis 18, 1909-1915.

Katz, E., and Willner, I. (2004). Biomolecule-functionalized carbon nanotubes: applications in nanobioelectronics. Chemphyschem : a European journal of chemical physics and physical chemistry 5, 1084-104.

Kevin, L. G., Camara, A. K. S., Riess, M. L., Novalija, E., and Stowe, D. F. (2003). Ischemic preconditioning alters real-time measure of O2 radicals in intact hearts with ischemia and reperfusion. American journal of physiology. Heart and circulatory physiology 284, H566-74.

Kisker, C., Schindelin, H., and Rees, D. C. (1997). Molybdenum-cofactor-containing enzymes: structure and mechanism. Annual review of biochemistry 66, 233-67.

Korshunov, S. S., Krasnikov, B. F., Pereverzev, M. O., and Skulachev, V P (1999). The antioxidant functions of cytochrome c. FEBS letters 462, 192-8.

Kosaka, A., Yamamoto, C., Morishita, Y., and Nakane, K. (1987). Enzymatic determination of bilirubin fractions in serum. Clinical Biochemistry 20, 451-458.

Kowaltowski, A. J., Souza-Pinto, N. C. de, Castilho, R. F., and Vercesi, A. E. (2009). Mitochondria and reactive oxygen species. Free radical biology & medicine 47, 333-43.

Krylov, A. V., Beissenhirtz, Moritz Karl, Adamzig, H., Scheller, Frieder W., and Lisdat, F. (2004). Thick-film electrodes for measurement of superoxide and hydrogen peroxide based on direct protein-electrode contacts. Analytical and Bioanalytical Chemistry 378, 1327-1330.

Krylov, A. V., Sczech, R., and Lisdat, F. (2007). Characterization of antioxidants using a fluidic chip in aqueous/organic media. Analyst 132, 135-141.

Laviron, E. (1979). General expression of the linear potential sweep voltammogram in the case of diffusionless electrochemical systems. Journal of Electroanalytical Chemistry 101, 19–28.

Lehninger, A. L., Nelson, D. L., and Cox, M. M. (2005). Lehninger principles of biochemistry (Wh Freeman).

Lei, C., Lisdat, F., Wollenberger, U., and Scheller, Frieder W. (1999). Cytochrome c/clay-modified electrode. Electroanalysis 11, 274–276.

Lisdat, F., Dronov, R., Möhwald, H., Scheller, Frieder W., and Kurth, D. G. (2009). Self-assembly of electro-active protein architectures on electrodes for the construction of biomimetic signal chains. Chemical communications (Cambridge, England), 274-83.

Lisdat, F., Ge, B., Ehrentreich-Forster, E., Reszka, R., and Scheller, Frieder W. (1999). Superoxide dismutase activity measurement using cytochrome c modified electrode. Analytical Chemistry 71, 1359-1365.

Lisdat, F., Ge, B., Reszka, R., and Kozniewska, E. (1999). An electrochemical method for quantification of the radical scavenging activity of SOD. Fresenius Journal of Analytical Chemistry 365, 494-498.

Liu, X., Kim, C. N., Yang, J., Jemmerson, R., and Wang, X. (1996). Induction of apoptotic program in cell-free extracts: requirement for dATP and cytochrome c. Cell 86, 147-57.

Lu, C., Song, G., and Lin, J. M. (2006). Reactive oxygen species and their chemiluminescence-detection methods. TrAC Trends in Analytical Chemistry 25, 985–995.

Lutkenhaus, J. L., and Hammond, P. T. (2007). Electrochemically enabled polyelectrolyte multilayer devices: from fuel cells to sensors. Soft Matter 3, 804.

Lvov, Y. M., Lu, Z., Schenkman, J. B., Zu, X., and Rusling, J. F. (1998). Direct Electrochemistry of Myoglobin and Cytochrome P450 c am in Alternate Layer-by-Layer Films with DNA and Other Polyions. Journal of the American Chemical Society 120, 4073-4080.

Lvovich, V., and Scheeline, A. (1997). Simultaneous superoxide and hydrogen peroxide detection in peroxidase/NADH oscillator. Analytica Chimica Acta 354, 315-323.

Ly, H. K., Marti, M. a, Martin, D. F., Alvarez-Paggi, D., Meister, W., Kranich, A., Weidinger, I. M., Hildebrandt, Peter, and Murgida, D. H. (2010). Thermal fluctuations determine the electron-transfer rates of cytochrome c in electrostatic and covalent complexes. Chemphyschem : a European journal of chemical physics and physical chemistry 11, 1225-35.

Ma, H., Hu, N, and Rusling, J. F. (2000). Electroactive myoglobin films grown layer-by-layer with poly (styrenesulfonate) on pyrolytic graphite electrodes. Langmuir 16, 4969-4975.

Mailer, K. (1990). Superoxide radical as electron donor for oxidative phosphorylation of ADP. Biochemical and biophysical research communications 170, 59–64.

Maly, J. et al., others (2002). Immobilisation of engineered molecules on electrodes and optical surfaces. Materials Science and Engineering: C 22, 257–261.

Marcus, R. A., and Sutin, N. (1985). Electron transfers in chemistry and biology. Biochimica et Biophysica Acta 811, 265-322.

Marklund, S. (1976). Spectrophotometric study of spontaneous disproportionation of superoxide anion radical and sensitive direct assay for superoxide dismutase. The Journal of biological chemistry 251, 7504-7.

McCord, J. M., and Fridovich, I. (1969). Superoxide dismutase. An enzymic function for erythrocuprein (hemocuprein). Journal of Biological Chemistry 244, 6049.

McCord, J. M., and Fridovich, I. (1968). The reduction of cytochrome c by milk xanthine oxidase. The Journal of biological chemistry 243, 5753-60.

McCord, J. M., and Fridovich, I. (1970). The utility of superoxide dismutase in studying free radical reactions. II. The mechanism of the mediation of cytochrome c reduction by a variety of electron. J Biol Chem 245, 1374-1377.

McNeil, C. J., Smith, K. a, Bellavite, P., and Bannister, J. V. (1989). Application of the electrochemistry of cytochrome c to the measurement of superoxide radical production. Free radical research communications 7, 89-96.

Mei, Y., Yong, J., Liu, Hongtu, Shi, Y., Meinkoth, J., Dreyfuss, G., and Yang, X. (2010). tRNA binds to cytochrome c and inhibits caspase activation. Molecular cell 37, 668-78.

Mesaros, S., Vankova, Z., Grunfeld, S., Mesarosova, A., and Malinski, T. (1998). Preparation and optimization of superoxide microbiosensor. Analytica Chimica Acta 358, 27-33.

Meyer, E., Giegé, P., and Gelhaye, E., N (2005). AtCCMH, an essential component of the c-type cytochrome maturation pathway in Arabidopsis mitochondria, interacts with apocytochrome c. Proceedings of the.

Mills, D. a, Geren, L., Hiser, C., Schmidt, B., Durham, B., Millett, F., and Ferguson-Miller, Shelagh (2005). An arginine to lysine mutation in the vicinity of the heme propionates affects the redox potentials of the hemes and associated electron and proton transfer in cytochrome c oxidase. Biochemistry 44, 10457-65.

Min, L., and Jian-xing, X. (2007). Detoxifying function of cytochrome c against oxygen toxicity. Mitochondrion 7, 13-6.

Mizutani, K. et al. (2010). X-ray analysis of bilirubin oxidase from Myrothecium verrucaria at 2.3 A resolution using a twinned crystal. Acta crystallographica. Section F, Structural biology and crystallization communications 66, 765-70.

Moore, G. R., and Pettigrew, G. W. (1990). Cytochromes c. Evolutionary, Structural and Physicochemical Aspects (Berlin, New York: Springer-Verlag).

Moraes, M. L., Rodrigues Filho, U. P., Oliveira, O. N., and Ferreira, M. (2007). Immobilization of uricase in layer-by-layer films used in amperometric biosensors for uric acid. Journal of Solid State Electrochemistry 11, 1489–1495.

Mozaffari, S. A., Chang, T., and Park, S.-M. (2009). Diffusional Electrochemistry of Cytochrome c on Mixed Captopril/3-Mercapto-1-propanol Self-Assembled Monolayer Modified Gold Electrodes. The Journal of Physical Chemistry C 113, 12434-12442.

Mufazalov, I. a et al. (2009). Preparation and characterization of mouse embryonic fibroblasts with K72W mutation in somatic cytochrome C gene. Molecular Biology 43, 596-603.

Murphy, M. P. (2009). How mitochondria produce reactive oxygen species. The Biochemical journal 417, 1-13.

Nicholson, R., and Shain, I. (1964). Theory of Stationary Electrode Polarography Single Scan and Cyclic Methods Applied to Reversible, Irreversible, and Kinetic Systems. Analytical Chemistry 36, 706-723.

Niki, Katsumi (2002). Interprotein Electron Transfer: An Electrochemical Approach. 電気化学および工業物理化学 70, 82-90.

Niki, Katsumi, Hardy, W., Hill, M., Li, H., and Sprinkle, J., E (2003). Coupling to lysine-13 promotes electron tunneling through carboxylate-terminated alkanethiol self-assembled monolayers to cytochrome c. J. Phys. Chem. 107, 9947-9949.

Ohsaka, T., and Tian, Y. (2002). A superoxide dismutase-modified electrode that detects superoxide ion. Chemical Communications(9, 990-991.

Olteanu, A., Patel, C. N., Dedmon, M. M., Kennedy, S., Linhoff, M. W., Minder, C. M., Potts, P. R., Deshmukh, M., and Pielak, G. J. (2003). Stability and apoptotic activity of recombinant human cytochrome. Biochemical and Biophysical Research Communications 312, 733-740.

Ow, Y.-L. P., Green, D. R., Hao, Z., and Mak, T. W. (2008). Cytochrome c: functions beyond respiration. Nature reviews. Molecular cell biology 9, 532-42.

Paradies, G., Petrosillo, G., Paradies, V., and Ruggiero, F. M. (2010). Oxidative stress, mitochondrial bioenergetics, and cardiolipin in aging. Free radical biology & medicine 48, 1286-95.

Pecina, P. et al. (2010). Phosphomimetic substitution of cytochrome C tyrosine 48 decreases respiration and binding to cardiolipin and abolishes ability to trigger downstream caspase activation. Biochemistry 49, 6705-14.

Penna, G. L., Furlan, S., and Banci, L. (2007). Molecular statistics of cytochrome c: structural plasticity and molecular environment. Journal of biological inorganic chemistry, 180-193.

Pepelina, T. Y., Chertkova, R. V., Dolgikh, D. a, and Kirpichnikov, M. P. (2010). The role of individual lysine residues of horse cytochrome c in the formation of reactive complexes with components of the respiratory chain. Russian Journal of Bioorganic Chemistry 36, 90-96.

Pereverzev, M. O., Vygodina, T. V., Konstantinov, A. A., and Skulachev, V. P. (2003). Cytochrome c, an ideal antioxidant. Biochemical Society transactions 31, 1312-5.

Perry, J. J. P., Shin, D. S., Getzoff, E. D., and Tainer, J. a (2010). The structural biochemistry of the superoxide dismutases. Biochimica et biophysica acta 1804, 245-62.

Pervaiz, S., and Clement, M.-V. (2007). Superoxide anion: oncogenic reactive oxygen species? The international journal of biochemistry & cell biology 39, 1297-304.

Pervaiz, S., and Clément, M.-V. (2002). A permissive apoptotic environment: function of a decrease in intracellular superoxide anion and cytosolic acidification. Biochemical and biophysical research communications 290, 1145-50.

Pielak, G. J., Concar, David W, Moore, G. R., and Williams, Robert J P (1987). The structure of cytochrome c and its relation to recent studies of long-range electron transfer. Protein Engineering 1, 83-88.

Pinton, P. et al. (2007). Protein kinase C beta and prolyl isomerase 1 regulate mitochondrial effects of the life-span determinant p66Shc. Science (New York, N.Y.) 315, 659-63.

Pollock, W. B., Rosell, F. I., Twitchett, M. B., Dumont, M. E., and Mauk, A. G. (1998). Bacterial expression of a mitochondrial cytochrome c. Trimethylation of lys72 in yeast iso-1-cytochrome c and the alkaline conformational transition. Biochemistry 37, 6124-31.

Polticelli, F., Battistoni, A., O□Neill, P., Rotilio, G., and Desideri, A. (1998). Role of the electrostatic loop charged residues in Cu, Zn superoxide dismutase. Protein Science 7, 2354–2358.

Polticelli, F., Bottaro, G., Battistoni, A., Carri, M. T., Djinovic-Carugo, K., Bolognesi, M., O□Neill, Peter, Rotilio, Giuseppe, and Desideri, Alessandro (1995). Modulation of the Catalytic Rate

of Cu,Zn Superoxide Dismutase in Single and Double Mutants of Conserved Positively and Negatively Charged Residues. Biochemistry 34, 6043-6049.

Pond, A., Ledbetter, A., Sono, M., and Goodin, D. (2001). Electron Transfer in Chemistry. In Structure V. Balzani, ed. (Weinheim, Germany: Wiley-VCH Verlag GmbH).

Privett, B. J., Shin, J. H., and Schoenfisch, M. H. (2010). Electrochemical sensors. Analytical chemistry 82, 4723-41.

Qi, P. X., Urbauer, J. L., Fuentes, E. J., Leopold, M. F., and Wand, A. J. (1994). Structural water in oxidized and reduced horse heart cytochrome c. Nature Structural & Molecular Biology 1, 378–382.

Quick, K. (2000). Rapid microplate assay for superoxide scavenging efficiency. Journal of Neuroscience Methods 97, 139-144.

Reece, S. Y., Stubbe, J., and Nocera, D. G. (2005). pH Dependence of charge transfer between tryptophan and tyrosine in dipeptides. Biochimica et biophysica acta 1706, 232-8.

Ren, Y., Wang, W.-H., Wang, Y.-H., Case, M., Qian, W., McLendon, G., and Huang, Z.-X. (2004). Mapping the electron transfer interface between cytochrome b5 and cytochrome c. Biochemistry 43, 3527-36.

Rhoten, M., Burgess, J., and Hawkridge, F. (2002). The reaction of cytochrome from different species with cytochrome oxidase immobilized in an electrode supported lipid bilayer membrane. Journal of Electroanalytical Chemistry 534, 143-150.

Rieder, R., and Bosshard, H. (1980). Comparison of the binding sites on cytochrome c for cytochrome c oxidase, cytochrome bc1, and cytochrome c1. Differential acetylation of lysyl residues in free and. Journal of Biological Chemistry 255, 4732-4739.

Ritzmann, M., and Bosshard, H. (1988). Sulfite oxidase from chicken liver. Further characterization of the role of carboxyl groups in the reaction with cytochrome c. European Journal of Biochemistry 381, 377-381.

Rivera, M., and Walker, F. Ann (1995). Biosynthetic Preparation of Isotopically Labeled Heme. Analytical Biochemistry 230, 295-302.

Rodríguez-Roldán, V., García-Heredia, J. M., Navarro, J. A., Hervás, M., De La Cerda, B., Molina-Heredia, F. P., and De La Rosa, M. A. (2006). A comparative kinetic analysis of the reactivity of plant, horse, and human respiratory cytochrome c towards cytochrome c oxidase. Biochemical and biophysical research communications 346, 1108-13.

Rudolph, M. J., Johnson, Jean L., Rajagopalan, K. V., and Kisker, C. (2003). The 1.2 Å structure of the human sulfite oxidase cytochrome b 5 domain. Acta Crystallographica Section D Biological Crystallography 59, 1183-1191.

Rusling, J. F., Hvastkovs, E. G., Hull, D. O., and Schenkman, J. B. (2008). Biochemical applications of ultrathin films of enzymes, polyions and DNA. Chemical communications (Cambridge, England), 141-54.

Sanders, S. P., Harrison, S. J., Kuppusamy, P., Sylvester, J. T., and Zweier, J. L. (1994). A comparative study of EPR spin trapping and cytochrome c reduction techniques for the measurement of superoxide anions. Free radical biology & medicine 16, 753-61.

Sarauli, D., Tanne, J., Schäfer, D., Schubart, I. W., and Lisdat, F. (2009). Multilayer electrodes: Fully electroactive cyt c on gold as a part of a DNA/protein architecture. Electrochemistry Communications 11, 2288-2291.

Sarsour, E. H., Kumar, M. G., Chaudhuri, L., Kalen, A. L., and Goswami, P. C. (2009). Redox control of the cell cycle in health and disease. Antioxidants & redox signaling 11, 2985-3011.

Scarpeci, T. E., Zanor, M. I., Carrillo, N., Mueller-Roeber, B., and Valle, E. M. (2008). Generation of superoxide anion in chloroplasts of Arabidopsis thaliana during active photosynthesis: a focus on rapidly induced genes. Plant molecular biology 66, 361-78.

Scheller, Frieder W., Jin, W., Ehrentreich-Forster, E., Ge, B., Lisdat, F., Buttemeyer, R., and Wollenberger, U. (1999). Cytochrome C based superoxide sensor for in vivo application. Electroanalysis 11, 703-706.

Schubert, K., Goebel, G., and Lisdat, F. (2009). Bilirubin oxidase bound to multi-walled carbon nanotube-modified gold. Electrochimica Acta.

Schulz, H., Hennecke, H., and Thöny-Meyer, L. (1998). Prototype of a heme chaperone essential for cytochrome c maturation. Science (New York, N.Y.) 281, 1197-200.

Scott, R., and Mauk, G. (1996). Cytochrome C: A Multidisciplinary Approach (Univ Science Books).

Seitz, P. M., Cooper, R., Gatto, G. J., Ramon, F., Sweitzer, T. D., Johns, D. G., Davenport, E. A., Ames, R. S., and Kallal, L. A. (2010). Development of a high-throughput cell-based assay for superoxide production in HL-60 cells. Journal of biomolecular screening : the official journal of the Society for Biomolecular Screening 15, 388-97.

Sezer, M., Spricigo, R., Utesch, T., Millo, D., Leimkühler, S., Mroginski, M. a, Wollenberger, U., Hildebrandt, Peter, and Weidinger, I. M. (2010). Redox properties and catalytic activity of surface-bound human sulfite oxidase studied by a combined surface enhanced resonance Raman spectroscopic and electrochemical approach. Physical chemistry chemical physics : PCCP 12, 7894-903.

Shi, L., Lu, Y., Sun, J., Zhang, J., Sun, C., Liu, J., and Shen, J. (2003). Site-selective lateral multilayer assembly of bienzyme with polyelectrolyte on ITO electrode based on electric field-induced directly layer-by-layer deposition. Biomacromolecules 4, 1161-7.

Shih, C. et al. (2008). Tryptophan-accelerated electron flow through proteins. Science (New York, N.Y.) 320, 1760-2.

Shimizu, A., Kwon, J. H., Sasaki, T., Satoh, T., Sakurai, N., Sakurai, T., Yamaguchi, S, and Samejima, T. (1999). Myrothecium verrucaria bilirubin oxidase and its mutants for potential copper ligands. Biochemistry 38, 3034-42.

Shleev, S., Elkasmi, a, Ruzgas, T, and Gorton, L (2004). Direct heterogeneous electron transfer reactions of bilirubin oxidase at a spectrographic graphite electrode. Electrochemistry Communications 6, 934-939.

Shleev, S., Tkac, J., Christenson, A., Ruzgas, Tautgirdas, Yaropolov, A. I., Whittaker, J. W., and Gorton, Lo (2005). Direct electron transfer between copper-containing proteins and electrodes. Biosensors & bioelectronics 20, 2517-54.

Simonneaux, G., and Bondon, A. (2005). Mechanism of electron transfer in heme proteins and models: the NMR approach. Chemical reviews 105, 2627-46.

Sinibaldi, F., Howes, B. D., Piro, M. C., Polticelli, F., Bombelli, C., Ferri, T., Coletta, M., Smulevich, G., and Santucci, R. (2010). Extended cardiolipin anchorage to cytochrome c: a model for protein-mitochondrial membrane binding. Journal of biological inorganic chemistry : JBIC : a publication of the Society of Biological Inorganic Chemistry 15, 689-700.

Sinibaldi, F., Howes, Æ. B. D., and Piro, Æ. M. C. (2006). Insights into the role of the histidines in the structure and stability of cytochrome c. Journal of Biological Inorganic Chemistry, 52-62.

Sklenar, V. (1993). Gradient-Tailored Water Suppression for 1H-15N HSQC Experiments Optimized to Retain Full Sensitivity. Journal of Magnetic Resonance, Series A 102, 241-245.

Skulachev, V. P. (1998). Cytochrome c in the apoptotic and antioxidant cascades. FEBS letters 423, 275-80.

Smirnov, V. V., and Roth, J. P. (2006). Mechanisms of electron transfer in catalysis by copper zinc superoxide dismutase. Journal of the American Chemical Society 128, 16424-5.

Song, M. I., Bier, F. F., and Scheller, Frieder W. (1995). A Method to Detect Superoxide Radicals Using Teflon Membrane and Superoxide-Dismutase. Bioelectrochemistry and Bioenergetics 38, 419-422.

Song, S., Liu, Hongyun, Guo, X., and Hu, Naifei (2009). Comparative electrochemical study of myoglobin loaded in different polyelectrolyte layer-by-layer films assembled by spin-coating. Electrochimica Acta 54, 5851-5857.

Speck, S., Koppenol, W., Dethmers, J., Osheroff, N., Margoliash, E., and Rajagopalan, K. (1981). Definition of cytochrome c binding domains by chemical modification. Interaction of horse cytochrome c with beef sulfite oxidase and analysis of steady state kinetics. Journal of Biological Chemistry 256, 7394.

Spricigo, R., Dronov, R., Lisdat, F., Leimkühler, S., Scheller, Frieder W., and Wollenberger, U. (2009). Electrocatalytic sulfite biosensor with human sulfite oxidase co-immobilized with cytochrome c in a polyelectrolyte-containing multilayer. Analytical and bioanalytical chemistry 393, 225-33.

Spricigo, R., Dronov, R., Rajagopalan, K V, Lisdat, F., Leimkühler, S., Scheller, Frieder W., and Wollenberger, U. (2008). Electrocatalytically functional multilayer assembly of sulfite oxidase and cytochrome c. Soft Matter 4, 972-978.

Spricigo, R., Richter, C., Leimkühler, S., Gorton, Lo, Scheller, Frieder W., and Wollenberger, U. (2010). Sulfite biosensor based on osmium redox polymer wired sulfite oxidase. Colloids and Surfaces A: Physicochemical and Engineering Aspects 354, 314-319.

Stoll, C., Gehring, C., Schubert, K., Zanella, M., Parak, W. J., and Lisdat, F. (2008). Biosensors and Bioelectronics Photoelectrochemical signal chain based on quantum dots on gold — Sensitive to superoxide radicals in solution. Biosensors and Bioelectronics 24, 260-265.

Stroppolo, M. E., Falconi, M., and Caccuri, A., A (2001). Superefficient enzymes. Cellular and Molecular 358, 347–351.

Sullivan, E. P., Hazzard, J. T., Tollin, G., and Enemark, J. H. (1993). Electron transfer in sulfite oxidase: Effects of pH and anions on transient kinetics. Biochemistry 32, 12465-12470.

Tammeveski, K., Tenno, T. T., Mashirin, A. A., Hillhouse, E. W., Manning, P, and McNeil, C. J. (1998). Superoxide electrode based on covalently immobilized cytochrome c: Modelling studies. Free Radical Biology and Medicine 25, 973-978.

Tang, H., Chen, J., Nie, L., Kuang, Y., and Yao, S. (2007). A label-free electrochemical immunoassay for carcinoembryonic antigen (CEA) based on gold nanoparticles (AuNPs) and nonconductive polymer film. Biosensors & bioelectronics 22, 1061-7.

Tang, Z., Wang, Y., Podsiadlo, P., and Kotov, N. a (2006). Biomedical Applications of Layer-by-Layer Assembly: From Biomimetics to Tissue Engineering. Advanced Materials 18, 3203-3224.

Terrettaz, S., Cheng, J., Miller, C., and Guiles, R. (1996). Kinetic parameters for cytochrome c via insulated electrode voltammetry. J. Am. Chem. Soc 7863, 7857-7858.

Tian, Y., Mao, L. Q., Okajima, T., and Ohsaka, T. (2005). A carbon fiber microelectrode-based third-generation biosensor for superoxide anion. Biosensors & Bioelectronics 21, 557-564.

Tian, Y., Mao, L. Q., Okajima, T., and Ohsaka, T. (2004). Electrochemistry and electrocatalytic activities of superoxide dismutases at gold electrodes modified with a self-assembled monolayer. Analytical Chemistry 76, 4162-4168.

Tian, Y., Mao, L, Okajima, T., and Ohsaka, T. (2002). Superoxide dismutase-based third-generation biosensor for superoxide anion. Analytical Chemistry 74, 2428-2434.

Tian, Y., Mao, Lanqun, and Ohsaka, T. (2006). Electrochemical Biosensors for Superoxide Anion. Current Analytical Chemistry 2, 51-58.

Trewhella, J., Carlson, V. a, Curtis, E. H., and Heidorn, D. B. (1988). Differences in the solution structures of oxidized and reduced cytochrome c measured by small-angle X-ray scattering. Biochemistry 27, 1121-5.

Tsujimura, S, Kano, K, and Ikeda, T. (2005). Bilirubin oxidase in multiple layers catalyzes four-electron reduction of dioxygen to water without redox mediators. Journal of Electroanalytical Chemistry 576, 113-120.

Turano, P. (2004). Insights into Partially Folded or Unfolded States of Metalloproteins from Nuclear Magnetic Resonance. Inorg. Chem. 43, 7945-7952.

Turner, A. P. F. (2000). BIOCHEMISTRY: Biosensors-Sense and Sensitivity. Science 290, 1315-1317.

Updike, S., and Hicks, G. (1967). The enzyme electrode. Nature 214, 986-988.

Van Gelder, B., and Slater, E. (1962). The extinction coefficient of cytochrome c. Biochimica et biophysica acta 58, 593.

Volkov, A. N., Ferrari, D., Worrall, J. A. R., Bonvin, A. M. J. J., and Ubbink, M. (2005). The orientations of cytochrome c in the highly dynamic complex with cytochrome b5 visualized by NMR and docking using HADDOCK. Protein Science 14, 799–811.

Wang, Joseph (2000). Analytical Electrochemistry. In Analytical Electrochemistry (New York: Wiley-VCH), pp. 36-39.

Wang, L., and Waldeck, D.H. (2008). Denaturation of Cytochrome c and Its Peroxidase Activity When Immobilized on SAM Films. Journal of Physical Chemistry C 112, 1351-1356.

Wang, M., Gao, J., Müller, P., and Giese, B. (2009). Electron transfer in peptides with cysteine and methionine as relay amino acids. Angewandte Chemie (International ed. in English) 48, 4232-4.

Webb, M., Stonehuerner, J., and Millett, F. (1980). The use of specific lysine modifications to locate the reaction site of cytochrome c with sulfite oxidase. Biochimica et Biophysica Acta (BBA) 593, 290–298.

Wherland, S., and Gray, H. (1976). Electron transfer mechanisms employed by metalloproteins. In Biological aspects of inorganic chemistry, p. 289.

Williams, G., Eley, C. G., Moore, G. R., Robinson, M. N., and Williams, R. J. (1982). The reaction of cytochrome c with [Fe(EDTA)(H2O)]-. FEBS letters 150, 293-9.

Winkler, J. R., Wittung-Stafshede, P., Leckner, J., Malmström, B. G., and Gray, H. B. (1997). Effects of folding on metalloprotein active sites. Proceedings of the National Academy of Sciences of the United States of America 94, 4246-4249.

Wu, Y., and Hu, S. (2007). Biosensors based on direct electron transfer in redox proteins. Microchimica Acta 159, 1-17.

Wu, Z., Zhao, Y., and Zhao, B. (2010). Superoxide anion, uncoupling proteins and Alzheimer□s disease. Journal of clinical biochemistry and nutrition 46, 187-94.

Xu, F., Shin, W., Brown, S., and Wahleithner, J., UM (1996). A study of a series of recombinant fungal laccases and bilirubin oxidase that exhibit significant differences in redox potential, substrate specificity, and stability. et Biophysica Acta (BBA 1292, 303-311.

Xu, J., and Bowden, E. F. (2006). Determination of the orientation of adsorbed cytochrome C on carboxyalkanethiol self-assembled monolayers by in situ differential modification. Journal of the American Chemical Society 128, 6813-22.

Xu, X., Thompson, L. V., Navratil, M., and Arriaga, E. a (2010). Analysis of superoxide production in single skeletal muscle fibers. Analytical chemistry 82, 4570-6.

Yamazaki, T., Kojima, K., and Sode, K. (2000). Extended-Range Glucose Sensor Employing Engineered Glucose Dehydrogenases. Analytical Chemistry 72, 4689-4693.

Ying, T., Wang, Z.-H., Lin, Y.-W., Xie, J., Tan, X., and Huang, Z.-X. (2009). Tyrosine-67 in cytochrome c is a possible apoptotic trigger controlled by hydrogen bonds via a conformational transition. Chemical communications (Cambridge, England), 4512-4.

Ying, T., Wang, Z.-H., Zhong, F., Tan, X., and Huang, Z.-X. (2010). Distinct mechanisms for the pro-apoptotic conformational transition and alkaline transition in cytochrome c. Chemical communications (Cambridge, England) 46, 3541-3.

Ying, T., Zhong, F., Xie, J., Feng, Y., Wang, Z.-H., Huang, Z.-X., and Tan, X. (2009). Evolutionary alkaline transition in human cytochrome c. Journal of bioenergetics and biomembranes 41, 251-7.

Yu, T., Wang, X., Purring-Koch, C., Wei, Y., and McLendon, G. L. (2001). A mutational epitope for cytochrome C binding to the apoptosis protease activation factor-1. The Journal of biological chemistry 276, 13034-8.

Yuasa, M., and Oyaizu, K. (2005). Electrochemical Detection and Sensing of Reactive Oxygen Species. Current Organic Chemistry 9, 1685-1697.

Yue, H., Waldeck, D.H., Schrock, K., Kirby, D., Knorr, K., Switzer, S., Rosmus, J., and Clark, R. a (2008). Multiple Sites for Electron Tunneling between Cytochrome c and Mixed Self-Assembled Monolayers. Journal of Physical Chemistry C 112, 2514-2521.

Zhao, W., Xu, J.-J., and Chen, H.-Y. (2006). Electrochemical Biosensors Based on Layer-by-Layer Assemblies. Electroanalysis 18, 1737-1748.

Zhou, Y.-H., Fu, H., Zhao, W.-X., Chen, W.-L., Su, C.-Y., Sun, H., Ji, L.-N., and Mao, Z.-W. (2007). Synthesis, structure, and activity of supramolecular mimics for the active site and arg141 residue of copper, zinc-superoxide dismutase. Inorganic chemistry 46, 734-9.

ACKNOWLEDGEMENTS

An dieser Stelle möchte die Möglichkeit nutzen, mich bei einigen Menschen zu bedanken, die mich auf dem Weg zu diesem Schriftstück begleitet haben. Besonderen Dank gilt meinem „Doktorvätern“ Prof. Möhwald und Prof. Lisdat, die es mir ermöglicht haben an diesem interessanten interdisziplinären Projekt zu arbeiten und mir stets für Diskussionen zur Seite standen.

Darüber hinaus bin ich Prof. Lisdat sehr dankbar, dass er mir mit seinem Fachwissen, der konstruktiven Kritik und seinen vielen Ideen immer wieder neue Anregungen gegeben hat. Sein großes Engagement ist für mich bemerkenswert.

Für die tägliche angenehme Arbeitsatmosphäre und Hilfsbereitschaft im Labor oder Büro bedanke ich mich bei Roman Dronov, Kirsten Schubert und David Saurali (auch als „Editor in Chief“) und bei allen aktuellen und ehemaligen Mitarbeitern der ehemaligen „Analytischen Biochemie“ der Universität Potsdam sowie der Abteilung Biosystemtechnik der TH Wildau. Insbesondere danke ich Frau Prof. Leimkühler für die freundliche Bereitstellung des Enzyms Sulfitoxidase für meine Experimente und Frau Prof. Wollenberger für die vielen hilfreichen Diskussionen und Ratschläge.

Ringrazio anche Paola, Marco e Andrea per il caro aiuto nel periodo di lavoravo al CERM (e dopo). Grazie a Paola per tutti gli spettri NMR fatti. E grazie a Marco per aiuto nell'espressione delle proteine. Senza di loro la tesi non sarebbe com’è adesso. Ringrazio anche per la loro collaborazione nello scrivere le pubblicazioni. Infine devo ringraziare tutti, ma tutti, gli (ex)CERMiani per aver reso il mio periodo fiorentino indimenticabile!

Wenn ich zurück blicke, dann waren die letzten Jahre eine sehr “bewegte” Zeit: Ich bin nicht nur zweimal mit dem Labor umgezogen, sondern war vor Allem viel auf Reisen und habe viele Erfahrungen sammel können: bei diversen Konferenzen, Tagungen, Sommerschulen und natürlich bei meinen Aufenthalten an der Universität Florenz. Für diese Möglichkeiten möchte ich mich bei der Max-Planck-Gesellschaft für die finanzielle Unterstützung bedanken. Aber auch Prof. Lisdat danke ich für den Ansporn für die Teilnahme an den Tagungen.

APPENDIX

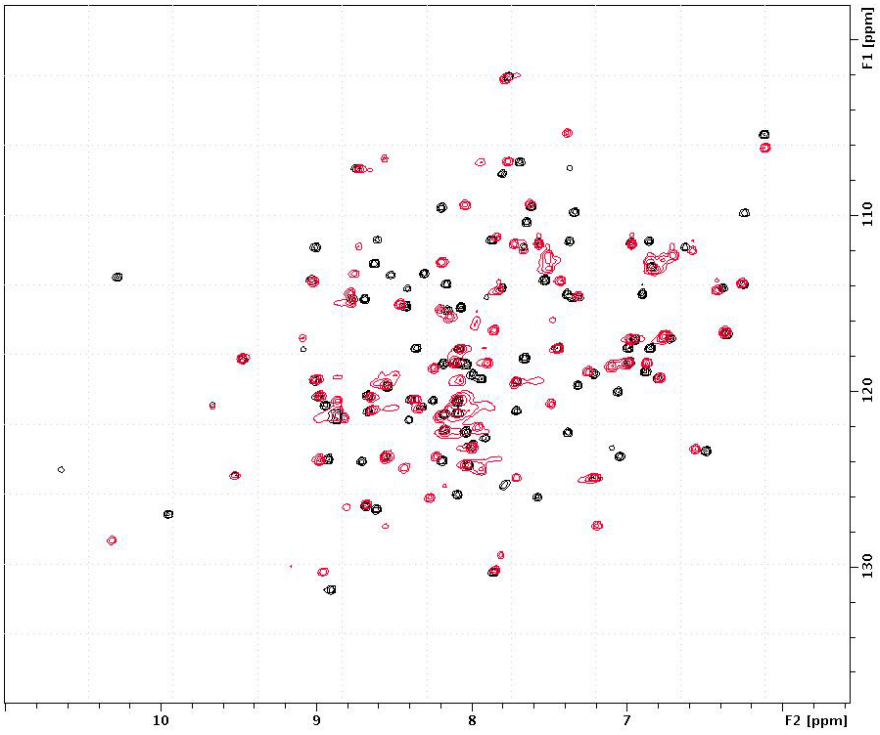

A1. Overlay of the ^{1}H-^{15}N HSQC spectra of the ferrous form of Y46K (red trace) and wild type (black trace) human cytochrome c.

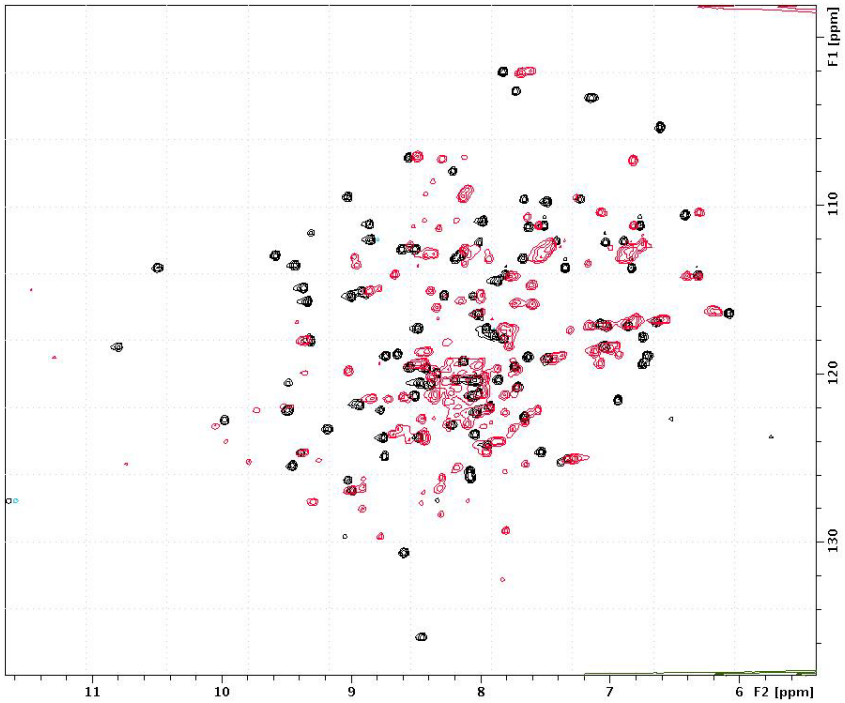

A2. Overlay of the ^{1}H-^{15}N HSQC spectra of the ferric form of Y46K (red trace) and wild type (black trace) human cytochrome c.

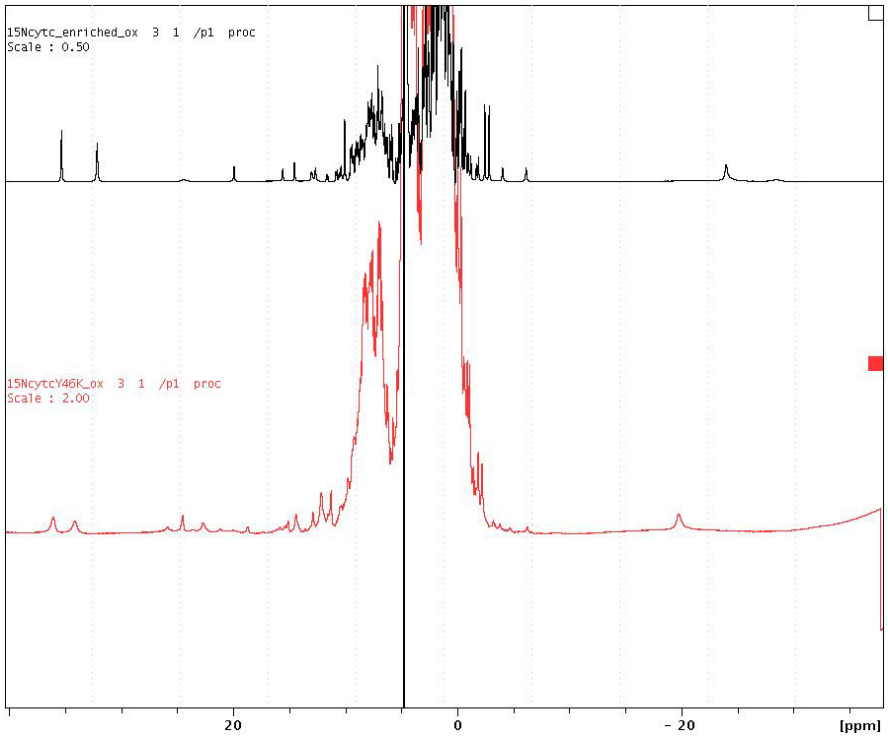

A3. Comparison of the hyperfine shifted resonances in the ^{1}H NMR spectra of the ferric form of (black) wild type, and (red) Y46K human cytochrome c.

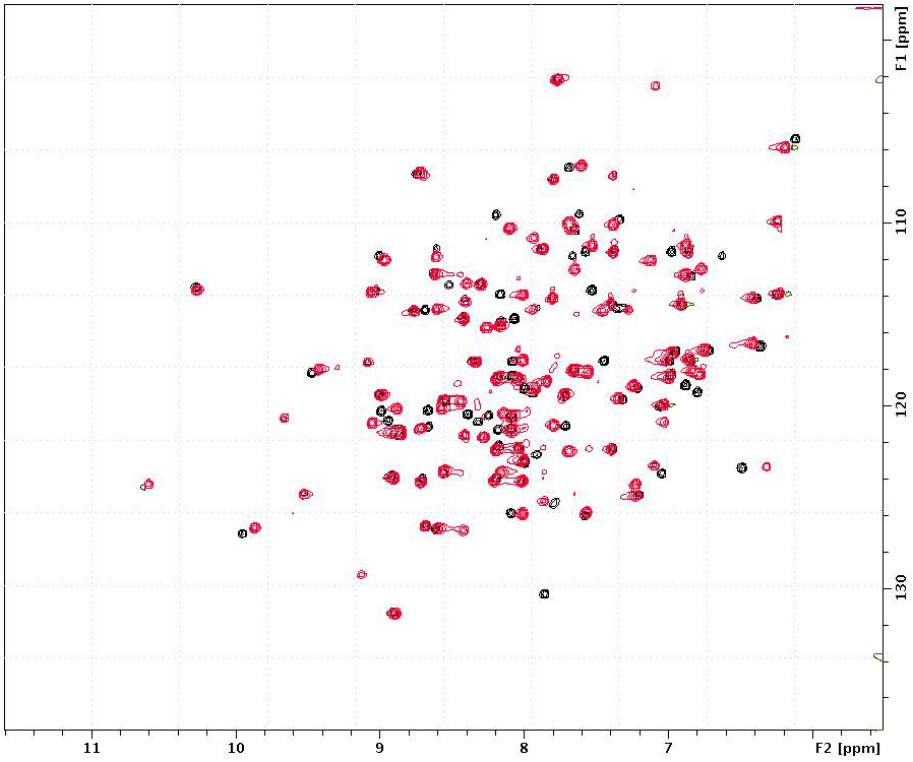

A4. Overlay of the ^{1}H-^{15}N HSQC spectra of the ferrous form of F82K (red trace) and wild type (black trace) human cytochrome c.

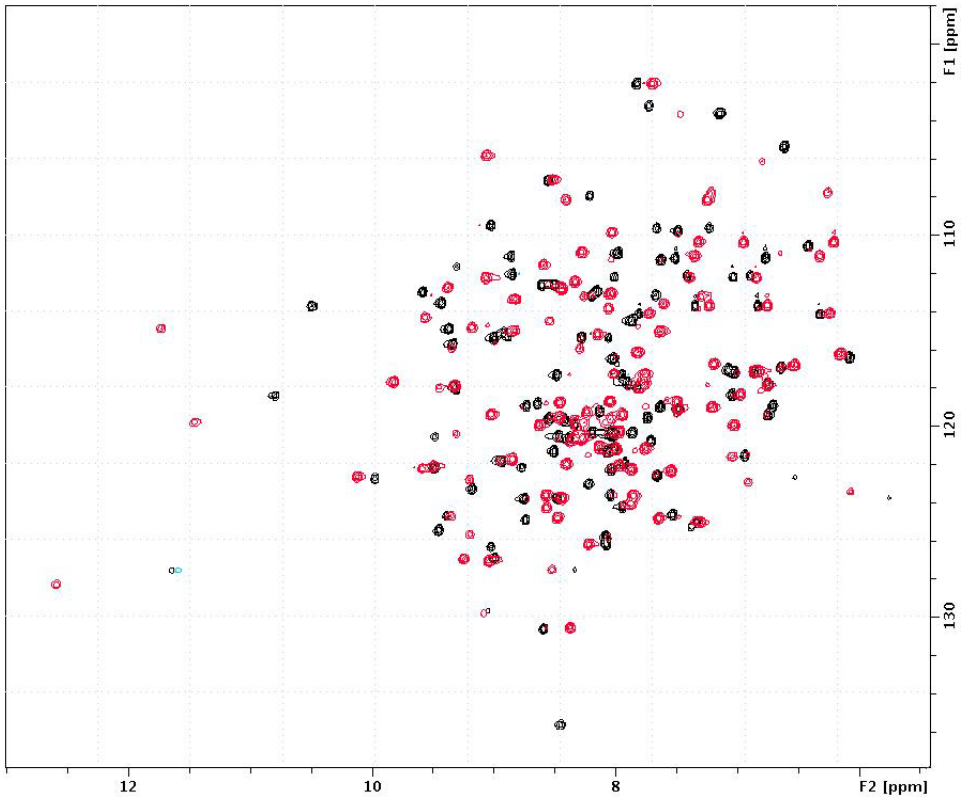

A5. Overlay of the ^{1}H-^{15}N HSQC spectra of the ferric form of F82K (red trace) and wild type (black trace) human cytochrome c.

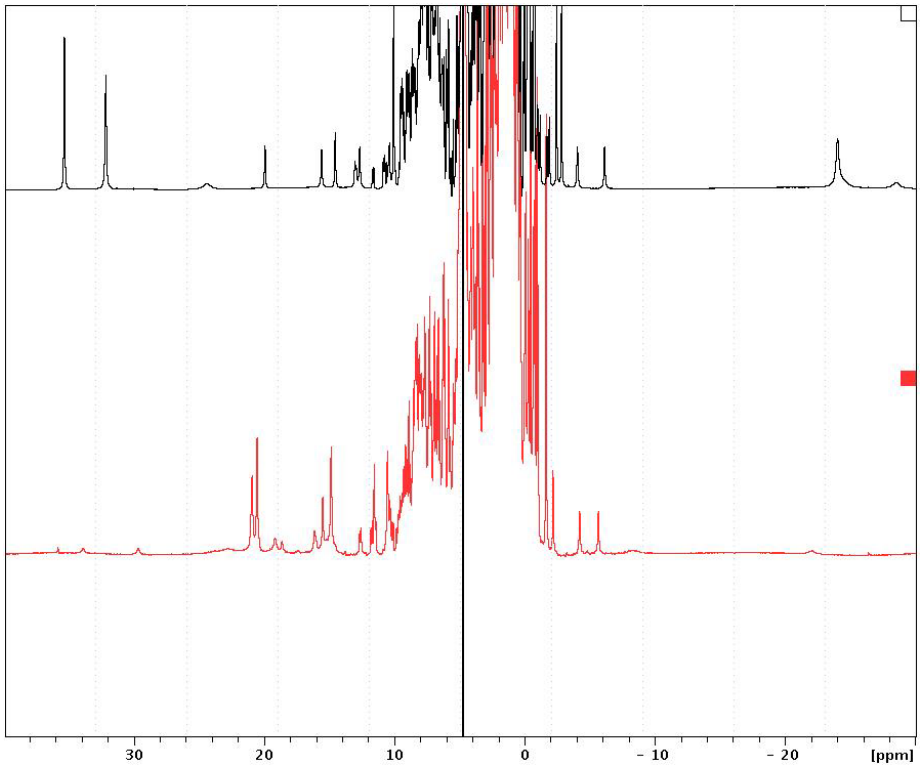

A6. Comparison of the hyperfine shifted resonances in the ^{1}H NMR spectra of the ferric form of (black) wild type, and (red) F82K human cytochrome c.

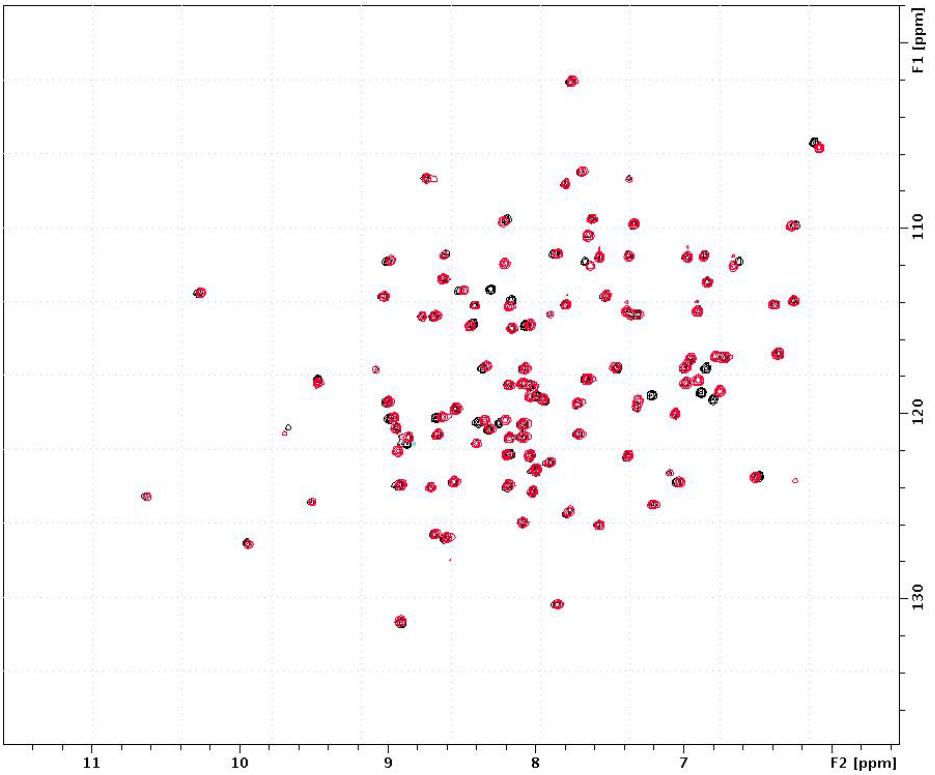

A7. Overlay of the ^{1}H-^{15}N HSQC spectra of the ferrous form of E66K (red trace) and wild type (black trace) human cytochrome c.

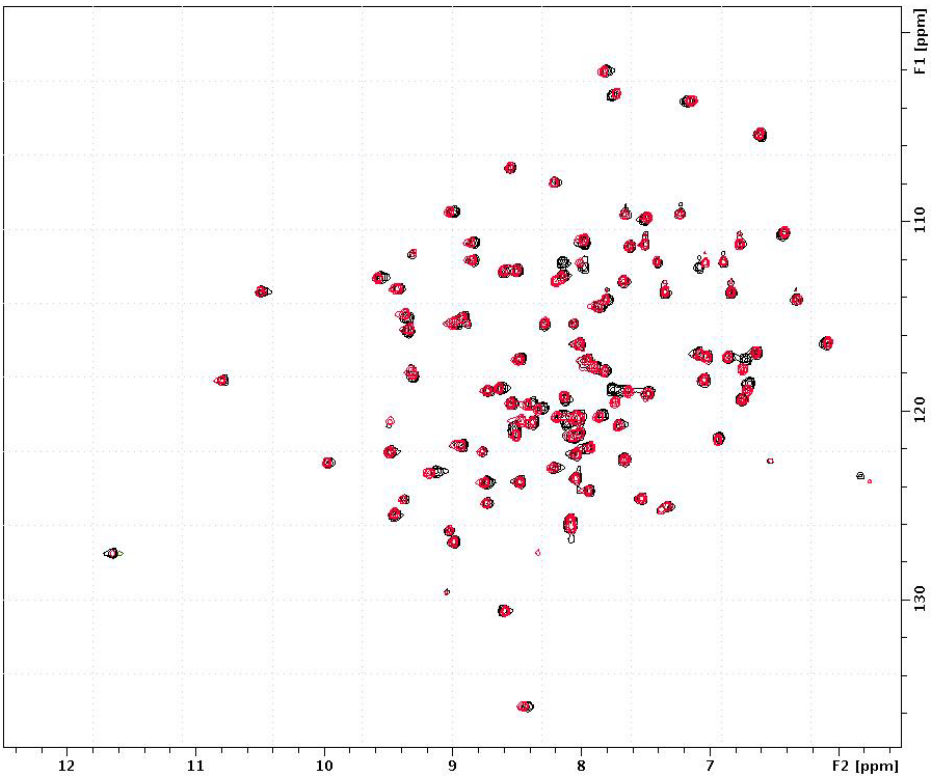

A8. Overlay of the ^{1}H-^{15}N HSQC spectra of the ferric form of E66K (red trace) and wild type (black trace) human cytochrome c.

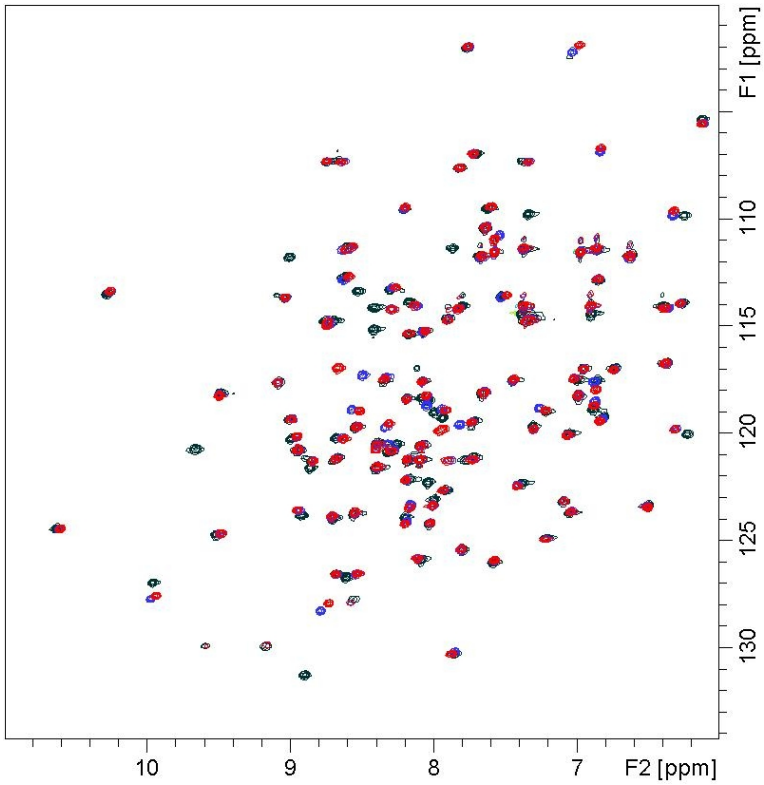

A9. Overlay of the ^{1}H-^{15}N HSQC spectra of the ferrous form of WT (black trace) with T63K (red trace) and T63R (blue trace).

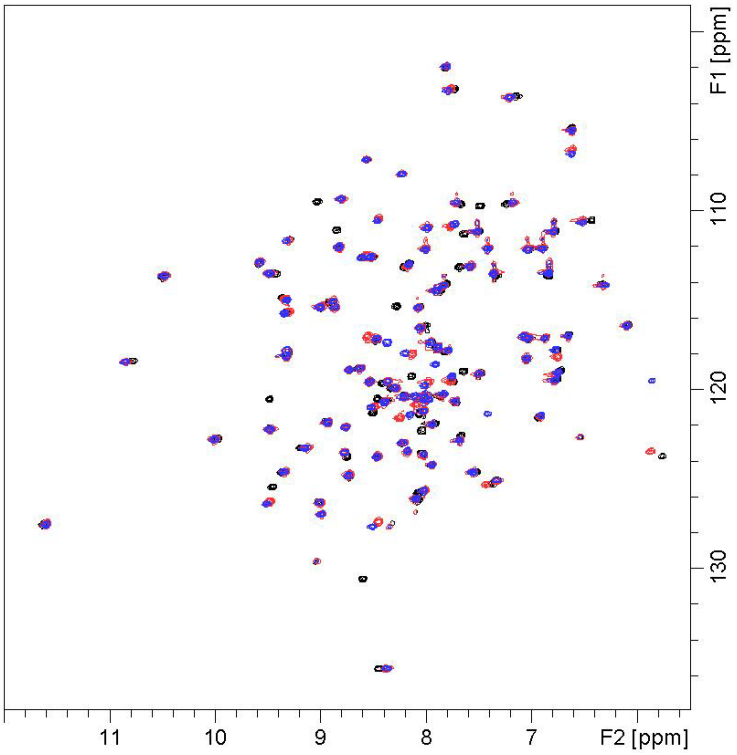

A10. Overlay of the ^{1}H-^{15}N HSQC spectra of the ferric form of WT (black trace) with T63K (red trace) and T63R (blue trace).

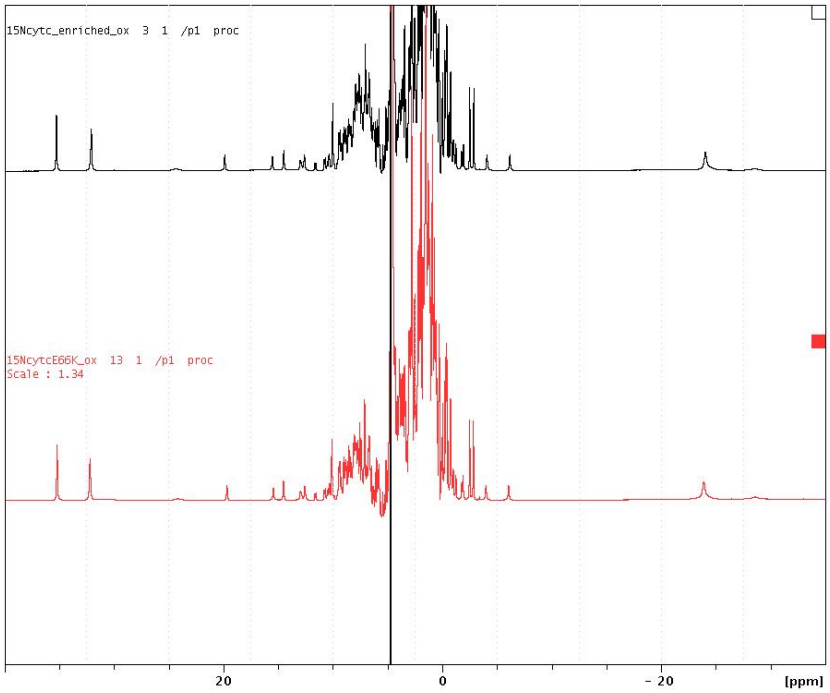

A11. Comparison of the hyperfine shifted resonances in the ^{1}H NMR spectra of the ferric form of (A) wild type, and (B) E66K human cytochrome c.

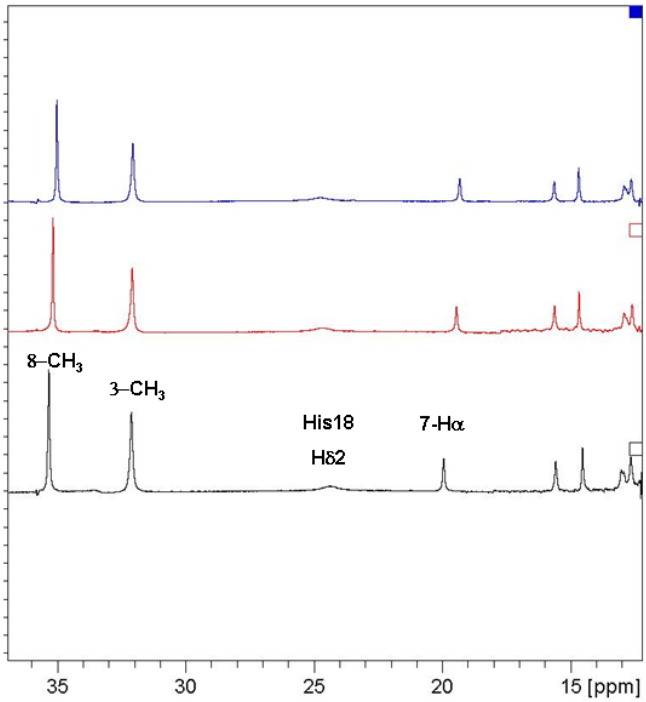

A12. The downfield regions of the 1D ^{1}H NMR spectra of oxidized WT (bottom black trace), T63K (middle red trace) and T63R (top blue trace). Some representative signals for the heme methyls and axial ligands are labeled in the WT spectrum and obviously recognizable in the other two spectra.

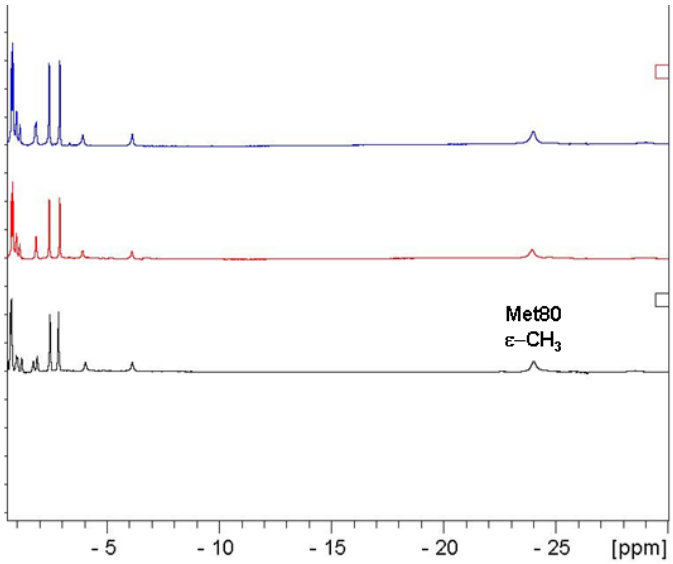

A13. The upfield regions of the 1D ^{1}H NMR spectra of oxidized WT (bottom black trace), T63K (middle red trace) and T63R (top blue trace). Some representative signals for the heme methyls and axial ligands are labeled in the WT spectrum and obviously recognizable in the other two spectra.

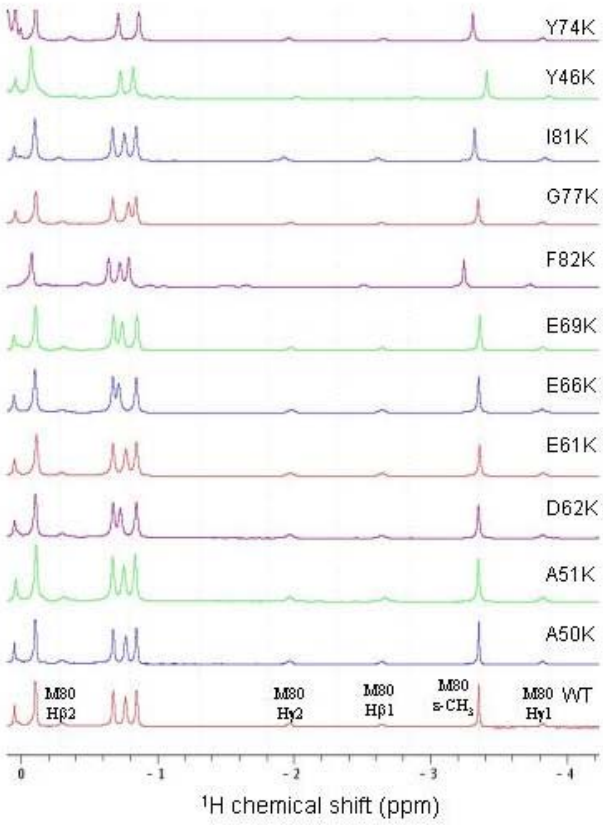

A14. Upfield part of the ^{1}H NMR spectra of wild type and mutated ferrous forms of human cytochrome c. The Met80 side chain resonances are labelled for the wild type protein according to the available assignment.

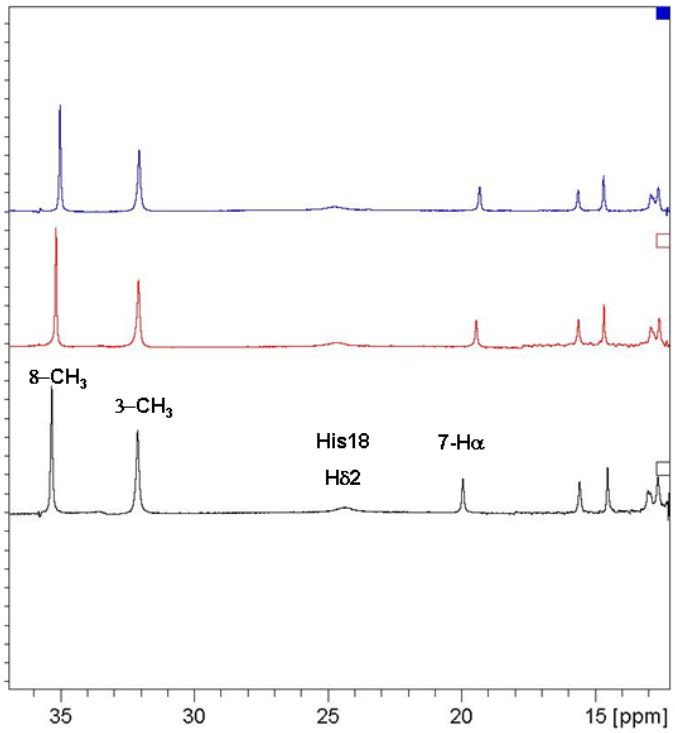

A15. The downfield regions of the 1D ^{1}H NMR spectra of oxidized WT (bottom black trace), T63K (middle red trace) and T63R (top blue trace). Some representative signals for the heme methyls and axial ligands are labeled in the WT spectrum and obviously recognizable in the other two spectra.

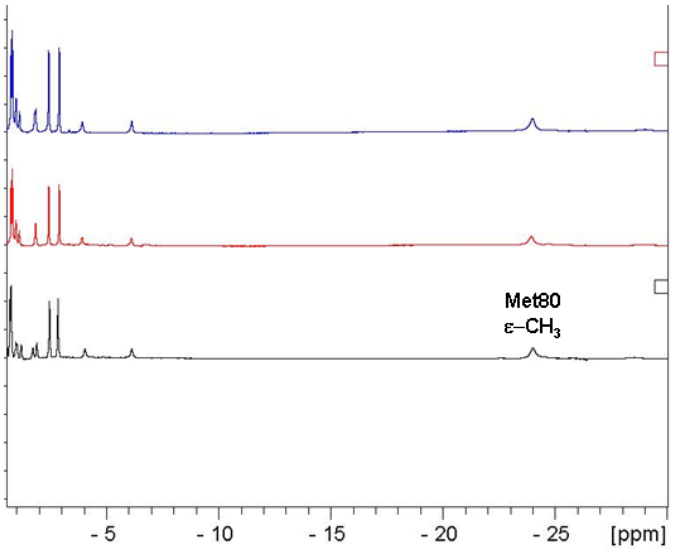

A16. The upfield regions of the 1D ^{1}H NMR spectra of oxidized WT (bottom black trace), T63K (middle red trace) and T63R (top blue trace). Some representative signals for the heme methyls and axial ligands are labeled in the WT spectrum and obviously recognizable in the other two spectra

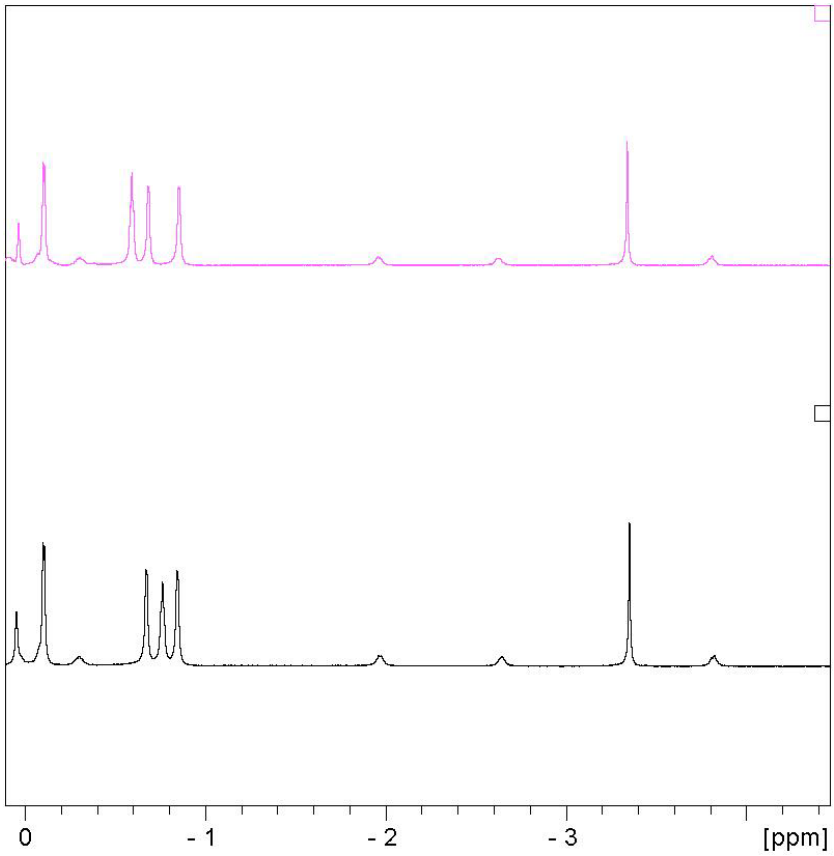

A17 Comparison of the ^{1}H NMR spectra of WT (lower black trace) and T63K-E66K variant (upper magenta trace) for the upfield region of the reduced form.

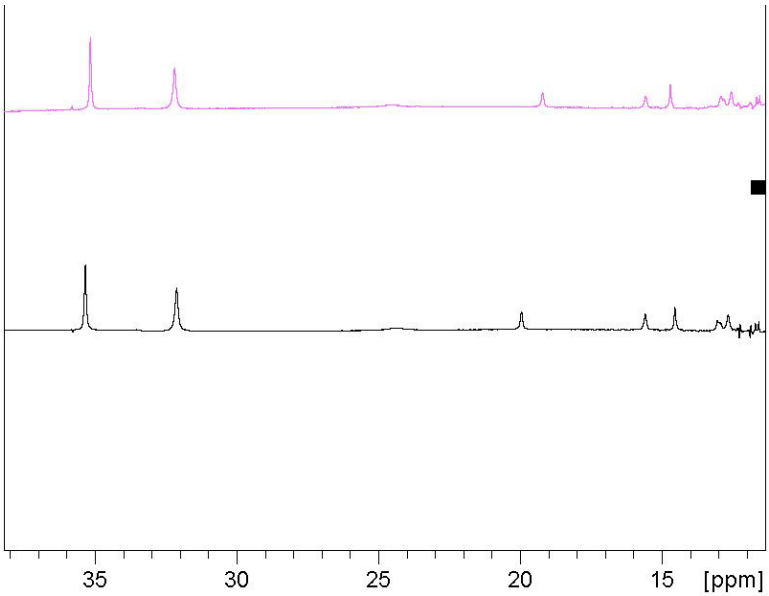

A18. Comparison of the ^{1}H NMR spectra of WT (lower black trace) and T63K-E66K variant (upper magenta trace) for the downfield region of the oxidized form.

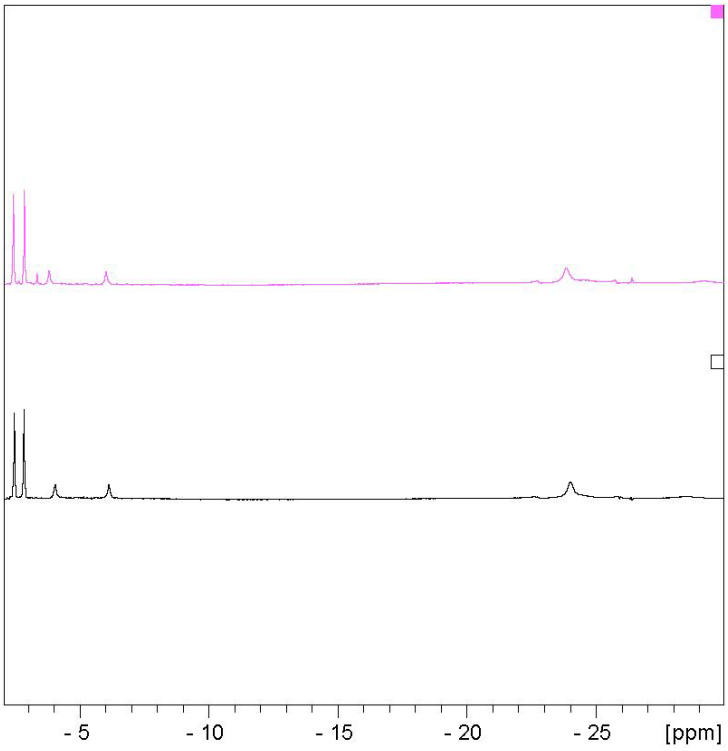

A19 Comparison of the ^{1}H NMR spectra of WT (lower black trace) and T63K-E66K variant (upper magenta trace) for the upfield region of the oxidized form.

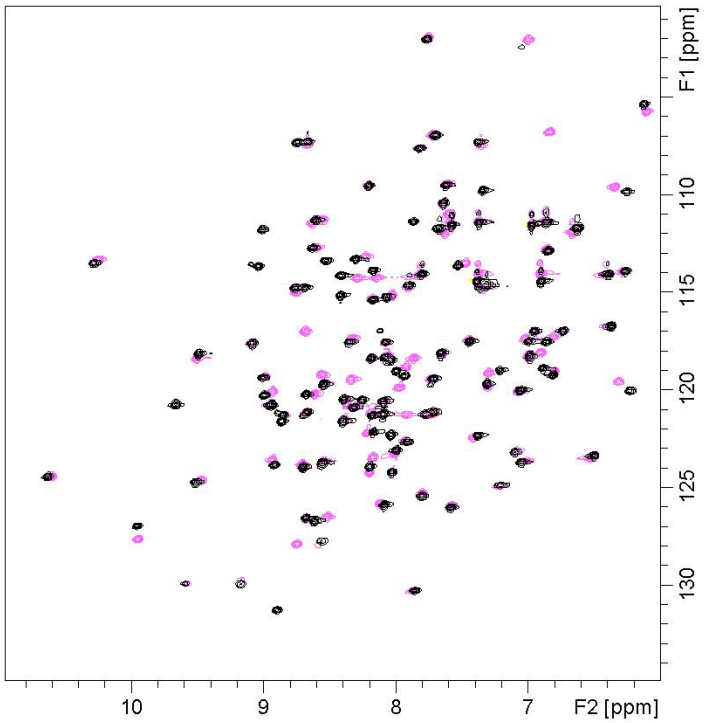

A19 Overlay of the ^{1}H-^{15}N HSQC spectra of the reduced forms of WT (black trace) and T63-KE66K (magenta trace).

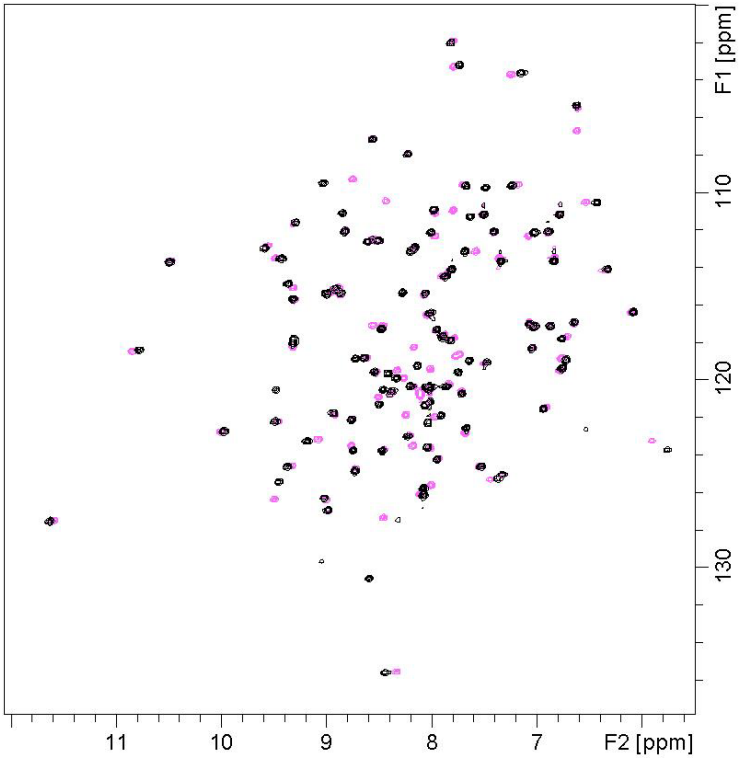

A20. Overlay of the ^{1}H-^{15}N HSQC spectra of the oxidized forms of WT (black trace) and T63KE66K (magenta trace).